FEASIBILITY STUDY OF A PORTABLE COUPLED ^{3}He DETECTOR WITH $LaBr_3$ GAMMA SCINTILLATOR FOR FIELD IDENTIFICATION AND QUANTIFICATION OF NUCLEAR MATERIAL

A Thesis

by

DANIEL CANADY STROHMEYER

Submitted to the Office of Graduate Studies of
Texas A&M University
in partial fulfillment of the requirements for the degree of

MASTER OF SCIENCE

May 2010

Major Subject: Health Physics

FEASIBILITY STUDY OF A PORTABLE COUPLED ^{3}He DETECTOR WITH $LaBr_3$ GAMMA SCINTILLATOR FOR FIELD IDENTIFICATION AND QUANTIFICATION OF NUCLEAR MATERIAL

A Thesis

by

DANIEL CANADY STROHMEYER

Submitted to the Office of Graduate Studies of
Texas A&M University
in partial fulfillment of the requirements for the degree of

MASTER OF SCIENCE

Approved by:

Chair of Committee,	William S. Charlton
Committee Members,	John W. Poston, Sr.
	Sunil Khatri
Head of Department,	Raymond Juzaitis

May 2010

Major Subject: Health Physics

ABSTRACT

Feasibility Study of a Portable Coupled ^{3}He Detector with $LaBr_3$ Gamma Scintillator for Field Identification and Quantification of Nuclear Material.

(May 2010)

Daniel Canady Strohmeyer, B.S., Texas A&M University;

Chair of Advisory Committee: Dr. William Charlton

In recent years, there have been several research endeavors to increase the ability to identify and quantify special nuclear material in field measurements. These have included both gamma spectroscopy and neutron coincidence systems that are portable and work in a variety of environments. In this work, a Monte Carlo Neutral Practicle X (MCNPX) model was used to design an instrument that includes four gamma detection slabs placed within four neutron detection slabs. The combination of gamma spectroscopy and neutron coincidence counting in a single instrument allows for direct measurement of plutonium (Pu) mass without need for assumptions or operator declarations. A combined neutron-gamma instrument was designed for use in characterizing and quantifying Pu in field samples. This detector consists of a plastic scintillator containing $LaBr_3$ nanoparticles and a polyethylene slab containing four ^{3}He tube detectors. The system was tested via simulation with MCNPX for four Pu samples of known quality and quantity. These samples had masses ranging from 100-300 g of Pu. It was found that the designed detector system could be used to determine ^{240}Pu-effective

mass to within 3.5% accuracy and to characterize the isotopic content of the Pu to within 2% accuracy for all isotopes except for ^{238}Pu and ^{242}Pu. The system could determine ^{238}Pu isotopic content to within 14% accuracy but is completely unable to determine ^{242}Pu content. This system has the ability to Four Plutonium (Pu) samples of known quantity were modeled and tested to determine what data was available from each individual signature. Each model included a separate MCNPX deck for each individual isotope that contributes to the gamma signature in photon mode and a spontaneous fission and (α,n) deck for the neutron signature. The first three samples were used to create spectrums and efficiency curves for each odd isotope as well as for a Pu effective mass for the neutron signature. The data from these simulations were then used to identify the isotopics in the fourth sample to within acceptable accuracy. From this data, a total Pu mass was obtained as well as an ability to determine the ratio of (α,n) to spontaneous fission neutrons without additional simulations. This provides a new method to detect and identify the Pu content within a sample without producing requiring supplemental additional information since isotopics can be determined with the combined use of the gamma and neutron systems.

ACKNOWLEDGEMENTS

I would like to thank everyone from the Nuclear Security Science and Policy Institute for making this work possible. I would like to specifically thank Grant Ford for his continuous assistance from beginning to completion. I would also like to thank my committee, especially the chair, Dr. Charlton, for their tireless efforts to help with the research, presentations, and writing. Dr. Charlton's guidance and wisdom will last long after this work is done, and hopefully lead to a long career in international safeguards and nonproliferation.

I would also like to thank my mother, Judy Joiner and my sister, Keana Frey, for their help with formatting and review of the entire document throughout the process. Without both of them I would not be where I am today.

TABLE OF CONTENTS

Page

LIST OF TABLES

Page

Page

LIST OF FIGURES

Page

Page

CHAPTER I

INTRODUCTION

1.1 MOTIVATION AND OBJECTIVES

The proliferation of nuclear weapons and materials is a continuing threat. This has garnered significant attention due to the second test of a nuclear weapon by North Korea and the continuing enrichment of uranium by Iran. The growth in nuclear material inventories and the future possibility of even larger growth has made nuclear terrorism a greater threat now than ever before. The US government has sworn to combat this threat, and techniques and instruments are needed.

Many radiation detectors exist today that identify and quantify nuclear material. Some weigh well over 50 kg and are large and difficult to move[2]. This limits the use of this equipment in field applications and has lead to research areas to design and develop a system that is portable and able to identify and quantify special nuclear material in the field. One previous example of this is the Portable Neutron Coincidence Counter[1-3] developed by A. Thornton and H. Menlove, which measures neutron coincidences to quantify plutonium (Pu). Other preliminary efforts have studied the use of both neutron and gamma signatures; however, none of these have been portable[4-5]. In this work, we develop a portable, combined neutron-gamma detection system. This system uses a combination of neutron coincidences and gamma spectroscopy to identify and quantify

---

This thesis follows the style of *Nuclear Technology*.

nuclear material in the field. We will focus on the use of this system for measurement of Pu but it may be useful for other nuclear materials as well.

The instrument designed here makes use of a slab detector that consists of a gamma scintillator adjacent to a slab of polyethylene with four ^{3}He tubes in it. This allows for simultaneous measurement of gamma and neutron radiation from the sample. The intention is to arrange four of these slabs in a collar-like configuration in which an unknown sample is placed in the middle of the collar. The scintillator material uses $LaBr_3$ nanocrystals embedded in an Oleic Acid matrix. This system makes use of advanced detection materials (some of which are not yet commercially available[6-9], specifically the scintillator materials). Since some of these materials could not be acquired commercially, the system was simulated using MCNPX for the design process; however, measured data was used to benchmark the simulations wherever possible.

1.2 SOURCES OF RADIATION FROM PLUTONIUM

1.2.1 NEUTRON SOURCES

Neutron detection systems have been in use for decades and are available in many different configurations. Early systems measured the gross count rate, or what today is known as singles or totals rates, meaning one count equals a single neutron interaction within the detector medium[10]. The totals rate can be used to determine if neutrons are being emitted from an unknown sample (which is often an indicator of the presence of nuclear material) and can be used to determine the total quantity of nuclear material for very simple (and well characterized) samples. For many applications, the totals rate is

not directly related to the quantity of Pu in a sample due geometry, matrix characteristics, and impurity isotopes.

If more than one neutron is born simultaneously, such as during a fission event, an alternate method to detecting neutrons is to count them simultaneously or in coincidence. This method is more costly, but provides more information about the source than the totals rate alone. Neutron coincidence counting is a passive non-destructive assay (NDA) method and is commonly used today as a quantitative and qualitative measurement technique[10]. NDA methods are generally preferred since they don't alter the state of the material. Thus, once the NDA measurement is complete, then the material can be returned or undergo additional measurements. Passive NDA methods make use of the spontaneously produced radiation from a material due to its natural radioactivity. Active NDA measurements are another NDA technique that actively induces a signal from a material using an external source. This method is commonly used on materials where the spontaneous fission (SF) rate is too low for a passive method, for example U. Plutonium on the other hand has a high SF rate that readily allows for passive methods to be used.

When a fission event occurs, many byproducts are produced. They include fission products, gamma rays, and neutrons. Between 0 and 8 neutrons can be produced simultaneously from the same fission events. These neutrons are known as coincident neutrons. When this coincident event caused by two neutrons occurs, it indicates that fissionable material is present, and in the case of passive detection systems a spontaneous fission has occurred[10].

The SF rate is a characteristic of the specific nuclide(s) present in the sample. Plutonium has high SF rates for the even numbered isotopes (i.e. ^{238}Pu, ^{240}Pu and ^{242}Pu). The SF information for Pu can be seen below in Table 1.

Table 1. Spontaneous fission neutron yields for Pu isotopes (data from Ref. 10).

Isotope	Spontaneous Fission Yield (n/s-g)	Spontaneous Fission Multiplicity (ν)	Induced Fission Multiplicity (ν)
^{238}Pu	2.59E+03	2.21	2.9
^{239}Pu	2.18E-02	2.16	2.88
^{240}Pu	1.02E+03	2.16	2.8
^{241}Pu	5.00E-02	2.25	2.8
^{242}Pu	1.72E+03	2.15	2.81

From Table 1, it can be seen that ^{240}Pu has a high yield and since it is the dominant isotope in low (~6%) to high (~15 to 25%) burn-up Pu, it is the primary isotope of interest. Because of this, when performing measurements on Pu an effective ^{240}Pu mass ($^{240}Pu_{eff}$) is used and is defined by[6]:

$$m_{eff}^{240} = 2.52m^{238} + m^{240} + 1.68m^{242} \quad [1]$$

This is the effective mass of ^{240}Pu only that would give the same coincidence response that would be obtained from an actual sample containing various even Pu isotopes. The coefficients in the equation are determined by the relative SF half-lives and the relative multiplicity distributions of each isotope, as well as the coincidence circuitry[10]. Since the

relative SF yields are the dominant effect, the change in circuitry would make only slight changes.

However, SF is not the only source of neutrons in a sample. In most samples that emit neutrons their primary mode of decay is via alpha decay and not SF. When an alpha is emitted it is possible to undergo an (α,n) interaction with matrix material (for example, the oxygen in oxide powders) and produce a neutron. Since these neutrons are only being produced in singles (i.e. one at a time), they should not affect the coincidence count rate. There will be a small number emitted close enough in time that will be counted as a coincidence event, but this will be a small variation. This allows coincidence measurements to be performed despite the other neutrons present from background or (α,n) reactions. Therefore this measurement can be performed in a variety of environments.

On the other hand, there is another source of coincidence neutrons in samples containing fissionable material. Whenever a neutron is born, either from SF or a (α,n) reaction, it can also induce fission. These induced fission neutrons can in turn induce additional fissions. This is called sample self multiplication (or the multiplication factor) and must be accounted for when measuring the sample.

1.2.2 GAMMA-RAY SOURCES

Pu produces a number of discrete gamma-rays that are emitted in coincidence during alpha or beta decay. The primary gamma-ray signatures from Pu are given in Table 2. As can be seen, Pu has a number of different gamma lines and they range over energies

from very low (~50-100 keV) to fairly high (~600 keV). A typical Pu gamma spectra will show a complex of gamma lines around 300-400 keV and another complex of gamma lines around 600 keV. This tends to make gamma-ray spectrum analysis for Pu complicated.

Table 2. Major Pu gamma-ray signatures (data from Ref. 10).

Isotope	Energy (keV)	Activity (□/g-s)
^{238}Pu	152.7	5.90E6
	766.4	1.387E5
^{239}Pu	129.3	1.436E5
	413.7	3.416E4
^{240}Pu	45.2	3.80E6
	160.3	3.37E4
	642.5	1.044E3
^{241}Pu	148.6	7.15E6
	208.0	2.041E7
^{241}Am	59.5	4.54E10
	125.3	5.16E6

Gamma rays most commonly interact in one of three ways: photoelectric effect, Compton scattering, and pair production[11]. All of these result in a free electron and an ionized nucleus. There are other types of gamma ray interactions, but these have low probabilities and are of little concern since they do not result in the transfer of energy to electrons[12]. The type of interaction that will occur depends on many factors, with gamma-ray energy and Z (or proton number) of the absorber being the essential components. Figure 1 shows the relationship between the Z of the absorber, the photon energy, and the type of reaction that is likely to occur.

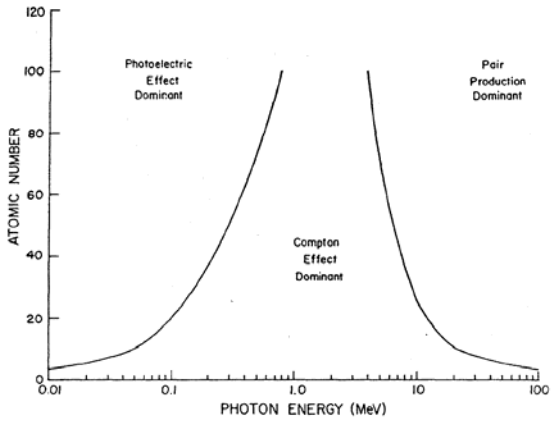

Figure 1. Relative importance of three major interactions (from Ref. 11).

The photoelectric effect is the predominant interaction for photons of less than 1 MeV for higher Z materials. The photoelectric effect results in the absorption of the gamma ray energy in its entirety. Some of the energy is used to free an electron from its orbit and the majority of the remaining energy is transferred to the electron itself. A minuscule amount of energy will be transferred to the recoil nucleus. This interaction can only take place with a bound electron since momentum has to be conserved. An illustration of photoelectric effect can be seen in Figure 2.

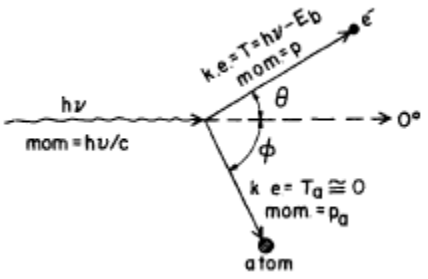

Figure 2. Kinematics of photoelectric effect (from Ref. 11).

Compton scattering is the midrange energy interaction. It is most probable for energies of 1-10 MeV for higher Z material. For low Z materials, it is the most probable independent of energy. This interaction still involves an electron, but the photon can interact with free electrons and loosely bound electrons that are usually on the outer most shell of the electron orbitals. Conservation of energy and momentum only allows a fraction of the photon energy to be transferred to the electron. The remainder of the energy remains with the outgoing photon. This results in a spectrum of photons essentially ranging from zero to close to the original photon energy. In Figure 3, an illustration of Compton scattering can be seen.

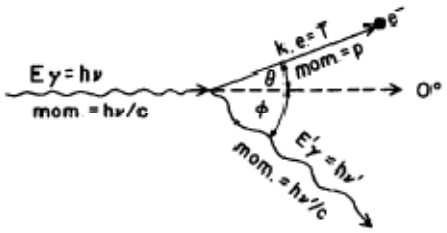

Figure 3. Kinematics of Compton scattering (from Ref. 11).

The third type of interaction is pair production and is least likely to occur except in high Z material with high energy photons. This reaction can only occur within the coulomb field of a nucleus[7]. The products of this reaction are a recoil nucleus, one electron (β^-), and one positron (β^+). In order for this reaction to occur, the photon must have at least 1.022 MeV. This is the rest mass of one β^- and one β^+. The β^+ will undergo pair annihilation quickly in most materials creating two 511 keV gamma rays traveling in opposite directions. An illustration of pair production can be seen in Figure 4.

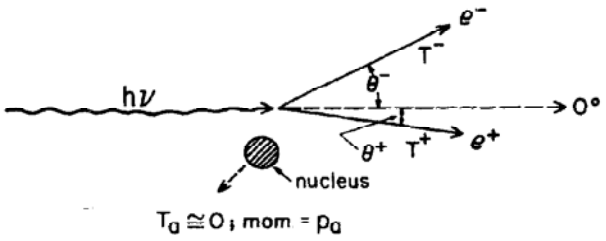

Figure 4. Kinematics of pair production (from Ref. 11).

1.3 NEUTRON DETECTION

1.3.1 NEUTRON DETECTION INSTRUMENTATION

Most nuclear detectors measure thermal neutrons (~0.25eV) since they are easier to detect than epithermal (0.25eV-1MeV) or fast (>1MeV) neutrons. Detection systems such as ^{3}He, $^{10}BF_3$, and fission chambers take advantage of the larger absorption cross sections at thermal energies (see Figure 5). All these detectors create charged particles via absorption reactions. These energetic charged particles then induce a current in the device. Fission chambers use a fission event to detect neutrons, and the detector fission events would create a fission neutron background that precludes their use in coincidence counting system. The most common detectors used are ^{3}He gas tubes. This type or detector is attractive due to its ruggedness, light weight, high efficiency, variety of sizes, and low gamma sensitivity[10].

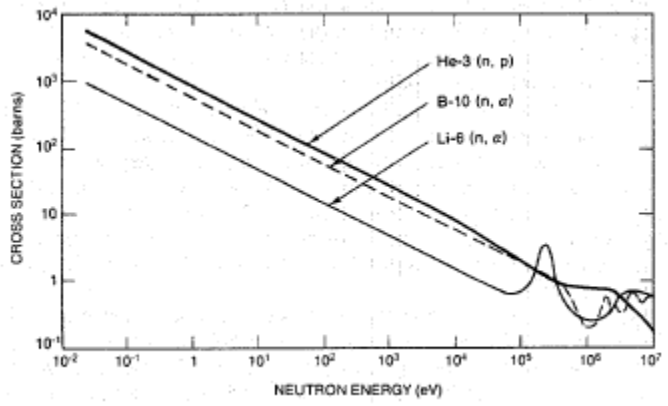

Figure 5. ^{3}He cross section versus energy.

^{3}He detects neutrons through an absorptions reaction producing a triton and proton:

$$^{3}_{2}He + ^{1}_{0}n \rightarrow ^{3}_{1}H + ^{1}_{1}p \qquad [2]$$

This results in ionized particles in an electric field. These ionized particles collide with gas atoms and liberate electrons. Inside the detector tube there is a positively charged (cathode) wall, usually made of aluminum or stainless steel, and a negatively charged (anode) gold plated tungsten wire[11]. This will allow the negatively charged electrons to move towards the anode and the ions to move to the cathode. This induces a current in the system.

Since the neutrons are going to be measured in the thermal range, the fast neutrons that are born from fission must be slowed down to interact with the detector medium. This requires a moderator to be placed between the detector tubes and the source. Most materials used for this process are hydrogen rich. One of the most common materials is High Density Polyethylene (C_6H_{12}). This slowing down to thermal energies will take a

significant amount of time, typically from 8-128 μsecs. We will consider the system to register a coincidence count when two neutrons "interact" in one or more detectors within a certain time frame (called the gate width). The optimal gate width varies depending on the design of the detector system. The electronics system will then register the number of coincidences that occurred during the total count time. One of the more common electronics systems used today are a shift registers.

Some common neutron instrumentation that is used today for neutron coincidence counting is well counters. These have been a staple in safeguards measurements for some time but come with several drawbacks. Most well counters are heavy and cumbersome. This makes them difficult to move. An example of a Canberra well counter currently available can be seen in Figure 6. This counter is 73 cm high and weighs 55 kg.

Figure 6. Canberra High-Level Neutron Coincidence Counter (see Ref 13).

1.3.2 NEUTRON COINCIDENCE COUNTING

In most modern neutron coincidence counting the Neutron Coincidence Point Model[10] is used to perform the analysis. This model provides equations relating the effective ^{240}Pu mass to the observed singles (*S*) and doubles (*D*) count rates:

$$S = m_{eff}^{240} F \varepsilon M \nu_{s1} (1 + \alpha) \quad [3]$$

$$D = m_{eff}^{240} \frac{F \varepsilon^2 f_d M^2}{2} \left[\nu_{s2} + \left(\frac{M - 1}{\nu_{i1} - 1} \right) \nu_{s1} (1 + \alpha) \nu_{i2} \right] \quad [4]$$

where m_{eff}^{240} is the mass in terms of ^{240}Pu$_{eff}$ given by Eq. (1), *F* is the spontaneous fission rate of ^{240}Pu of 473 fission/s-g, ε is the neutron detection efficiency, *M* is the neutron leakage multiplication, α is the (α,n) to spontaneous fission neutron ratio, f_d is the doubles gate fraction, $\nu_{s1,s2}$ are the first and second reduced moments of the spontaneous fission neutron distribution, and $\nu_{i1,i2}$ are the first and second reduced moments of the induced fission neutron distribution. Typically, we measure *S* and *D* for the sample, measure □ using a point ^{252}Cf calibration source, determine □ for known isotopes for the sample, set f_d based on the detector settings (the optimum value for which is usually calculated using Monte Carlo techniques for a particular detector configuration), and $\nu_{s1,s2}$ and $\nu_{i1,i2}$ are known from nuclear data. We can then solve for the mass (m_{eff}^{240}) and the sample multiplication (*M*) using the two equations of the point model. This process requires significant knowledge of the sample to determine □. This knowledge may not exist a priori or may need to be acquired from a declaration. In either case, the results could be suspect.

The point model has several assumptions. It assumes that all induced fission neutrons are emitted simultaneously with the original spontaneous fission or (α,n) reaction. Since the time scale on these types of reactions is extremely short relative to the neutron die-away time, this is an acceptable assumption. The neutron point model does not account for reflected neutrons that reenter the sample and induce fission. The detector efficiency is assumed to be uniform over the entire volume of the sample. (This is where the name "point model" was derived because it assumes that all neutrons are born from a single point within the sample.) It assumes that (α,n) neutrons and spontaneous fission neutrons have the same energy spectrum. For most neutron sources this assumption is not valid, but for plutonium oxide (PuO_2) the (α,n) and spontaneous fission neutrons have comparable energies with different spectrum shapes. This allows the values for F, $\nu_{s1,s2}$, $\nu_{i1,i2}$ and ε to be the same for both types of equations.

There are a number of other assumptions made such as the amount of neutron capture without fission is negligible, that the distributions of neutron multiplicity and neutron energy are not correlated, and that the neutron die-away time in the sample/detector combination is well approximated by a single exponential time constant. With small detectors and samples, these assumptions will be valid.

1.3.3 PORTABLE NEUTRON COINCIDENCE COUNTER

Since many models manufactured today are not as portable as desired, there have been many research projects to increase the portability of a neutron coincidence counter without loss of the many advance features available in other models. One detector

recently developed was the Portable Neutron Coincidence Counter (PNCC) by H. Menlove, A. Thornton, and W. Charlton[2-3]. The PNCC is considered extremely portable compared to other models available. The purpose for the development of the PNCC was to aid the International Atomic Energy Agency (IAEA) with measurements of nuclear material. This detector system was chosen incorporated in this research.

The PNCC consists of multiple slabs of polyethylene with ^{3}He tubes embedded in them. Each slab consists of four ^{3}He tubes which extend the full length of the polyethylene and are connected via a junction box on top of the slab (Figure 7). It can be operated in more than one arrangement. The preferred arrangement is have four slabs arranged as a collar (Figure 8). The PNCC was shown to have excellent capability in measuring samples with masses ranging from 100-400 g. The PNCC had a detector efficiency of 8.9% when arranged as shown in Figure 8.

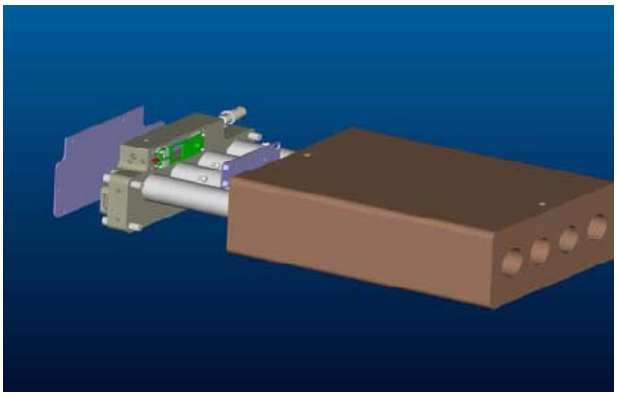

Figure 7. PNCC slab illustration (from Ref 2).

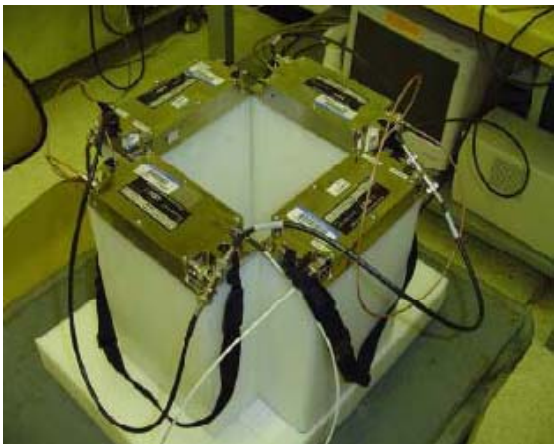

Figure 8. PNCC four slab setup (from Ref 2).

1.4 GAMMA-RAY DETECTION

When an isotope of Pu decays via alpha decay, the resulting gamma rays are unique to the parent isotope. Using a gamma spectroscopy system, one can identify which isotope(s) are present in the source material. An example of a generic spectrum can be seen in Figure 9. Each different letter in Figure 9 represents an area that is common to most spectra: A is the photopeak (or full-energy peak), B is the Compton continuum and is a byproduct of Compton scattering reactions, C is the Compton edge and corresponds to the maximum energy that can be transferred in a single Compton event, D is the Compton valley and is caused by multiple Compton events, E is the backscatter peak and is caused by gamma rays from the source that interact by Compton scattering in the materials that are surrounding the source such as a shield, F is the excess region and is produced by high energy background gammas such as cosmic rays, and G is the low energy rise and is caused by electronic noise. The photopeak is usually the main area of

interest since its area can be directly related to the number of photons of that energy entering the detector. There are two additional features that are not shown on that spectrum in Figure 9. If the gamma ray has sufficient energy to undergo pair production there will be a single escape peak at 511 keV below the original photon energy escape peak at 1.022 MeV below the original photon energy. There may also be a peak at 511 keV as a byproduct from the annihilation photons.

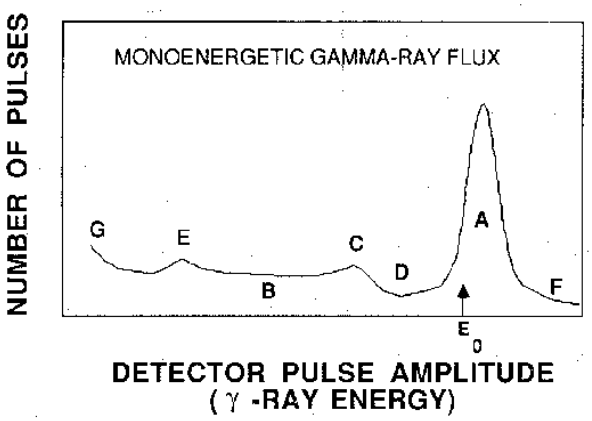

Figure 9. Generic gamma spectrum (from Ref. 11).

1.4.1 SOLID-STATE DETECTORS

When it comes to gamma spectroscopy, two main detector systems are commonly used today: solid state and scintillator detectors. Each has advantages and disadvantages and careful consideration must be taken to decide which is best for a certain application. Solid state detectors, and specifically high purity germanium (HPGe), have the highest resolution available on the market today. If that is the only consideration of importance, then HPGe detectors are the right choice. Outside of the energy resolution advantage, there are many drawbacks to HPGe detector systems. One of the disadvantages to the

HPGe detectors is that it must be kept at liquid nitrogen (LN) temperatures in order to work properly. This means that independent of the environment of operation, cooling must be provided. In most situations, this is solved with the use of a dewar that stores the LN for several days. If portability is a major concern, there are several options available. This includes a smaller dewar system that will last for 1-3 days. Mechanical cooling, which provides complete independence from LN, has been an attractive alternative in recent years. However, many of the mechanical systems have slight vibration issues that degrade the detector resolution. In the last few years, great strides have been made to reduce the vibration or to use another type of mechanism, such as wave technology, that has been incorporated in the Canberra Falcon 5000.

Another disadvantage to the HPGe is the geometry of the design. Not only are the crystal sizes limited, but the detector systems as a whole are difficult to maneuver. The crystal size will limit the efficiency that is available for a system.

1.4.2 SCINTILLATOR DETECTORS

On the other hand, scintillator systems can be extremely portable. Overall, there are several different types of scintillators. For gamma spectroscopy, sodium iodide (NaI) is the most common. This system has much higher efficiency than HPGe due to larger crystal sizes available and higher density. They also are able to operate at room temperature. However, NaI has a much lower resolution than HPGe. A comparison of HPGe and NaI resolution can be seen in Figure 10.

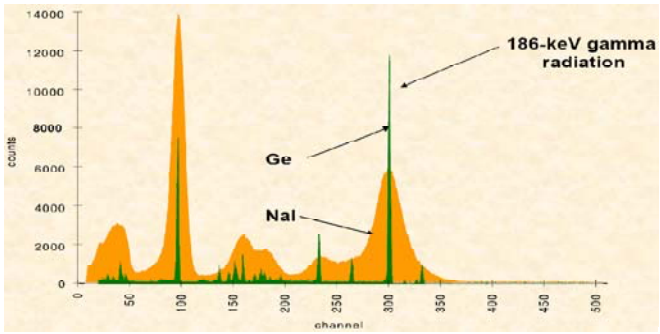

Figure 10. HPGe and NaI spectrum comparison

In recent years, there has been tremendous research to increase the portability and resolution of scintillator detector systems. One area has been to use other inorganic scintillator materials that produce better resolution than NaI. Lanthanum Bromide ($LaBr_3$) has been one of these materials. It has one of the highest light outputs of all the scintillators and will be discussed in more detail in a later section.

1.5 MCNPX

MCNPX is the Monte Carlo Neutral Particle transport code and is an enhanced version of MCNP developed by Los Alamos National Laboratory (LANL). This code has the ability to simulate both neutron and gamma interactions separately. It can be used to simulate measured gamma-ray spectra and coincidence counting data (both using the F8 tally). For all of the design work performed here, MCNPX was used to simulate the output of the detector designs and to predict detector signals.

CHAPTER II

$LaBr_3$ DETECTION SYSTEM

Since the gamma spectroscopy system included in the system design is not commercially available, simulations were performed to estimate the response of this detector to nuclear material using MCNPX. To help validate the MCNPX simulations for $LaBr_3$, MCNPX simulations were also performed for a commercially available $LaBr_3$ probe and compared to experimental results. $LaBr_3$ was chosen as the scintillator material for this design due to its superior energy resolution compared to NaI. However, $LaBr_3$ has several disadvantages compared to NaI as well. The $LaBr_3$ crystal size is currently limited (though this is becoming less of an issue as the research in this area continues). Also, the price for $LaBr_3$ is considerably higher than that of NaI. However, it is being considered a widespread replacement for NaI and prices may decrease in the future.

One research area that may lead to an elimination of the size constraints for $LaBr_3$ crystals involves the use of nano-size crystals within a matrix. This will provide greater choice in geometry than the standard probe. Some of this research is ongoing at LANL[6-9]. This use of nanocrystals will be discussed in more detail in Chapter III.

2.1 CANBERRA INSPECTOR 1000™

The Canberra Inspector 1000™ Digital Hand-Held Multichannel Analyzer with the IPROL-1 Intelligent Probe with Sourceless Stabilization (Figure 11) was chosen as the benchmark system. The Inspection 1000™ can be used for a variety of different

purposes. It is extremely portable compared to other systems currently available.[13] The detector dimensions are 19.0 cm x 16.5 cm x 6.4 cm with a weight of less than 2.4 kg.

Figure 11. Inspector 1000^{TM} System

The Inspector 1000 includes software that is in principle a portable version of the Canberra Genie 2000 Gamma Spectroscopy software[14] that is also commercially available. The MCA consists of 512 channels with an energy range of 30 keV to 3 MeV with the LaBr detector. The input has a maximum count rate of 500,000 cps when not limited by the detection probe. Its environmental limitations are -10 to +50 ^{o}C and a humidity of up to 80%.

2.2 IPROL-1 $LaBr_3$ DETECTION PROBE

One of the more advanced gamma spectroscopy methods available with the aforementioned system is the IPROL-1 Detector Probe (see Figure 12). This probe contains a 1.5 in x 1.5 in $LaBr_3$ scintillation crystal. This probe is considered advanced

because of its increased resolution compared to NaI. The increased resolution of $LaBr_3$ compared to NaI lends to better peak identification.

Figure 12. IPROL-1 $LaBr_3$ Detector Probe

The IPROL-1 probe was modeled in MCNPX to benchmark the ability to simulate the spectrum produced by the detector. The probe houses a 3.81-cm radius by 3.81-cm length crystal within an aluminum housing. The exterior of the can is made of a 3.035 cm aluminum cylinder that is 1.25 mm thick. There is a gap between the exterior cylinder and the crystal. There is a thin aluminum shell that surrounds the crystal at the center of the exterior shell. The crystal is coupled to the PMT tube at the top of the crystal. The PMT is 16 cm and is coupled to an electronics section that is 4.49 cm long. The entire probe is encased in an aluminum shell that is 1.25 mm thick. The density for the $LaBr_3$ is 5.1 g/cc, and the density of the aluminum is 2.7 g/cc. The PMT had an assumed density of 0.6 g/cc as a mixture of air and glass. The electronics section has an assumed density of 2.0 g/cc as a mixture of aluminum, silicon, and air. A visualization, of the MCNPX input deck can be seen in Figure 13.

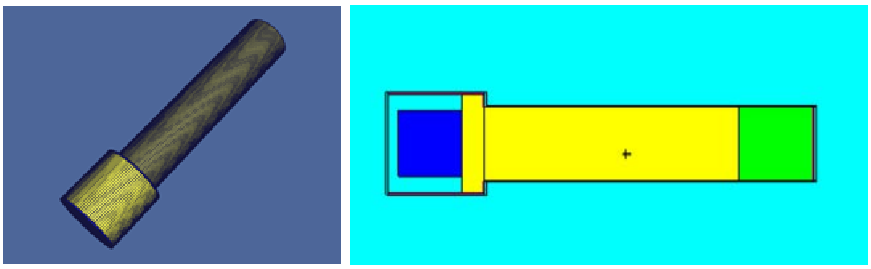

(A) (B)

Figure 13. MCNP model of IPROL-1 probe (A) 3D and (B) cross-section using VISED.

2.3 MEASUREMENTS USING IPROL-1

2.3.1 BACKGROUND MEASUREMENTS

An example of a $LaBr_3$ background spectrum can be seen in Figure 14. The spectrum was taken for 1800 sec in an interior room in a building with no windows. The majority of these counts are due to the natural radioactivity of La[15]. Lanthanum is made of 99.908% ^{139}La and 0.0902% ^{138}La. ^{138}La is radioactive and decays via two modes. One method is electron capture that produces an X-ray and a 1.435 MeV gamma ray with a yield of 66.40%. The peak caused by the reaction is shown in red.

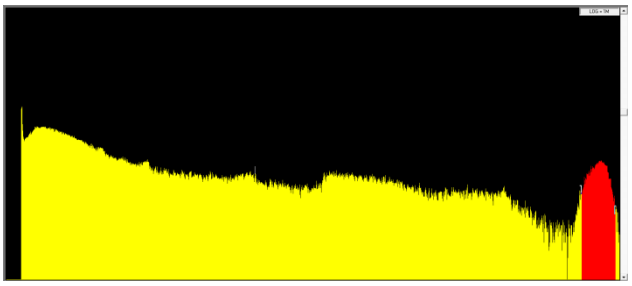

Figure 14. $LaBr_3$ background spectrum

The other mode is via beta decay. This mode produces a 788 keV gamma, a β^- particle, and a neutrino. This mode occurs 33.60% of the time. The β particle emitted with an energy spectrum ranging from zero to 253 keV. Decay information for the $LaBr_3$ in the detector is given in Table 3. This is peak is not highlighted in the figure since it was assumed to be covered by background at the time of measurement.

Table 3. $LaBr_3$ Decay Information

Molecular Mass of LaBr3	3.786E+02	g/mol
Crystal Volume	4.344E+01	cc
Crystal Mass	2.215E+02	g
La Mass	8.127E+01	g
La-138 Mass	7.000E-02	g
La-139 Mass	8.120E+01	g
Fraction of La in LaBr3	3.700E-01	
Specific Activity of La-138	9.142E+02	Bq/g
Activity of Crystal	6.702E+01	Bq
Decay Rate via 788 keV Branch	2.305E+01	Bq
Decay Rate via 1435 keV Branch	4.397E+01	Bq
Time	1.800E+03	sec
Number of 788 keV gammas born	4.150E+04	Bq
Number of 1435 keV gammas born	7.914E+04	Bq
Number of 253 keV Betas ONLY	4.150E+04	Bq

It was not determined until later when the simulations were ran why the 700 keV regions was oddly shaped. This was caused by the second mode of decay by the Lanthanum. Since it is beta decay the beta energy was being absorbed within crystal at 100% efficiency. The caused the peak from the resulting gamma to be broadened from 700-1000 keV.

2.3.2 CS-137 AND CO-60 POINT SOURCES

Both of these measurements were taken separately with the probe positioned horizontally within a lead shield surrounding both the source and the probe. The source was positioned 3 cm from the detector along the axis. The counts were performed for 3600 seconds with a maximum energy range of 1.5 MeV, with the results seen in Figure 15.

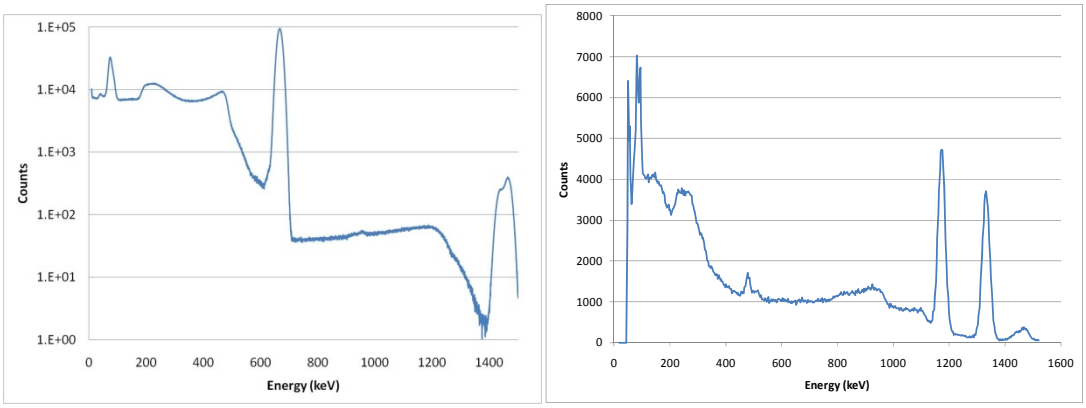

(A) (B)

Figure 15. (A) ^{137}Cs and (B) ^{60}Co Spectrums from IPROL-1 Probe

2.3.3 PLUTONIUM OXIDE MEASUREMENTS

The samples used in the PNCC measurements were unavailable, but a small Pu sample was able to be measured from ORNL and the associated data. The set up for the experiment can be seen in Figure 16.

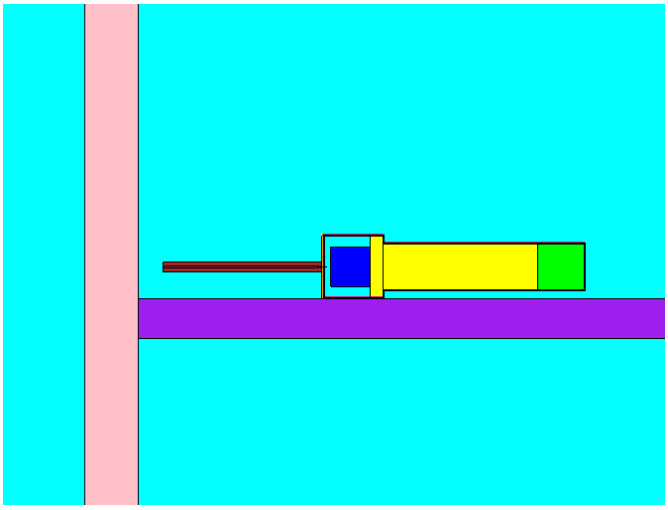

Figure 16. PuO_2 measurement setup

The exact detail of the interior of the sample was not able to be obtained, but some reasonable assumptions were made. The sample was embedded within a plastic tube that stretched 15.24 cm with a radius of 0.5 cm and a density of 1.050 g/cc. The sample was completely surrounded by plastic at the bottom of the tube. The sample was small enough that it could be modeled as a point source that was placed in a Pu sphere with a radius of only .05 cm. This allows for virtually no shielding by the Pu sphere from the point source. The interior of the tube was filled with air with a density of 0.001293 g/cc. This same air also filled the entire space around the setup. The purple region represents

the countertop that it was placed on. The countertop was an epoxy with a density of 1.250 g/cc and measures 91.44x3.81x91.44 cm in volume. The gray area is a concrete wall that the sample was right next to. It was 5.08x91.44x91.44 cm with a density of 2.300 g/cc.

This was an extremely small sample, but the gamma signature of PuO_2 is strong enough to still be able to distinguish some of the different peaks (see Figure 17). The isotopics of the sample used can be seen in the Table below.

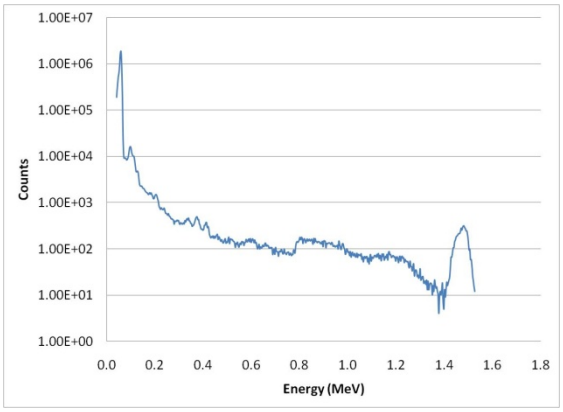

Figure 17. Pu spectrum from IPROL-1 Detector Probe

Table 4. Pu sample isotopics

Isotope	Mass (mg)	Mass %
Pu-238	7.00E-04	2.37E-04
Pu-239	2.42E+00	8.18E-01
Pu-240	1.72E-01	5.81E-02
Pu-241	4.00E-03	1.35E-03
Pu-242	1.03E-02	3.49E-03
Pu Total	2.60E+00	8.81E-01
O	3.49E-01	1.18E-01
Am-241	3.36E-03	1.14E-03
Totals	2.95E+00	1.00E+00

2.4 MCNPX SIMULATIONS OF IPROL-1 MEASUREMENTS

2.4.1 BACKGROUND

MCNPX does not have the ability to model coincident particles directly. Thus to properly model the background spectrum we must generate separate input decks for each different decay process that takes place. Since the 1.435 MeV mode of decay is electron capture, and therefore will produce several low energy x-rays that will not escape the crystal, we will simply simulate a single photon source with energies 1.4617 MeV (46.13%), 1.471 MeV (10.13%), and 1.439 MeV (9.37%). This source was added to an MCNPX deck for the IPROL-1 probe executed with 1E7 particles. The resulting spectrum will have the peak in the correct location, but the magnitude of the peak will be low. This is due to a remnant of MCNPX treats an F8 tally.

When MCNPX runs an F8 pulse height, it determines the energy deposition by taking the energy of the particle as it enters the tally cell and the energy leaving and

determining the difference. This value is recorded as a pulse within that cell. Since the source cell and the tally cell are the same, MCNP does not tally the pulses correctly. To accommodate for the deficiency, a correction factor of 4.8 was used for the entire background spectrum (i.e. the counts in each bin due to background only was multiplied by a sealing factor of 4.8).

The 788 keV gammas will be simulated directly within MCNPX, however the beta decay energy that is deposited in coincidence with the gamma must be included in an external routine. The beta has an extremely short mean free path in $LaBr_3$ and its entire energy will be absorbed in the crystal. The 788 keV gamma ray has a mean free path that is much greater than the beta and has a chance to escape the detector or could undergo Compton scattering. Thus, an MCNPX input deck was created for the IPROL-1 probe with just the 788 keV gamma ray as the source. The deck was executed with 1E7 particles. The resultant F8 tally spectrum was then broadened by adding the beta spectrum energy to the F8 tally data points. A more detailed discussion of this process can be seen in Appendix A.

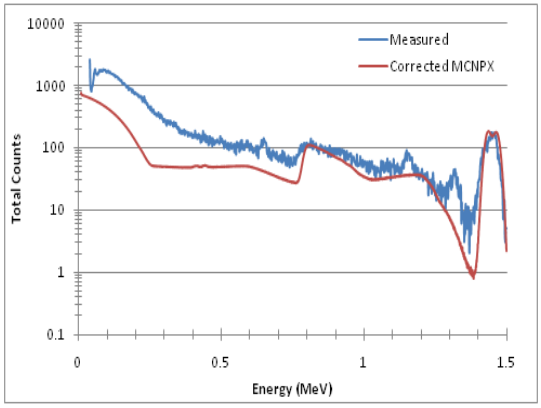

Figure 18. Measured vs. Corrected MCNPX simulation

In Figure 18 the corrected MCNPX spectrum can be seen in comparison to the measured. It can be seen that the higher energies match up very well in both peak placement and magnitude. The lower energy discrepancies were attributed to random background error. With the model now simulating the background correctly it was considered to accurate for the use of this experiment.

2.4.2 CS-137 AND CO-60 POINT SOURCES

The same setup was modeled within MCNPX as the previous measurement. For all the decks, 4000 energy bins were used ranging from 10 keV to 1.5 MeV with 0.373 keV per energy bin. The resulting spectra for the ^{137}Cs and ^{60}Co sources can be seen in Figure 17. The Gaussian Energy Broadening (GEB) function was used to account for peak broadening using measured Full Width at Half Maximums (FWHM) for the probe.

When the spectrums are compared, all the peaks match up well (see Figure 19). The background, however, did not. This was attributed to a possible alternate source contribution that was located in another area in the room from the measurement area. When trying to determine the source of the additional background it lead to the discovery of the β broadening that was discussed in the background model.

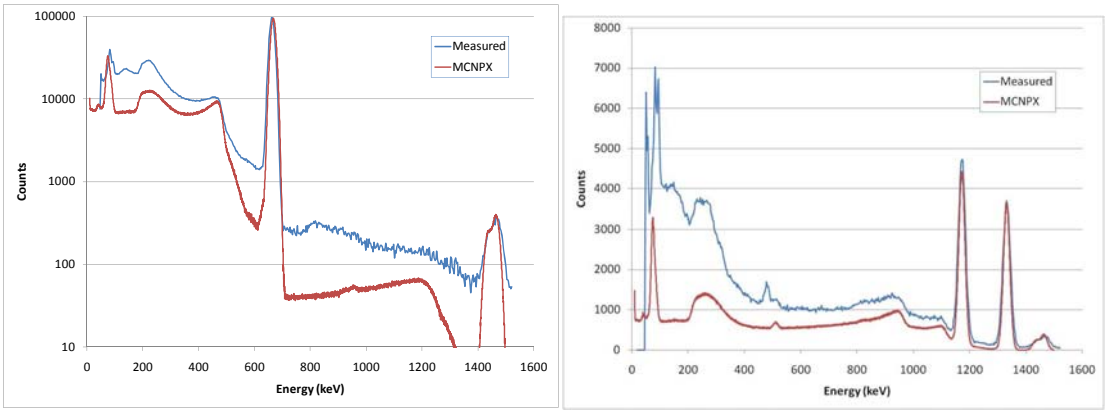

(A) (B)

Figure 19. Measured and MCNPX simulated spectra for the (A) Cs-137 and (B) Co-60

Since the background matched up well mention in the previous section and the peaks from these two sources were simulated accurately it was consider a good model for the interactions taking place within $LaBr_3$.

2.4.3 PLUTONIUM OXIDE

A Pu sample contains hundreds of gamma lines, but they vary greatly in yield. When all of the gamma lines are added, it increases the error in the pulse height tallies of MCNPX to almost unusable values. To account for this, only the useful gamma ray peaks were used with enough yield to correctly represent the spectrum[6]. It should be noted that no peaks were listed for ^{242}Pu in the reference material and therefore, not used in the code.

Table 5. Useful gamma rays in various energy regions

Region	Pu-238		Pu-239		Pu-240		Pu-241		Am-241	
(keV)	keV	γ/s-g	keV	γ/s-g	keV	γ/s-g	keV	γ/s-g	keV	γ/s-g
40-60	43.48	2.49E+08	51.63	6.19E+05	45.23	3.80E+06			59.54	4.54E+10
90-105	99.86	4.59E+07	98.78	2.80E+04	104.24	5.86E+05	103.68	3.86E+06	98.95	2.57E+07
									102.97	2.47E+07
120-450	152.68	6.05E+06	129.29	1.44E+05	160.28	3.38E+04	148.57	7.15E+06	125.29	5.16E+06
			203.54	1.28E+04			164.58	1.73E+06	335.4	6.28E+05
			345.01	1.28E+04			208	2.04E+07		
			375.04	3.60E+04			332.35	1.14E+06		
			413.71	3.43E+04			370.93	1.04E+05		
450-800	766.41	1.39E+05	645.97	3.42E+02	642.48	1.06E+03			662.42	4.61E+05
			717.72	6.29E+01					721.99	2.48E+05
Total		3.01E+08		8.87E+05		4.42E+06		3.44E+07		4.55E+10

There are still a number of peaks within the above table that would cause gross error in the output tallies when ran as a single deck. In order to minimize the error in the output, each isotope was ran individually and each spectrum was summed together to get a full spectrum. To determine the appropriate amount of counts per isotope, the total number of gammas from each isotope was multiplied by the mass of that isotope. This requires a total number of gammas/sec that can be directly multiplied by the output deck to create the spectrum. When the first spectrums were run, the 208 keV region was significantly below the measured value. Under closer inspection it was found that there is a peak from ^{241}Am that has enough yield to affect the peak. When this peak was added to the input deck, the problem was corrected. When all of the outputs were summed together, it yielded the Figure 20 below. Note that the La correction factor and broadening is only used for the La and not for another analysis.

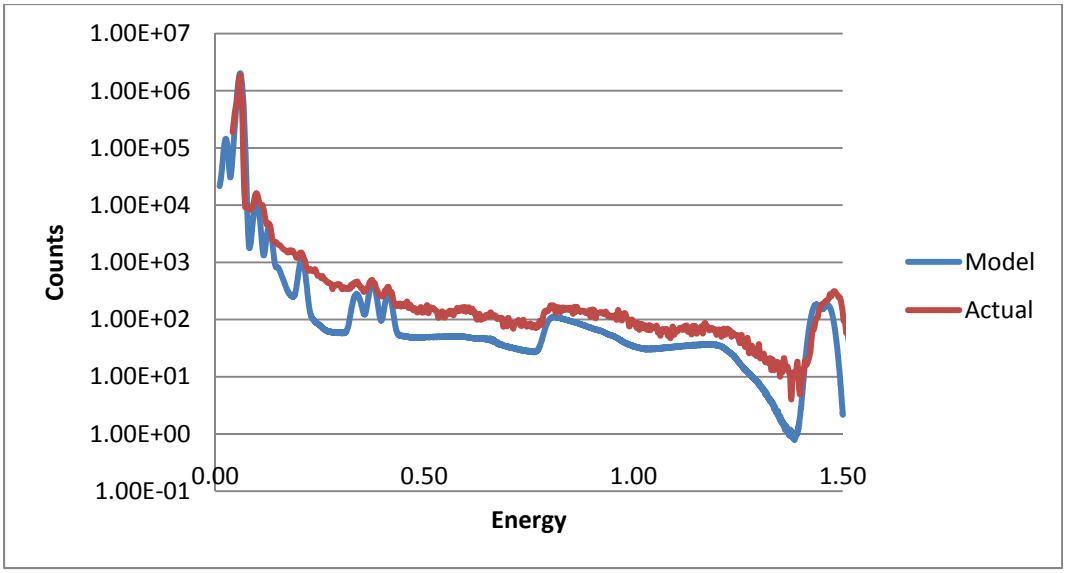

Figure 20. Plutonium comparison spectrum

There are some discrepancies that should be noted. First, a different detector system was used since it was at a different location. This is the cause of the La 1.435 MeV peak seeming slightly higher energy than the model. This was caused by a small variation in the calibration of the instrument. It also had a slightly higher background than normal, but was minimized as much as possible. The peak at ~330 keV is slightly lower than was expected, but the data on the peak yields was checked to ensure that the correct values were used. In all models the background produced was lower than the actual spectrum and was accredited to MCNPX not being able to account for natural background that can sometimes not be excluded from the spectrum. The use of a lead shield was brought up, but since this creates an x-ray in the same region as the 60 keV peak from ^{241}Am, it was excluded to ensure that the ^{241}Am was being simulated correctly.

With the above data it was concluded that the model was simulating $LaBr_3$ correctly and could be used to produce alternate detectors with the same information.

CHAPTER III

DETECTOR SYSTEM DESIGN OPTIMIZATION

3.1 DETECTOR DESIGN CONCEPT

The basic detector system concept developed here is shown in Figure 19. It consists of a slab detector with a gamma detector in front of a neutron detector. The gamma detector is composed of $LaBr_3$ nanocrystals suspended in an Oleic Acid matrix. The neutron detector consists of four ^3He tubes embedded in polyethylene. Figure 21 shows four slabs together in a collar configuration. This system was modeled in MCNPX. The system was optimized to minimize over system weight and maximize neutron and gamma efficiency.

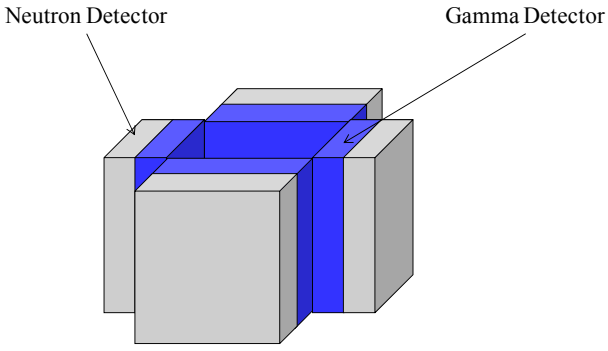

Figure 21. Four slab design

The gamma detector is based on a scintillator currently under development at LANL. This development includes the use of nanocomposite scintillators in an Oleic acid

matrix. This results in a gel-like matrix with up to 60% loading[6-9]. This type of material is known to maintain its transparency to around 1 cm in thickness. Since the research is still under development, for the purpose of this experiment the thickness was allowed to be increased under the assumption that the 1 cm will be overcome as the work continues. If this is not possible, then a segmented detector may need to be considered in the future. There were other matrix materials for the nanocrystals mentioned in the literature[6-9], but the Oleic acid matrix was chosen due to its high nanocrystals loading.

3.2 DETECTOR OPTIMIZATION SIMULATIONS

The neutron detector design was based off the design by Thornton et.al.[2-3] To simplify the combined system, it was desirable to leave the neutron detector design static and to modify the gamma slab thickness and nanocrystals loading. Since the peak gamma efficiency will occur with the maximum nanocrystal loading, the only variable perturbed in the optimization was the gamma slab thickness. The nanocrystal loading was set at 50% by volume in the Oleic acid matrix and the gamma slab thickness was altered from 1.0 cm to 3.81 cm.

We seek to minimize the detector weight while maximizing gamma detector efficiency and maximizing the neutron detector efficiency. The detector mass will be at its minimum with the thinnest slab. The gamma detector efficiency will be at its maximum with the thickest slab. It may not be intuitively obvious at what thickness the neutron efficiency will be at its maximum. The neutron detector from Thornton et al. is under moderated. Thus, it is expected that by adding the gamma slab between the detector and

the source, the neutron efficiency will increase due to increased neutron moderation. However, at some point, it is expected that the absorption of neutrons in the gamma slab will offset the efficiency gain from the increased moderation and the neutron efficiency will once again decrease.

The detector system was modeled as shown in Figure 19 using MCNPX. The gamma detectors had a length and height of 14.82 cm and 22.75 cm, respectively. The gamma detector width was varied from 1.0 cm to 3.81 cm. The gamma detector was composed of a 50% by volume loading of $LaBr_3$ nanocrystals in an Oleic acid ($C_{14}H_{34}O_2$) matrix. This mixture has a density of 3.00 g/cc and essentially consists of the nuclides shown in Table 5.

Table 6. Nuclide abundance by mass in scintillator detector material.

Nuclide	Composition (weight percent)
^{1}H	1.81%
^{12}C	11.40%
^{16}O	1.69%
^{138}La	0.03%
^{139}La	31.20%
^{79}Br	27.30%
^{81}Br	26.60%

A point source emitting monoenergetic photons of 662 keV was placed in the center region of the detector (i.e. at the detector midplane and equidistant from all four detector slabs). An F8 tally was used to calculate the pulse heights in the detector and the GEB function from Chap. 2 was used. The counts about the 662 keV photo peak were tallied to determine the total photopeak area. A plot of the simulated spectrum for a 1.0-cm

thick detector is shown in Figure 22. The MCNPX deck used for these simulations is shown in Appendix C. Each deck was executed using 1E9 particles. The detector efficiency was calculated as the ratio of the photo peak area to the number of source particles simulated.

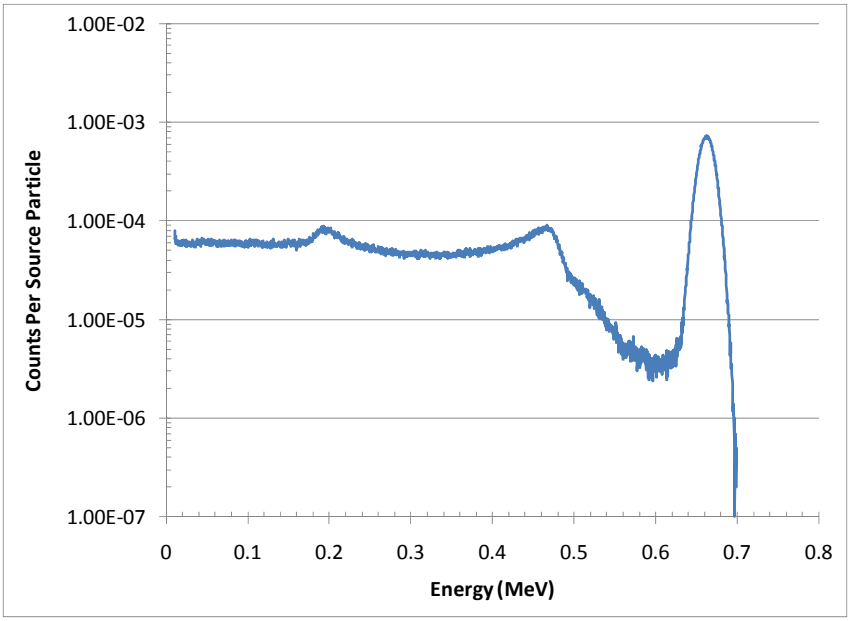

Figure 22. MCNPX simulated spectrum from point ^{137}Cs source.

The same MCNPX input decks were used to tally the neutron counts in the neutron detectors with the varying gamma slab thickness. Each deck was executed with 1E7 particles with a 195 g Pu source in the center of the detector system (i.e. at the detector midplane and equidistance from all detector slabs). The (n,p) interaction rate of the ^{3}He tubes was tallied using an F4 tally an FM4 multiplier card. Examples of the input decks for these simulations are shown in Appendix C.

A plot of the detector neutron and gamma efficiencies versus detector thickness is shown in Figure 23. As can be seen, the gamma efficiency increases significantly with increased slab thickness, but the neutron efficiency changes only slightly. Also, as expected, the peak gamma efficiency occurs when the detector slab is the thickest. The data used in this plot is also shown in Table 6.

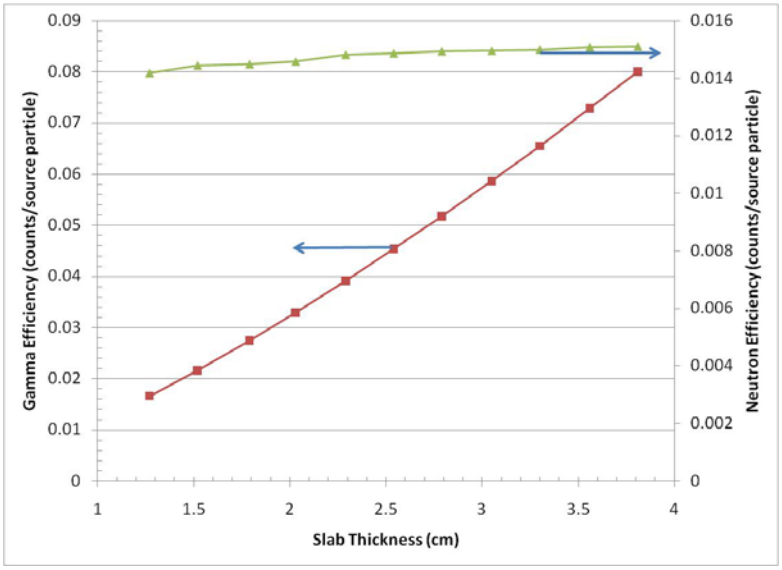

Figure 23. Simulated gamma and neutron detector efficiencies versus thickness of gamma detector slab

Table 7. Photon and neutron efficiencies versus thickness.

Thickness (cm)	Photon Efficiency (%)	Neutron Efficiency (%)
1.27	1.66	1.418
1.52	2.16	1.444
1.79	2.75	1.449
2.03	3.29	1.458
2.29	3.91	1.481
2.54	4.53	1.486
2.79	5.17	1.493
3.05	5.86	1.495
3.3	6.54	1.499
3.56	7.28	1.507
3.81	8.00	1.510

3.3 MULTI-VARIATE OPTIMIZATION FOR SLAB THICKNESS

Since the gamma efficiency and the slab mass are diametrically opposed, the optimum will occur at some point between the minimum and maximum slab thickness. To determine the optimum slab thickness, a multi-variate optimization was performed to minimize slab mass, maximize gamma efficiency, and maximize neutron efficiency. We performed this optimization by minimizing an objective function for the slab thickness. We will define our objective function as:

$$\Omega(t) = G(t)N(t)M(t) \qquad [5]$$

where *G(t)*, *N(t)*, and *M(t)* are utility functions for the gamma efficiency, neutron efficiency, and slab mass as a function of slab thickness (*t*), respectively. These utility functions relate the importance of the variable to the objective function.

We define the utility function for gamma efficiency as:

$$G(t) = 1 - A\left[\frac{\varepsilon_\gamma(t) - \varepsilon_\gamma^{min}}{\varepsilon_\gamma^{min}}\right] \quad [6]$$

where A is a constant defined such that the function $G(t)=1$ for $t=t_{min}$ and $G(t)\approx 0$ for $t=t_{max}$. For this set of data with t_{min}=1.27 cm and t_{max}=3.81 cm, A=0.25. It should be noted that $\varepsilon_\gamma^{min} = 1.664\%$.

We define the utility function for neutron efficiency as:

$$N(t) = 0.1\left\{1 - B\left[\frac{\varepsilon_n(t) - \varepsilon_n^{min}}{\varepsilon_n^{min}}\right]\right\} \quad [7]$$

where B is a constant defines such that $N(t)=0.1$ for $t=t_{min}$ and $N(t)\simeq 0$ for $t=t_{max}$. For this set of data, B=15.0. It should also be noted that $\varepsilon_n^{min} = 1.419\%$.

We define the utility function for mass as

$$M(t) = C\left[\frac{m(t) - m_{min}}{m_{min}}\right]^2 \quad [8]$$

where C is a constant defined such that $M(t)\simeq 0$ for t_{min} and M(t)=1 for t_{max}. The fact that the percent change in mass is varied to the second power is present to increase the importance of minimizing the slab mass. Decreasing this power would decrease the importance of slab mass and increasing this power would increase that importance.

A plot of the utility functions versus slab thickness is shown in Figure 24. Also a plot of the objective function versus slab thickness is shown in Figure 25. As can be seen from Figure 25, based on this objective function, the optimum slab thickness is 2.5 cm. For simplicity sake, this was rounded to 2.54 cm to result in a 1” thick slab.

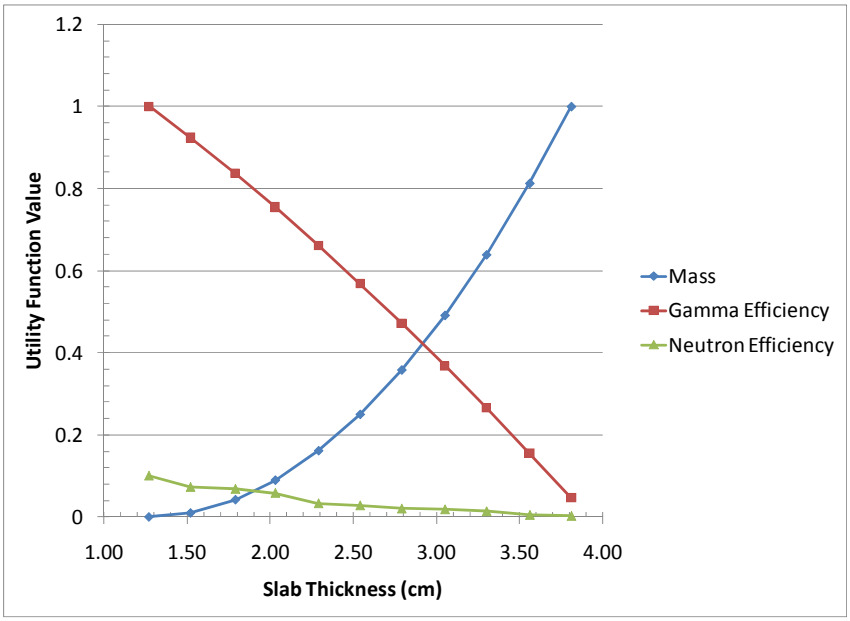

Figure 24. Utility functions for mass, γ efficiency, neutron efficiency vs. slab thickness

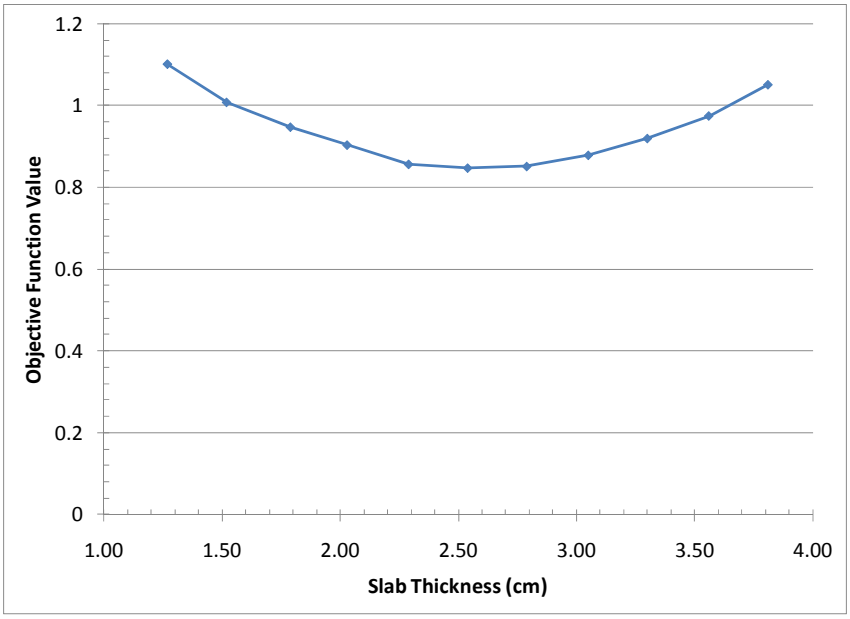

Figure 25. Objective function vs. slab thickness

3.4 *OPTIMIZED DETECTOR GEOMETERY*

The completed system was named the Portable Gamma-Neutron Counter (PGNC). The neutron potion of the system consisted of four HDPE slabs. Each slab has a density of 0.96 g/cc and dimensions of 7.62 cm x 17.78 cm x 22.86 cm. Each slab has four 2.8575 diameter holes bored out of the full length of the slab. In each hole is a ^{3}He tube that is 17.78 cm long by 1.19 cm in radius, with a ^{3}He density of 2.45E-5 g/cc. The tubes are manufactured out of 0.76 mm thick aluminum with a density of 2.7 g/cc. The area between the tube and the slabs are filled with air that has a density of 0.001239 g/cc as well as the inactive regions of the tubes. The top of each slab has an electronics portion that consists of iron with a lower than normal density of 2.0 g/cc. This lower density accounts for the air space between the electronic materials.

The gamma system consisted of four slabs that fit within the neutron system as shown in Figure 19. Each slab had dimensions of a 2.54 cm x 14.82 cm x 22.75 cm. Each slab consisted of 50% loaded by volume mixture of $LaBr_3$ and Oleic acid, with a density of 3.00 g/cc. Placed on top of the scintillator material is the PMT that consists of a glass and air mixture that has dimensions of 2.54 cm x 14.82 cm x 2.44 cm with a density of 0.6 g/cc. Both the scintillator material and the PMT are encased in aluminum that is 1 mm thick with a density of 2.7 g/cc. Both the gamma and neutron system sit atop a solid HPDE slab has dimensions of 46.02 cm x 34.32 cm x 5.08 cm.

The entire system visualized with VISED[16] is shown in Figures 26 and 27.

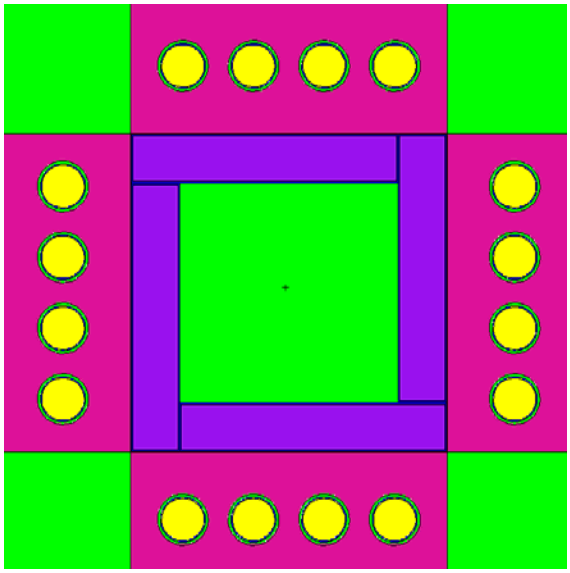

Figure 26. Over head view of PGNC

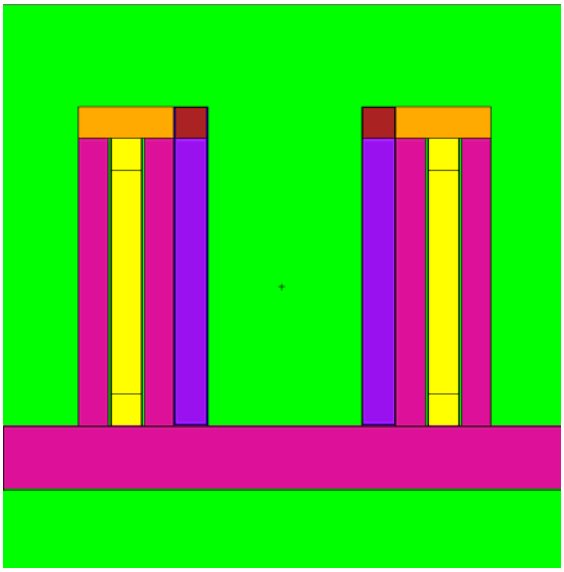

Figure 27. Cross section view of PGNC including ^{3}He tubes

In Figures 26 and 27, the different colors represent different materials. The pink material is the HDPE. The yellow is the ^{3}He active area. The area between the active area and the HDPE is green and represents air; and is also surrounding the entire system. On top of that is the electronics section in orange. The purple represents the $LaBr_3$/Oleic acid mixture with the PMT in maroon on top of that. Although difficult to see in these images, there is aluminum casing on the ^{3}He tubes, scintillator, and PMT.

CHAPTER IV

DATA ANALYSIS

To be able to compare the results of the simulations with the PNCC experiment the same source information was used. This includes the same masses, densities, heights, and radii. There were four different sources used in the PNCC experiment with an assumed density of 0.9 g/cc. This was based on the material being fabricated from left over production of feed fuel for the Fast Flux Test Facility in Richland, WA. This feed is composed of highly pure PuO_2 and UO_2, with a density range of 0.7-1.2 g/cc. Since 0.9 g/cc is in the middle of this range it was chosen. [2]

In this experiment the density will also have an influence on the gamma signature. If the Pu was in metallic form, the gammas detected would only be from the outer most shell of the sample. This is called infinite thickness, because the gammas in the interior will never be seen. However, since this is an oxide in powder form with a much lower density the affect will be less. The gamma signature is several orders of magnitude above the neutron, so the gamma signature will still be strong enough to measure.

This material is a powder, which in turn means that its density is hard to measure since it can vary depending on the settling. This can also affect the fill height of the sample which was shown to affect the count rate in the PNCC. The neutron multiplication and absorption, which can cause changes for the results, was not recalculated here since this was shown in detail for the PNCC experiment. Again, the fill height can have an effect

on the gamma signature as well, but since the fill height and density are directly correlated, it was thought to cause little change.

This experiment was not able to obtain the samples directly, but the data for the PNCC experiment was able to be obtained. The same values were used for this simulation to maintain consistency. The information for the four different samples used can be seen below.

Table 8. Sample dimension information

Sample ID	Mass	Density	Radius	Height
	(g)	(g/cc)	(cm)	(cm)
LAO-251	195	0.9	5.4356	2.33
LAO-252	365	0.9	5.4356	4.39
LAO-255	617	0.9	5.4356	7.38
LAO-255	436	0.9	5.4356	5.23

Table 9. Pu sample isotopic ratios

Sample ID	Pu Mass	Pu238	Pu239	Pu240	Pu241	Pu242	Am241	O16
	(g)	(w%)	(w%)	(w%)	(w%)	(w%)	(w%)	(w%)
LAO-251	195.00	0.05	72.91	14.52	0.41	0.31	0.85	11.8
LAO-252	365.00	0.05	73.04	14.41	0.4	0.31	0.82	11.8
LAO-255	617.00	0.05	73	14.44	0.4	0.3	0.82	11.8
LAO-256	436.00	0.05	73.05	14.43	0.4	0.3	0.8	11.8

Table 10. Pu sample mass data

Sample ID	Pu Mass	Pu238	Pu239	Pu240	Pu241	Pu242	Am241	O16
	(g)	(g)	(g)	(g)	(g)	(g)	(g)	(g)
LAO-251	195.00	0.0975	142.1745	28.314	0.7995	0.6045	1.6575	23.01
LAO-252	365.00	0.1825	266.596	52.5965	1.46	1.1315	2.993	43.07
LAO-255	617.00	0.3085	450.41	89.0948	2.468	1.851	5.0594	72.806
LAO-256	436.00	0.218	318.498	62.9148	1.744	1.308	3.488	51.448

4.1 GAMMA ANALYSIS

The first step was to perform a background analysis for the PGNC in the same manner as the probe that was discussed earlier. Each slab must detect the decay within it, as well as the gammas detected by the other slabs. The same procedure was used as before to determine the affect the beta particle had on the spectrum. Two separate F8 tallies we used to account for the decay in one slab, and the detection by the others. Once the counts were calculated for each tally they were both multiplied by four and summed together. This was done under the assumption that since the geometry is the same no matter what direction it is looked at, each slab would yield the same counts per slab. The information for the La in one slab, as well as the simulated background spectrum can be seen below in Table 11 and Figure 28.

Table 11. La decay information for one slab

Molecular Mass of LaBr3	378.62
Slab Volume	8.56E+02
Slab Mass	2.61E+02
LaBr3 Mass	2.22E+03
La Mass	8.14E+02
La-138 Mass	7.34E-01
La-139 Mass	8.13E+02
Fraction of La in LaBr3	0.366874
Specific Activity of La-138	914.2306
Activity of Slab	6.71E+02
Decay rate via 788 keV branch	2.25E+02
Decay rate via 1435 keV branch	4.46E+02
T	600
Number of 788 keV gammas born	1.00E+05
Number of 1435 keV gammas born	2.67E+05
Number of 253 keV Betas ONLY	1.00E+05

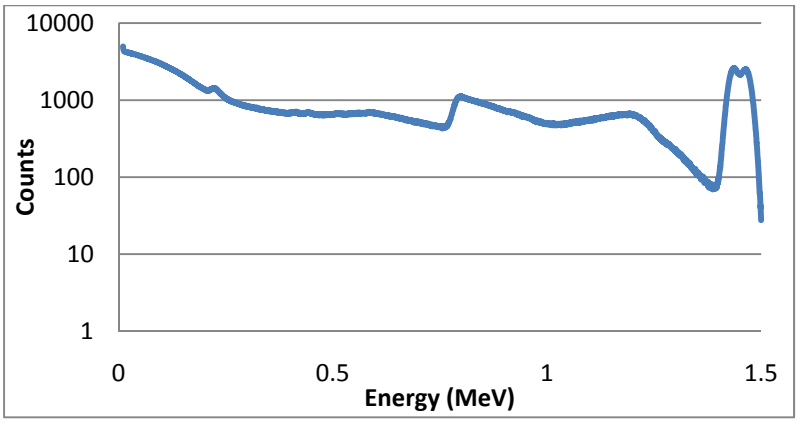

Figure 28. Total La background spectrum for PGNC

The gamma simulation was run separately from the neutron deck although the exact same geometry was used for each case. As was previously stated, there was a separate deck for each isotope to minimize the error in the photopeak. The yield for each isotope can be seen in the table below.

Table 12. Total yield for each isotope per sample

Sample ID	Pu238	Pu239	Pu240	Pu241	Am241		Total
	γ/s	γ/s	γ/s	γ/s	<60kev	>60 keV	γ/s
LAO-251	2.936E+07	1.262E+08	1.252E+08	2.749E+07	7.525E+10	9.597E+07	7.565E+10
LAO-252	5.495E+07	2.366E+08	2.325E+08	5.020E+07	1.359E+11	1.733E+08	1.366E+11
LAO-255	9.289E+07	3.997E+08	3.939E+08	8.486E+07	2.297E+11	2.929E+08	2.310E+11
LAO-256	6.564E+07	2.826E+08	2.781E+08	5.997E+07	1.584E+11	2.019E+08	1.592E+11

It should be noted that the ^{241}Am was split into two different decks. This was done since the 59.54 keV is several orders of magnitude higher than the rest of the peaks. This caused the error in the output deck to be too high for use in the higher energy peaks that have low yield. Each deck was run with 1E8 particles with 4000 energy bins between

0.010-1.5 MeV. The same GEB function was used with the IPROL-1 probe. Each output tally was then multiplied by the above value for each isotope. All the isotopes were summed together along with the La data and this created a simulation of a spectrum.

To get an idea of the contribution of each isotope, Figure 29 shows each isotope independently. Below the 200 keV region it is almost impossible to distinguish between the different contributing isotopes. This prevents any of the data in this region to be usable with a system with a resolution of $LaBr_3$ or lower.

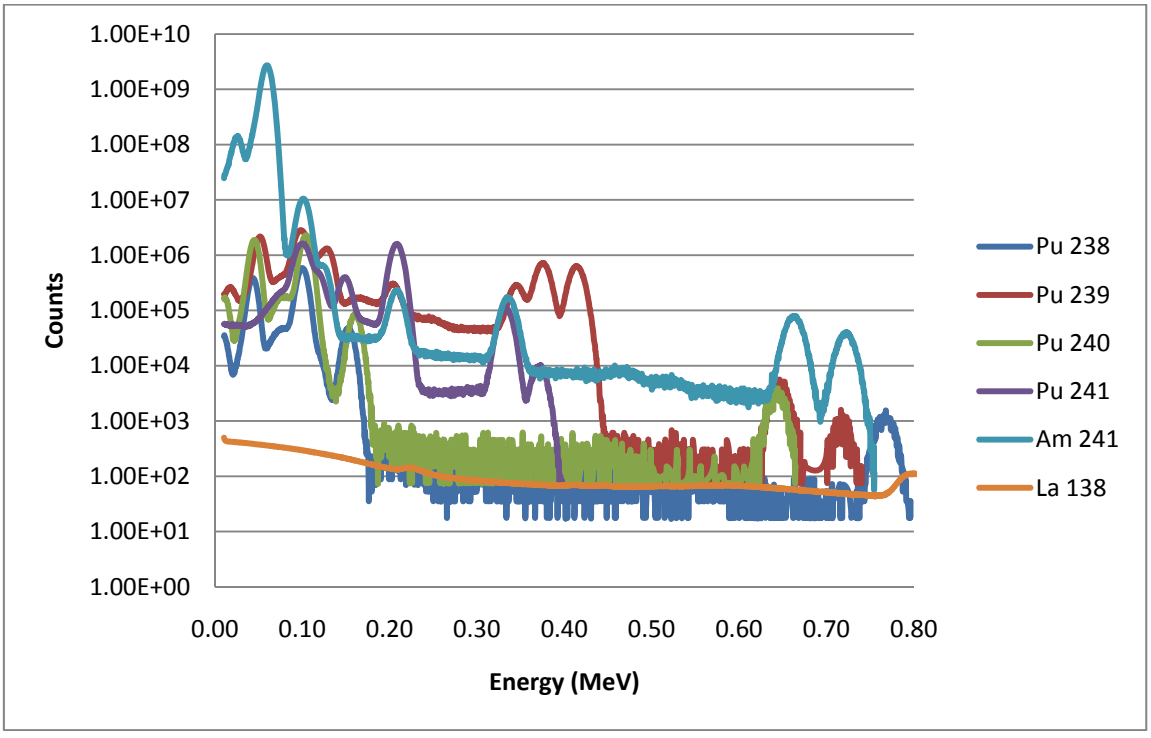

Figure 29. Separated gamma lines from MCNPX output for LAO-251

To get the total spectrum a sum each of the above peaks is needed, which is what MCNPX simulates. While useful, is not very realistic. Under normal circumstances the

spectrum would be analyzed in some type of software that is able to perform much of the necessary data on the spot. There are several types of software on the market but since Genie 2K® (Genie) was used with the IPROL-1 measurements and it was also chosen here.

In order to import the data from Excel into Genie, a special file needs to be created. To do this, open a notepad file that is empty and copy over the total counts per energy bin. This should be one single column that corresponds to only the counts. No other information is necessary. It should be noted that the counts must be rounded to the nearest whole number in the notepad file. Save the file with the extension .TKA. When in Genie open a file, but under file type choose PC-Toolkit. This TKA file should be visible in this format; open the file. The rest of the data that was associated in Excel, such as energy per bin, will be lost.

To reenter the energy calibration data, an energy calibration curve needs to be determined. Note that the equation is linear and is in MeV. It needs to be changed to keV by multiplying by 1000. This equation for the line should be entered in the energy coefficient box in the calibrate menu. The other value in the box is the FWHM data. The FWHM in the 660 keV region was known, and the following equation was solved to determine the coefficient. The 0.3724 keV value was used since it is the energy per bin

$$22.314\ keV = .3724\ keV + xE^{\frac{1}{2}} \qquad [9]$$

in the MCNPX deck. The resulting value for x from the equation is 0.854. Since the FWHM is energy dependent, and not count dependent, the same procedure was used for

each sample tested. This allowed for consistency in the results much like using an actual detector. It should be noted that these values differ from the one used for the IPROL-1 detector, but both yielded close to the same FWHM value. In Figure 30 the spectrum from sample LAO-251 can be seen in Genie. This plot is shown on log scale with the maximum value being 1E9 counts.

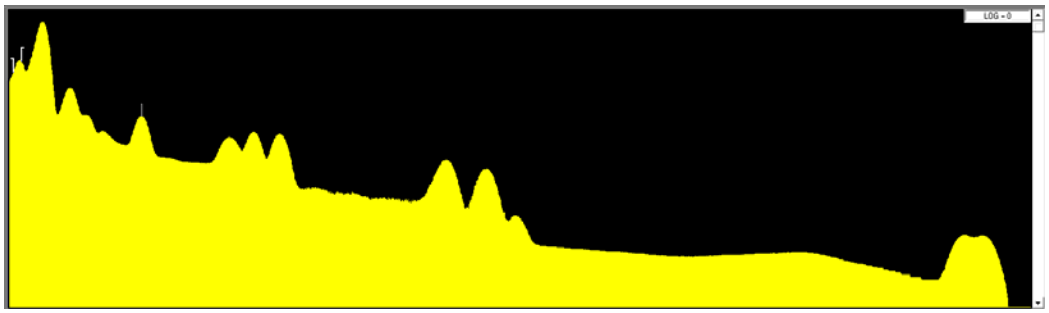

Figure 30. LAO-251 spectrum in Genie

To find the necessary peak, Genie has to ability to distinguish between the continuum and the peaks. To perform this, the analyze mode is used within Genie. The peak locate option will locate the peaks based on the significance threshold value. For this, a value of 100.00 was used to identify only the usable peaks. Lower values than this will place peaks in unnecessary locations. In future experiments this value can be changed to best identify the peaks. The tolerance was set to 1.00 FWHM value. When completed, it identifies 11 peaks in the spectrum. The next step is to use the peak area analysis to determine the counts within each individual peaks. This yields the same 11 peaks, with some of them interacting with each other. In Figure 31, it shows the same spectrum with the peaks located. The blue peaks indicate a multiple, meaning more than one peak is

included in the results. When the peak area is given in the report window it shows the peaks separately but notes them as a multiple region of interest or ROI.

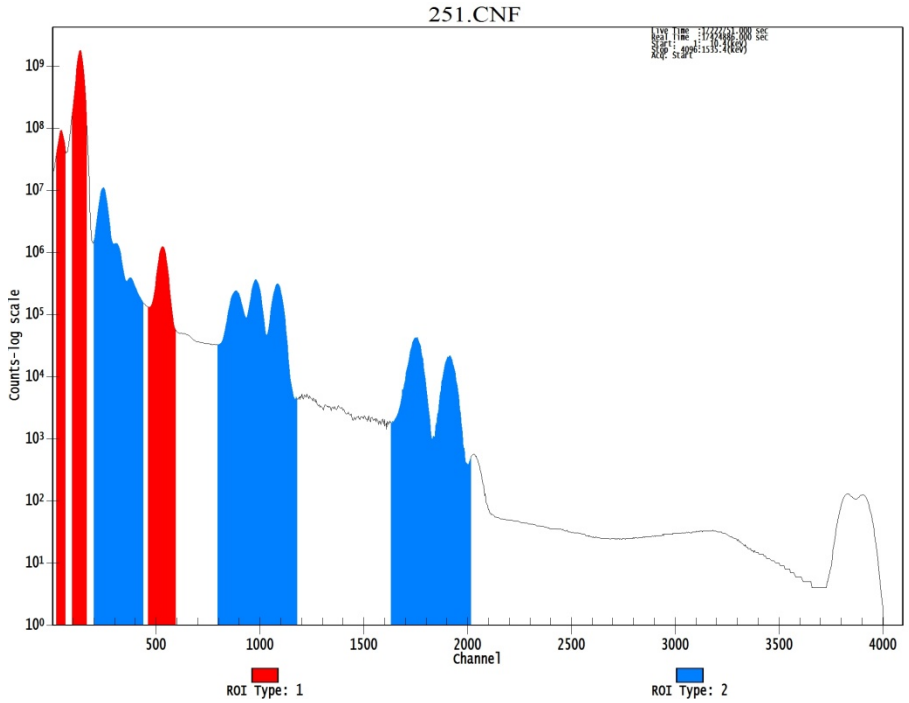

Figure 31. LAO-251 analyzed spectrum

The largest peak occurs at the 60 keV region, and is from ^{241}Am. Even though there are a tremendous number of counts from this gamma line, it was ignored because of the extremely low efficiency: < 1% for each sample.

With those peaks being ignored, it leaves the peaks between approximately 200 keV to 766 keV. When this is considered, there are 7 usable peaks. The peak in the 208 keV region is largely due to ^{241}Pu. The triple peak between the 345 keV and 415keV is

caused by ^{239}Pu and the double peak between 660 keV and 720 keV is mainly due to ^{241}Am, as well as a peak at 766 keV caused by ^{238}Pu.

When the data was analyzed, there was one peak from the usable data that the calculated efficiency was unreasonably high; this was in the 345 keV region. When a closer look was taken at the individual peaks, it was caused by more than one isotope contributing to the peak above the continuum. When a peak was chosen to use to quantify the material this peak was disregarded to minimize the error if there was a change in isotopic ratio, and was not included in the efficiency curve. The energy vs. efficiency plot can be seen in Figure 32 for sample LAO-251, LAO-252, and LAO-255. Equation 18 is used to calculate the peak efficiencies. The LAO-256 sample will be discussed in a later chapter.

$$Peak\ Efficiency = \frac{Cts_{Detected}}{Cts_{Total}} \quad [10]$$

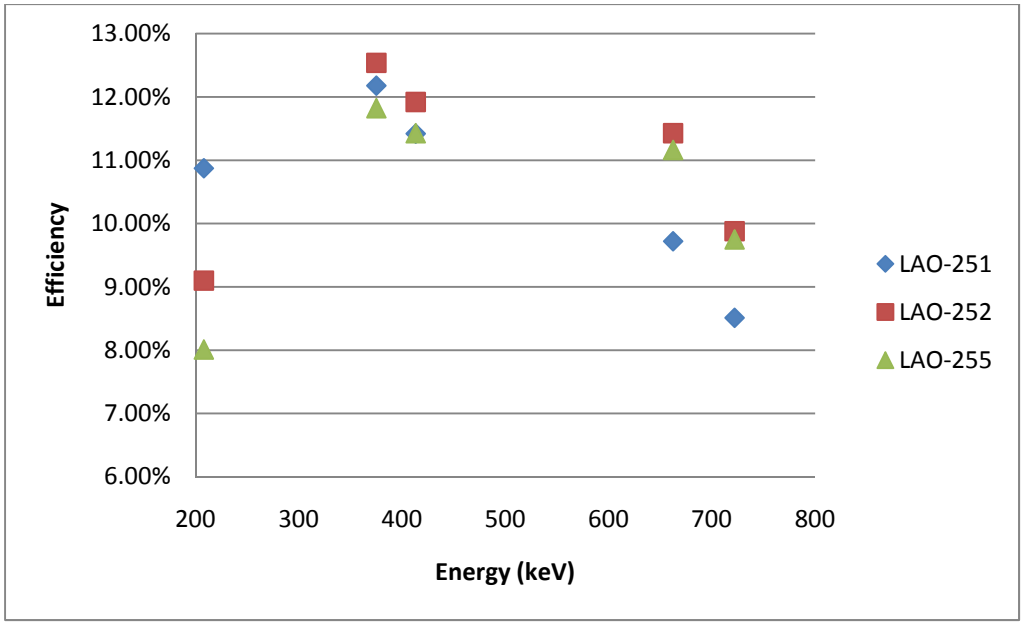

Figure 32. Energy vs. efficiency

4.2 NEUTRON ANALYSIS

The neutron analysis was done with the exact same geometry as the gamma with MCNPX operating in mode N. There was a deck written for each decay mode being SF or (α,n) for each sample. Each deck was run for 1E7 histories. Each SF deck with the source being identified as PAR=SF for the source definition. This allows the material within the source to produce SF neutrons and will only do so if the material in the material card is able to spontaneously fission. In order to simulate the coincidence capability, two F8 tallies were included in the deck. In each tally a CAP 2003 command was included, meaning the capture by ^{3}He. The first tally has no gate width or pre-delay information, and is an infinite gate that provides the singles efficiency. The second tally had a 64 μsec gate width and a 4.5 μsec pre-delay that provides the doubles efficiency.

Both tallies provide efficiency for the sum of all four slabs. There was also a F4 tally in the deck that is another value for the singles efficiency. These samples include the Multiplicity (M) that is seen with in the neutron point model. If these values are used to solve for those equations, M should be set to unity.

This will not produce (α,n) neutrons and a separate deck must be run with this type of source definition. This is included in the source specification and includes a distribution by including the energy of the α particle with a correlated yield for that energy. The information for this distribution was obtained from the PNCC experiment. The same tallies were used for the (α,n) deck, as were for the SF deck, and is also summed over all four slabs.

The singles efficiencies can be seen in Table 12 for SF, and Table 13 for (α,n). There is a slight variation between the SF and (α,n) efficiencies. This is caused by the higher energy of the (α,n) neutrons and the system having a lower efficiency for neutrons of that energy.

Table 13. Spontaneous fission singles efficiencies

	F4 Tally		F8 Tally	
Sample	**Efficiency**	**error**	**Efficiency**	**error**
LAO-251	8.33%	0.0083%	8.34%	0.0058%
LAO-252	8.75%	0.0087%	8.76%	0.0061%
LAO-255	9.35%	0.0084%	9.35%	0.0065%

Table 14. (α,n) singles efficiencies

	F4 Tally		F8 Tally	
Sample	**Efficiency**	**error**	**Efficiency**	**error**
LAO-251	7.53%	0.0083%	7.53%	0.0113%
LAO-252	7.90%	0.0087%	7.89%	0.0111%
LAO-255	8.39%	0.0092%	9.35%	0.0084%

When calculating the doubles efficiency, only the F8 tally produces this value, and is in Table 14. Since the (α,n) reaction only produces singles neutron, the efficiency should be near zero. Since the neutron can go on and induce fission, and there is a small chance that two reactions may take place within the gate width time, there will be some doubles detection. Also, since the detection rate is so low, it will cause the error to be large.

Table 15. Doubles efficiencies from F8 tally

	SF		Alpha,n	
Sample	Efficiency	error	Efficiency	error
LAO-251	0.45%	0.0016%	0.04%	0.0007%
LAO-252	0.51%	0.0017%	0.05%	0.0008%
LAO-255	0.60%	0.0019%	0.07%	0.0010%

In order to calculate the number of neutron counts the values for the simulations, a value for the total neutrons being born with in the sample had to be calculated, meaning the sum of the neutrons from all the isotopes. Equation 10 is the equation to determine the total counts per second where efficiency is the singles or doubles value, respectively. The value for the yield of each mode of decay can be seen in Table 15. These values were used with Table 13 to determine the total yield of the sample. Table 16 and 17 shows the count rate determined for both the singles and doubles count.

$$CPS = (\varepsilon_{SF} * Y_{SF}) + (\varepsilon_{\alpha,n} * Y_{\alpha,n}) \quad [11]$$

Table 16. Neutron yield values

Isotope	SF yield (n/s-g)	(a,n) Yield (n/s-g)
Pu238	2.59E+03	1.34E+04
Pu239	2.18E-02	3.81E+01
Pu240	1.02E+03	1.41E+02
Pu241	5.00E-02	1.30E+00
Pu242	1.72E+03	2.00E+00
Am241	1.18E+00	2.69E+03

Table 17. Singles count rate

		F4 Tally		F8 Tally	
Sample	Pu240eff (g)	Cts/sec	error	Cts/sec	error
LAO-251	29.6	3656	4	3659	3
LAO-252	55.0	7122	8	7130	6
LAO-255	93.0	12845	14	12857	11

Table 18. Doubles count rate

Sample	Pu240eff (g)	Cts/sec	error
LAO-251	29.6	142	1
LAO-252	55.0	307	1
LAO-255	93.0	606	2

From this data it can be seen that even with the gamma detector slab on the interior of the neutron tubes, it still has good efficiencies as a singles and doubles neutron counter. Therefore it still could be used as a neutron coincidence counter in the field.

CHAPTER V

MASS DETERMINATION

With all the information that was provided, the fourth sample was simulated as an unknown value. This was done to determine if an approximate mass could be determined from the simulation results of the fourth and the previous three samples. As stated previously, this usually requires other simulations to be run in order to solve for all the unknowns of the sample and detector.

An efficiency curve was created for each peak that was able to be resolved from the simulated spectrum. Only peaks where the main contributor was one isotope were used. For instance, while there is a distinctive peak in the 100 keV region, it is caused by a multitude of isotopes. The Genie software is able to fit the peaks with multiple isotopic contributions some of the time, and if this was possible, the peak was used. However, when there are several isotopes contributing, this is not able to be done since the resulting error will be too high for use. Six peaks were resolved and were able to be used to create efficiency curves. They can be seen in the table below.

Table 19. Gamma detection efficiencies

Isotope	Energy	Efficiency		
	(keV)	LAO-251	LAO-252	LAO-255
Pu-241	208.00	10.87%	9.10%	8.01%
Pu-239	375.04	12.18%	12.54%	11.82%
Pu-239	413.17	11.42%	11.92%	11.43%
Am-241	662.42	9.72%	11.43%	11.16%
Am-241	721.99	8.51%	9.88%	9.75%
Pu-238	766.41	7.49%	8.31%	7.86%

With these six peaks, efficiency curves for four different isotopes were created. ^{239}Pu and ^{241}Am had two separate peaks and this allowed a comparison of the different peaks to ensure that their variation was consistent across the energy ranges. All four plots for each isotope can be seen in the figures below. Each figure is plotted to show the total counts per second (cps) versus mass of the isotope in the sample. There is error associated with these values, but is small and unable to be seen on Figures 33-36.

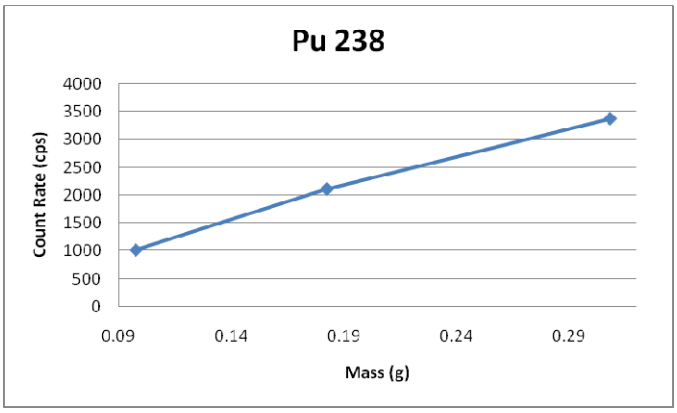

Figure 33. Count rate vs. Pu-238 mass

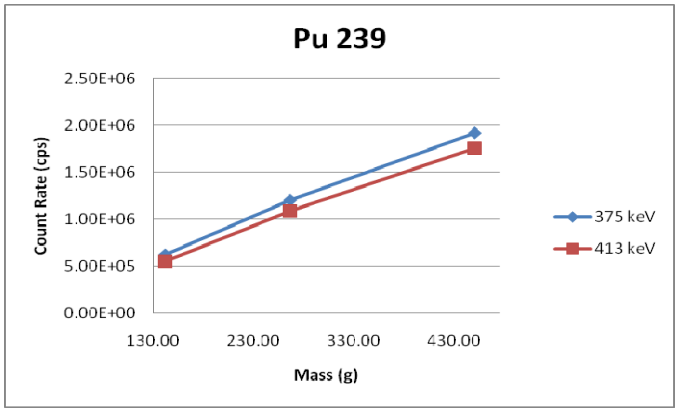

Figure 34. Count rate vs. Pu-239 mass

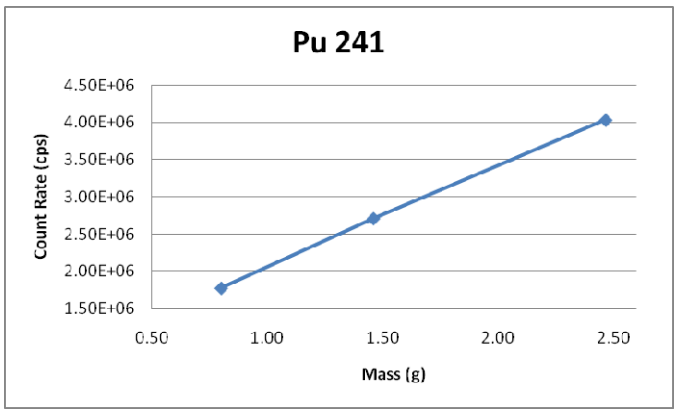

Figure 35. Count rate vs. Pu-241 mass

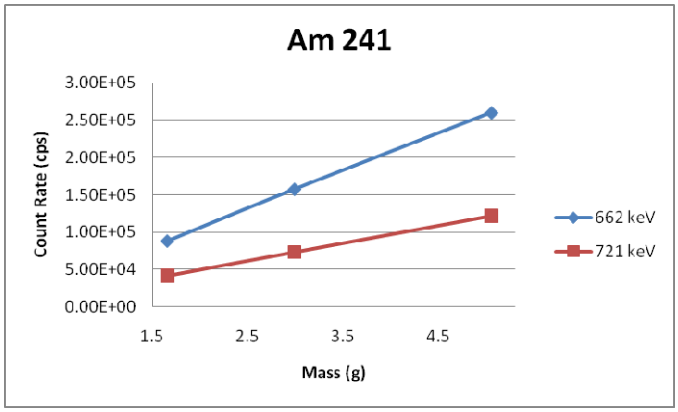

Figure 36. Count rate vs. Am-241 mass

Each plot was used to form a linear relationship and an equation was ascertained from this data. It should be noted that only the raw count data and the given information about the samples was used, meaning no outside information about the sample or the detector was used. For Pu-239 and Am-241, the equation with the R^2 value closest to one was used in the calculation. The equations for each isotope are given by:

$$CPS = 1.10 \times 10^4 M^{Pu238} - 7.900 \times 10^0 \quad [12]$$

$$CPS = 3.894 \times 10^3 M^{Pu239} + 1.913 \times 10^4 \quad [13]$$

$$CPS = 1.351 \times 10^6 M^{Pu241} + 7.098 \times 10^5 \quad [14]$$

$$CPS = 2.380 \times 10^4 M^{Am241} + 1.962 \times 10^3 \quad [15]$$

From this, it can be seen that the primary gamma producing isotopes are odd numbered. This makes sense since the even isotopes spontaneously fission much more frequently than the odd. This allows the neutron signature from the even isotopes to determine

additional information about them. For the neutron, signature individual isotopes are not able to be seen and the previously discussed $^{240}Pu_{eff}$ value must be used and can be seen in Equation 2. The ^{238}Pu value can be determined from the gamma signature leaving ^{240}Pu and ^{242}Pu. The ^{242}Pu value can be assumed as zero since it is always extremely small compared to ^{240}Pu and is produced by neutron absorption. This allows the equations to be solved for ^{240}Pu which is the main contributing isotope from the equation. Please note that the doubles values were used to determine these values.

With all the equations, used masses were able to be calculated for each individual isotope there was a signature for and those masses can be seen in the table below.

Table 20. Calculated vs. actual mass

Nuclide	Calculated Mass (g)	Actual Mass (g)	Percent Error (%)
^{238}Pu	0.250	0.218	14.7
^{239}Pu	314.679	18.498	-1.2
^{240}Pu	62.670	62.915	-3.9
^{241}Pu	1.725	1.744	-1.1
^{242}Pu	0.000	1.308	n/a
^{241}Am	3.534	3.488	1.3
$^{240}Pu_{eff}$	63.300	65.612	-3.5

The table also shows the variation between the calculated value and the actual value. All were less the 15% except for the assumed zero value for ^{242}Pu. While this could be considered a large amount of error the calculated values for ^{239}Pu and ^{240}Pu are 87% of the total mass and are the primary isotopes of interest. These values can be further interpreted to calculate the α value. The value for α can be seen in Table 20.

Table 21. Calculated vs. actual α value

	Calculated	Actual	Percent Difference (%)
α	0.522	0.497	5.0

This calculation yields an error of less the 5% which is the goal for most types of systems. This allows for all unknowns to be solved for as a system of equations and provides a method to determine the total mass of the sample without additional simulations. With the singles and doubles equations used, it calculates a M of 1.08224 and a $^{240}Pu_{eff}$ of 60.7862 g. The $^{240}Pu_{eff}$ is lower than both the calculation and actual but that was expected since M was included in the simulation of MCNPX. This shows that the isotopics can be determined with this experiment with little or no information about the sample.

CHAPTER VI

CONCLUSIONS

In summary, the portable neutron-gamma coincidence counter that was presented here is meant to be an extension of work of PNCC to increase the ability of that detector. The characterization and simulations performed were to determine the feasibility of this type of system. The sensitivity to the gammas emitted by a plutonium source was sought as well as what peaks were able to be resolved from the $LaBr_3$ system using a simulated detector in MCNPX. To determine the spectrum ability as well as determine what information could be used in conjunction with the neutron system, the same four standards were used that were in the PNCC work and compared to the previous values. The ability of the interaction of gammas with the scintillation material was used

The neutron detection abilities were performed by using the same methodologies as the PNCC. The Neutron Coincidence Point Model was used in conjunction with the new capabilities of MCNPX. This was done to ensure that the variation in neutron sensitivity was minimized when the gamma detection system was added in front of the neutron counter. This confirmed that MNCPX still simulated the neutron interaction correctly, even with the added material, and could eliminate the use of the point model in calculations.

6.1 MCNPX BENCHMARKING

The Canberra Inspector 1000 was used in conjunction with the IPORL-1 $LaBr_3$ gamma detection probe. This probe a 1.5"X1.5" cylindrical crystal and was modeled to that specification within MCNPX. This model was compared to the results of a ^{60}Co and ^{137}Cs source to ensure consistency across a wide energy range. When this was performed, it was shown that MCNPX correctly simulates the interaction of the gammas within the crystal.

However, when the model was compared to the actual spectrum, the background of the spectrum did not match up well. When an isolated background spectrum was taken with the probe, it should that the decay methods included in the model were not adequate. When further investigation was performed, it was determined that the reason for this was twofold. First, it was determined that there was an inherent flaw within the MCNPX code that caused the simulated counts to be lower than actual. This was because MCNPX was not designed to have the detection crystal being radioactive.

The second reason was due to the fact that one of the modes of decay for La is with a 788 keV beta decay. When beta decay occurs, it allows for a continuous energy spectrum from 0 keV to $beta_{max}$. Since this simulation was performed in mode P of MCNPX, this was not accounted for. Because of this, the output deck of the MCNPX file had to be adjusted to account for the energy broadening with the beta energy spectrum. Once this was performed, the resulting spectrum matched quite well with the actual spectrum from the IPROL-1 probe. Additional measurements were taken of a

small Pu source to ensure that the model accurately simulated the multitude of gammas for that source.

It was determined that MCNPX properly simulated the Pu source with the probe model. It was concluded that it could be used to model the nano-composite material that was used for this design.

6.2 MODEL GEOMETRIC DESIGN

The final design of the PNGC ensured that each signature was not affected too much by the other. Since the gamma was placed in front of the neutron system, the thickness of the material had to be varied to determine the impact on the neutron system as well as provide a high enough gamma signature to be used. The moderator material was also varied to determine if it should be changed since there was additional material between the source and the detection tubes.

Once several variations were tested, it was determined that the gamma detection slab should be one inch thick and fit inside of the neutron detection system, somewhat like a sleeve. While modifications to the moderator material was tested, it was determined that its' present form provides the best results. This also allowed for direct comparison of the PNCC data since the two systems were identical.

6.3 SIMULATION AND RESULTS

MCNPX input decks were written for the same four samples that were previously tested. To maintain consistency, the same parameters were used. This included four Pu cans that ranged from 195.00-617.00 g. This allowed for a wide change in both the neutron and

gamma signature. All four samples were run with the same diameter with only the fill height to account for the increase of material and the same density of 0.9 g/cc was used for each can.

For the gamma measurement, a deck was written for each isotope of interest and included the most predominate gamma lines. Each simulation had 4000 energy bin and a GEB function and was executed 1E8 particle tracks. The simulation created a spectrum that had several peaks that were able to be identified from 60-770 keV. Some of the peaks are caused by multiple isotopes and, if they could not be distinguished either visually or with the assistance of peak fitting software, they were not used. The peak efficiencies ranged from 7.49% to 12.54% and varied by isotope and by which sample was being simulated; with ^{238}Pu, ^{239}Pu, ^{241}Pu, and ^{241}Am being identified with the six peaks being used.

The same sample geometry was used with two decks for SF and (α,n) for the neutron signature. An MCNPX capture tally was used for both decks with 1E7 particles executed. An infinite gate width with no pre-delay was used for singles counts and a 64 μsec gate width with a 4.5 μsec pre-delay for the doubles counting. The simulation yielded a singles count rate of 3656-12845 cps with the F4 tally and the F8 resulted in a 3659-12857 cps. The doubles count rate from the F8 tally was 147-606 cps. These were consistent with the PNCC.

With both the neutron and gamma signature analyzed an estimate of the isotopics and mass of an unknown sample was able to be determined. Count Rate vs Mass curves from

the gamma analysis were created for ^{238}Pu, ^{239}Pu, ^{241}Pu, and ^{241}Am. This allowed for the mass of the material to be estimated. With a combination of the gamma values and the neutron values the isotopic were able to be determined within 15%. The majority isotopes were able to be determined to less than 2%. This also provided a method to calculate an α value to within 5% accuracy and M was also determine. This was able to be done with no additional simulations needed.

6.4 FINAL CONCLUSIONS AND RECOMMENDATIONS

The method presented here provides a new means to determine the isotopic of an unknown Pu sample. Normal to determine mass the other simulations or information must be obtained in order to determine the same information. This experiment was a feasibility study to see if it could be done. While it was there are some aspects that were not tested for this experiment and could be tested in future work.

Sample size and composition is one example. This experiment used the same sample geometry throughout the experiment. Samples of different radii should be tested and a sample that has a hole in the center should be tested to determine the variation of shelf-shielding which could lead to false results.

Also it the use of a gamma-neutron count was not tested. Since the samples that were used in this work had extremely high count rates this was not able to be done. However, if a small sample was used and the gamma count was low enough, it might be possible to determine if a gamma and neutron are products of the same event. In addition to the low count rate, a device with a higher resolution should be used.

In the mass determination the ^{240}Pu mass was assumed to be zero in order to determine the mass and isotopic of the sample. This would be a valuable piece of information if it was able to be determined from the gamma spectrum, but with this systems resolution is not possible. If a system with the resolution capabilities of an HPGe system or greater it should be possible to resolve a ^{240}Pu peak enough to extract the necessary data.

Even with these negative aspects it is still believed that once the gamma detection medium is available the dual use detector system should be explored further and a prototype produced.

REFERENCES

1. MCNPX. Computer software. Vers. 2.5. Los Alamos, NM: Los Alamos National Laboratory (2005).

2. A. L. THORNTON. "Development of a Portable Neutron Coincidence Counter for Field Measurements of Nuclear Materials Using the Advanced Multiplicity Capabilities of MCNPX 2.5.F and the Neutron Coincidence Point Model", MS Thesis, Texas A&M University (2007).

3. A. L. THORNTON, W.S. CHARLTON, H. MENLOVE, and M. MILLER, "Development and Characterization of a Portable Neutron Coincidence Counter" *Proc. of the 46th Annual Meeting of the Institute for Nuclear Materials Management*, Nashville, Tennessee, July 16-20, 2006 (2006).

4. I. PAZSIT, L. PAL, A. ENQVIST, and S. A. POZZI, "The Joint Distribution of Detected Neutrons and Gamma Photons from Fissile Samples and its Application in Nuclear Safeguards," *SPIE Fluctuations and Noise*, La Pietra Conference Center, Florence, Italy, May 20-24 (2007).

5. A. ENQVIST, I. PAZSIT, and S. A. POZZI, "The Detection Statistics of Neutrons and Photons Emitted from a Fissile Sample," *Proc. Of the 47th Annual Meeting of the Institute of Nuclear Materials Management Annual Meeting*, Tucson, Arizona, July 8-12 (2007).

6. McKIGNEY et al., NIM/A, 579, pp. 15-18 (2007).

7. DEL SESTO et al., LALP-07-030, Los Alamos National Laboratory (2007).

8. STRANGE et al., 2008 IEEE Nuclear Science Symposium Conference Record, pp. 3529-3532 (2008).

9. R. E. DEL SESTO, E. A. Mckigney, R. E. Muenhausen, K. C. Ott, R. D. Gilbertson, T. M. McCleskey, M. Bacania, L. G. Jacobson, A. K. Burnell, B. L. Bennet, S. C. Sitarz, and J. F. Smith. *Development of Nanocomposite Scintillators*. (2007)

10. D. REILLY, N. ENSSLIN, and H. SMITH. Passive Nondestructive Assay of Nuclear Material. Springfield, VA: National Technical Information Service, (1991).

11. G. F. KNOLL. Radiation Detection and Measurement. New York: Wiley-Interscience (2000).

12. F. H. ATTIX. Introduction to radiological physics and radiation dosimetry. New York: Wiley (1986).

13. "Products." *CANBERRA, Measurement Solutions for Nuclear Safety and Security | Radiation Detection*. Web. 02 Sept. 2009. <http://www.canberra.com>.

14. GENIE 2000. Computer software. Vers. 3.1A. Meriden, CT: Canberra (2006).

15. "SPECT Hardware Requirements." *UBC PhysAstro: Home Page*. Web. 02 Sept. 2009. <http://www.physics.ubc.ca/~mirg/home/tutorial/hardware.html>.

16. MCNP-VISED 4C2, http://www.rist.or.jp/rsicc/app/MCNP-VISEd4C2.html, (2006).

APPENDIX A

The secondary decay mode of ^{138}La is β^- decay and includes a 788 keV gamma, β^-, and a neutrino; it can be seen in the following[14]:

$$^{138}_{57}La \rightarrow 788keV\ \gamma + \beta^- + \nu \qquad [16]$$

The 788 keV gammas is a discrete energy but due to the laws of physics the beta particle and the neutrino are not, and at first were not considered to be included in the code. When the 788 keV gamma and its yield were added to the input deck it performed normally; creating a peak in that region with the number of counts determined by the yield of the peak. This produced a spectrum that had two peaks at the corresponding gamma lines but this is not what is seen in the background spectrum as seen in Figure 17. When more research was done to determine cause of the missing peak, it was concluded that the β^- was causing some issues with the 788 keV region. The beta and the gamma are produced in coincidence and was being detected within the crystal. The dilemma that this created was being counted with vastly different ratios. The beat is a charged particle which has an extremely short mean free path, and its entire energy of 253 keV is being absorbed within the crystal. The gamma, on the other hand, is not. Its mean free path is much greater than the beta and has a chance to escape from the detector. Not only is there a probability that it will escape with its entire energy, but it also has a chance to undergo Compton and deposit a fraction of its energy that would then be recorded in the Compton continuum. This created a unique challenge to model

since normally the scintillation crystal does not have the issue of being radioactive and only the gammas need to be accounted for.

The first step to account for this energy is to take a closer look at the beta decay process. The neutrino in the equation can be disregarded since it has an interaction probability of essentially zero. When the gamma and beta impart energy in the scintillator, it does so at essentially the same time. Instead of producing two separate events it is counted as one. In order to account for this, the energy distribution of the beta must be determined. Unlike the gamma that creates peak at certain energy E, the beta has a continuous energy distribution with the ability to produce a beta with energy 0 to E_{max}, being 0-253 keV. The remaining energy is imparted into the neutrino particle. By definition, the sum of these energies is E_o where E_o/c^2 is the nuclear mass difference. The equations to determine the total transition rate (dR) for decays can be seen below.

$$dR = \frac{G_w^2 |M_F|^2}{2\pi^3 \hbar^7 c^6} S_o(E_e) dE_e \qquad [17]$$

where:

$$S_o(E_e) = [(E_o - E_e)^2 - m_v^2 c^4)]^{\frac{1}{2}} (E_o^2 - E_e)(E_e^2 - m_e^2 c^4)^{\frac{1}{2}} E_e \qquad [18]$$

This formula can be improved if the interaction between the electron and the Coulomb field of the daughter nucleus is taken into account. To do this, $S_o E_e$ is modified to Equation 12.

$$S_c(E_e) = F(Z_d, E_e) S_o(E_e) \qquad [19]$$

where:

$$F(Z, E_e) = \frac{2\pi\eta}{1 - e^{-2\pi\eta}}, with\ \eta = \frac{\pm Ze^2}{4\pi\varepsilon_o \hbar v} \quad [20]$$

The constants for the above equations can be seen in Table 2.

Table 22. Beta decay values

Constants	
Gamma Energy (eV)	788742
Gw	1
Mf	1
h/	1.05E-34
c	3.00E+08
eps0	8.85E-12
dEe [eV]	1.00E+01
me*c2 [eV]	5.11E+05
mneutrino*c2 [eV]	1.00E+00
MeV/(amu*c2)	9.31E+02
FSC	0.0072974

By making a spreadsheet with the same energy/bin, 373 keV, an estimate of what the beta spectrum could look like can be obtained. Each value that varies with energy was calculated for each energy bin over the entire energy of the beta particle. A calculation was then performed to determine the probability of a beta at energy *E* for each bin out of the total S_oE. A graph of the results can be seen in Figure 12.

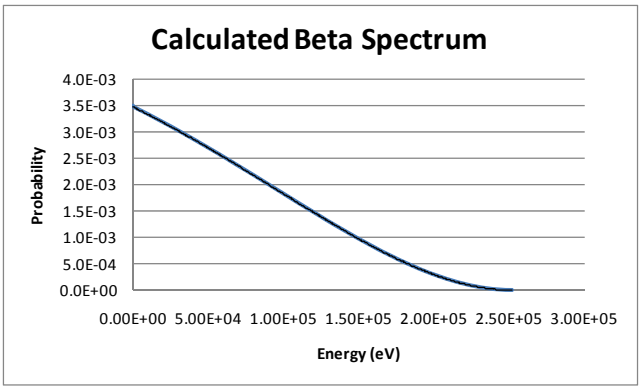

Figure 37. Beta Spectrum

In order to be able to use this data a trendline was added to calculate the interaction which was being counted in coincided with a gamma and can be seen in Equation 14.

$$y = 3.087E-25x^4 + 5.726E-20x^3 - 3.258E-14x^2 - 1.414E-08x + 3.473E-03 \quad [21]$$

When used in a calculation, these values were taken out to the 16th decimal place to ensure accuracy. The first attempt to use this information was to directly add it to the spectrum around the 788 keV region. While the results were somewhat similar, there was significant differences in the counts. When a comparison of the spectrums was made, it was noticed that the shape of the calculated peak was close to the actual. It was determined that the difference in counts was due to not including all of the Compton gammas that were being counted in coincidence with the beta particle along with the beta particles being counted when the gamma escaped. This required determining the numbers of counts that are from the Compton region as well as in the 788 keV region.

The original output deck was used in order to know what the simulated values were for the spectrum. The two different decay modes we ran into separate decks to ensure that

only the 788 keV gammas were being broadened since the 1.435 MeV were not produced in coincidence with the beta. The counts were determined in each energy bin by multiplying the output probability by the total number of decays produced by the β^- decay mode. The total number of β^- decays can be seen in Table 2. These counts were then broadened using Equation 14 over the entire β^- energy spectrum. To ensure that it was only the energy of the bin plus the β^- two IF statements were used to cutoff the below and above energy, this is shown in Equation 15.

$$IF(E_1 - E_2) < 0, [IF(E_2 - E_1) < 253keV\ \{EQ\ 14\} * CTS, 0], 0 \quad [22]$$

Where

$$x = (E_2 - E_1)$$

In the equation, E_1 and E_2 are defined numbers by the value of the energy bins used. A matrix was created with the axis and abscissa being the energy bin values. This creates a 4000x4000 element matrix with E_1 being the axis and E_2 abscissa. The value in each column is summed as well as the corresponding counts for that bin. To ensure that the calculation was correct, each row was summed and divided by the counts from the output deck. Each value was greater than 99% of the original value. This accounts for the counts that are produced from the gamma and beta being detected in coincidence, but it does not account for the remaining beta being stopped without a gamma. To account for that, the difference between the detected counts and the total disintegrations was multiplied by the beta energy spectrum as seen in Figure 19.

APPENDIX B

MCNPX INPUT DECKS

Spontaneous Fission Input Deck

```
MCNP Project (HANDHELD)
c     - cell card -
1   11 -0.96     18  21  24  27       u=1     imp:n=1     $poly box
2   14 -0.001293    -18  19           u=1     imp:n=1     $air space
3   14 -0.001293    -21  22           u=1     imp:n=1     $air space
4   14 -0.001293    -24  25           u=1     imp:n=1     $air space
5   14 -0.001293    -27  28           u=1     imp:n=1     $air space
6   12 -2.70        -19  20  31  32   u=1     imp:n=1     $Al clad
7   12 -2.70        -22  23  33  34   u=1     imp:n=1     $Al clad
8   12 -2.70        -25  26  35  36   u=1     imp:n=1     $Al clad
9   12 -2.70        -28  29  37  38   u=1     imp:n=1     $Al clad
10  13  2.4463e-4   -20              u=1     imp:n=1     $active He
tube
11  13  2.4463e-4   -23              u=1     imp:n=1     $active He
tube
12  13  2.4463e-4   -26              u=1     imp:n=1     $active He
tube
13  13  2.4463e-4   -29              u=1     imp:n=1     $active He
tube
14   0               30                      imp:n=0     $outside
universe
15  14 -0.001293    -30 #24 #25 #26 #33 #34
                        #31 #32 #27 #36 #30
                        #37 #38 #39 #40 #41
                        #42 #43 #44 #45 #46
                        #47 #48      imp:n=1     $sphere
16  13  2.4463e-4   -31              u=1     imp:n=1     $inactive
length
17  13  2.4463e-4   -32              u=1     imp:n=1     $inactive
length
18  13  2.4463e-4   -33              u=1     imp:n=1     $inactive
length
19  13  2.4463e-4   -34              u=1     imp:n=1     $inactive
length
20  13  2.4463e-4   -35              u=1     imp:n=1     $inactive
length
21  13  2.4463e-4   -36              u=1     imp:n=1     $inactive
length
22  13  2.4463e-4   -37              u=1     imp:n=1     $inactive
length
23  13  2.4463e-4   -38              u=1     imp:n=1     $inactive
length
24   0                      -17     fill=1          imp:n=1   $poly box
with tubes
25  like 24 but trcl=(0 0 0  -1 0 0  0 -1 0  0 0 1) imp:n=1   $opposite
poly/tubes
```

```
26  like 24 but trcl=(0 0 0  0 -1 0  1 0 0  0 0 1)  imp:n=1
$poly/tube slab
27  like 24 but trcl=(0 0 0  0 1 0  -1 0 0  0 0 1)  imp:n=1
$polt/tubes
c 29  15 -2.5        -41  42                          imp:n=1   $glass
jar
30  16 -0.900          -42 -43                       imp:n=1   $Pu mix
sample
c 35  18 -10e-20     -45 46 -47 48 -49 50             imp:n=1   $Cf-252
31  17 -2.0            -44                           imp:n=1   $metal
top
32  like 31 but trcl=(0 0 0  -1 0 0  0 -1 0  0 0 1) imp:n=1   $metal
top
33  like 31 but trcl=(0 0 0  0 -1 0  1 0 0  0 0 1)  imp:n=1   $metal
top
34  like 31 but trcl=(0 0 0  0 1 0  -1 0 0  0 0 1)  imp:n=1   $metal
top
36  11 -0.96  -51                                   imp:n=1   $bottom
poly slab
37  19 -3.00  -52 #41                                   imp:n=1   $LaBr
Slab
38  like 37 but trcl=(0 0 0  -1 0 0  0 -1 0  0 0 1) imp:n=1   $LaBr
Slab
39  like 37 but trcl=(0 0 0  0 -1 0  1 0 0  0 0 1)  imp:n=1   $LaBr
Slab
40  like 37 but trcl=(0 0 0  0 1 0  -1 0 0  0 0 1)  imp:n=1   $LaBr
Slab
41  12 -2.70  -53 52 54                             imp:n=1   $Al Shell
42  like 41 but trcl=(0 0 0  -1 0 0  0 -1 0  0 0 1) imp:n=1   $LaBr
Slab
43  like 41 but trcl=(0 0 0  0 -1 0  1 0 0  0 0 1)  imp:n=1   $LaBr
Slab
44  like 41 but trcl=(0 0 0  0 1 0  -1 0 0  0 0 1)  imp:n=1   $LaBr
Slab
45  20 -0.6   -54                                   imp:n=1   $PMT
46  like 45 but trcl=(0 0 0  -1 0 0  0 -1 0  0 0 1) imp:n=1   $LaBr
Slab
47  like 45 but trcl=(0 0 0  0 -1 0  1 0 0  0 0 1)  imp:n=1   $LaBr
Slab
48  like 45 but trcl=(0 0 0  0 1 0  -1 0 0  0 0 1)  imp:n=1   $LaBr
Slab

c     - surface cards -
17 BOX  -16.51 -8.89 -11.43   7.62 0 0   0 17.78 0   0 0 22.86
18 RCC  -12.7  -5.953 -11.43   0 0 22.86   1.42875         $void hole
19 RCC  -12.7  -5.953 -11.43   0 0 22.86   1.27            $Al clad
cylinder
20 RCC  -12.7  -5.953 -8.890   0 0 17.78   1.19380         $He cylinder
21 RCC  -12.7  -1.984 -11.43   0 0 22.86   1.42875         $void hole
22 RCC  -12.7  -1.984 -11.43   0 0 22.86   1.27            $void hole
23 RCC  -12.7  -1.984 -8.890   0 0 17.78   1.19380         $He cylinder
24 RCC  -12.7   1.984 -11.43   0 0 22.86   1.42875         $void hole
25 RCC  -12.7   1.984 -11.43   0 0 22.86   1.27            $Al clad
cylinder
```

```
26 RCC  -12.7   1.984 -8.890   0 0 17.78   1.19380         $He cylinder
27 RCC  -12.7   5.953 -11.43   0 0 22.86   1.42875         $void hole
28 RCC  -12.7   5.953 -11.43   0 0 22.86   1.27            $Al clad
cylinder
29 RCC  -12.7   5.953 -8.890   0 0 17.78   1.19380         $He cylinder
30 SPH   0 0 0 40
31 RCC  -12.7 -5.953  8.890   0 0 2.540   1.19380         $inactive
length
32 RCC  -12.7 -5.953 -11.43   0 0 2.540   1.19380         $inactive
length
33 RCC  -12.7 -1.984  8.890   0 0 2.540   1.19380         $inactive
length
34 RCC  -12.7 -1.984 -11.43   0 0 2.540   1.19380         $inactive
length
35 RCC  -12.7  1.984  8.890   0 0 2.540   1.19380         $inactive
length
36 RCC  -12.7  1.984 -11.43   0 0 2.540   1.19380         $inactive
length
37 RCC  -12.7  5.953  8.890   0 0 2.540   1.19380         $inactive
length
38 RCC  -12.7  5.953 -11.43   0 0 2.540   1.19380         $inactive
length
39 BOX  -16.51 8.900 -11.43   26.035 0 0   0 5.08 0   0 0 22.86
40 BOX  -16.51 -13.97 -13.97   26.035 0 0   0 27.94 0   0 0 2.54
41 RCC   0 0 -3.81     0 0 15.24           3.81
42 RCC   0 0 -10.666   0 0 2.33345133      5.4356             $Pu
cylinder
43 PZ   -8.33254867                                         $Pu
cylinder
44 BOX  -16.51 -8.89 11.43   7.62 0 0   0 17.78 0   0 0 2.54
45 PZ   11.43
46 PZ  -11.43
47 PX   8.89
48 PX  -8.89
49 PY   8.89
50 PY  -8.89
51 BOX -22.51 -17.31 -11.43   46.02 0 0   0  34.32 0   0 0 -5.08  $Poly
slab
52 BOX -8.78  -8.78  -11.32   2.54  0 0   0  14.82 0   0 0  22.75 $LaBr
Slab
53 BOX -8.88  -8.88  -11.42   2.74  0 0   0  15.02 0   0 0  25.39 $Al
Shell
54 BOX -8.78  -8.78   11.43   2.54  0 0   0  14.82 0   0 0   2.44 $PMT

c     - data cards -
mode n
print
sdef   pos=0 0 -9.499274335 par=sf axs=0 0 1 rad=d2 ext=d3
si2    0 5.4356
si3   -1.166725665 1.166725665
fq0   e t f
f4:n  10 11 12 13 t
fm4   -1 13 103
sd4    1 1 1 1 1
```

```
t4     450 6850 1E12
f14:n ((10 11 12 13) < 24)
fm14   -1 13 103
sd14    1
f24:n ((10 11 12 13) < 25)
fm24   -1 13 103
sd24    1
f34:n ((10 11 12 13) < 26)
fm34   -1 13 103
sd34    1
f44:n ((10 11 12 13) < 27)
fm44   -1 13 103
sd44    1
f8:n  10 11 12 13 t
ft108   cap 2003
fc108 Mulitplicity Count Rate (Infinite Gate)
f108:n  (10 11 12 13)
ft118  cap 2003 gate 450 2400
fc118 Multiplicity Count Rate (24us Gate)
f118:n  (10 11  12 13)
ft128  cap 2003 gate 450 6400
fc128 Multiplicity Count Rate (64us Gate)
f128:n  (10 11 12 13)
c     t4   300 1100 1900 3500 6700 13100
c f8:p    37
c f18:p  (37 38 39 40)
c ft8   GEB 0.007167 0.019027 -0.141
c ft18  GEB 0.007167 0.019027 -0.141
c e0    0.01  4000i  1.5
m11    6000.60c 0.333 1001.60c 0.667         $HDPE density=0.96 g/cm3
mt11   poly.01t
m12   13027.60c 1.000                        $Al   density=2.70 g/cm3
m13    2003.60c 1.000                        $He-3,10 atm,den=2.4463e-4
at/barn-cm
m14    8016.60c 0.210 7014.60c 0.790         $air
m15   14000.60c 0.334 8016.60c 0.666         $glass
m16   94238.60c -0.00048891
      94239.60c -0.72910337
      94240.60c -0.14524399
      94241.60c -0.00412629
      94242.60c -0.00306266
      95241.60c -0.00846288
       8016.60c -0.11797470
c      1001.60c -                            $Pu mix sample
m17   26000 1                                $Iron box
m18   98252.60c 1.000                        $Cf-252 source density
10e-20
m19    1001.60c -0.018112917
       6012.60c -0.114265632
       8016.60c -0.016921527
      57138.31c -0.000280893
      57139.31c -0.311822943
      35079.31c -0.273018919
      35081.31c -0.265586169                   $LaBr Crystal
```

```
m20    8016  .324  7014  .593  14000  .083     $Glass/Air Mix
nps   10000000

tmesh
rmesh1:n flux
cora1 -25 99i 25
corb1 -25 99i 25
corc1 -25 25
rmesh2
cora2 -25 99i 25
corb2 -25 99i 25
corc2 -25 25
rmesh3
cora3 -25 99i 25
corb3 -25 99i 25
corc3 -25 25
endmd
```

(α,n) Input Deck

```
MCNP Project (HANDHELD)
c     - cell card -
1   11 -0.96     18  21  24  27       u=1     imp:n=1     $poly box
2   14 -0.001293    -18  19           u=1     imp:n=1     $air space
3   14 -0.001293    -21  22           u=1     imp:n=1     $air space
4   14 -0.001293    -24  25           u=1     imp:n=1     $air space
5   14 -0.001293    -27  28           u=1     imp:n=1     $air space
6   12 -2.70        -19  20  31  32   u=1     imp:n=1     $Al clad
7   12 -2.70        -22  23  33  34   u=1     imp:n=1     $Al clad
8   12 -2.70        -25  26  35  36   u=1     imp:n=1     $Al clad
9   12 -2.70        -28  29  37  38   u=1     imp:n=1     $Al clad
10  13  2.4463e-4   -20              u=1     imp:n=1     $active He
tube
11  13  2.4463e-4   -23              u=1     imp:n=1     $active He
tube
12  13  2.4463e-4   -26              u=1     imp:n=1     $active He
tube
13  13  2.4463e-4   -29              u=1     imp:n=1     $active He
tube
14   0               30                      imp:n=0     $outside
universe
15  14 -0.001293    -30 #24 #25 #26 #33 #34
                        #31 #32 #27 #36 #30
                        #37 #38 #39 #40 #41
                        #42 #43 #44 #45 #46
                        #47 #48      imp:n=1     $sphere
16  13  2.4463e-4   -31               u=1     imp:n=1     $inactive
length
17  13  2.4463e-4   -32              u=1     imp:n=1     $inactive
length
18  13  2.4463e-4   -33              u=1     imp:n=1     $inactive
length
19  13  2.4463e-4   -34              u=1     imp:n=1     $inactive
length
20  13  2.4463e-4   -35              u=1     imp:n=1     $inactive
length
21  13  2.4463e-4   -36              u=1     imp:n=1     $inactive
length
22  13  2.4463e-4   -37              u=1     imp:n=1     $inactive
length
23  13  2.4463e-4   -38              u=1     imp:n=1     $inactive
length
24   0                     -17     fill=1          imp:n=1   $poly box
with tubes
25  like 24 but trcl=(0 0 0  -1 0 0  0 -1 0  0 0 1) imp:n=1   $opposite
poly/tubes
26  like 24 but trcl=(0 0 0  0 -1 0  1 0 0  0 0 1)  imp:n=1
$poly/tube slab
27  like 24 but trcl=(0 0 0  0 1 0  -1 0 0  0 0 1)  imp:n=1
$polt/tubes
```

```
c 29  15 -2.5        -41  42                          imp:n=1   $glass
jar
30  16 -0.900          -42 -43                       imp:n=1   $Pu mix
sample
c 35  18 -10e-20     -45 46 -47 48 -49 50             imp:n=1   $Cf-252
31  17 -2.0            -44                           imp:n=1   $metal
top
32  like 31 but trcl=(0 0 0  -1 0 0  0 -1 0  0 0 1) imp:n=1   $metal
top
33  like 31 but trcl=(0 0 0  0 -1 0  1 0 0  0 0 1)  imp:n=1   $metal
top
34  like 31 but trcl=(0 0 0  0 1 0  -1 0 0  0 0 1)  imp:n=1   $metal
top
36  11 -0.96  -51                                   imp:n=1   $bottom
poly slab
37  19 -3.00  -52 #41                                  imp:n=1   $LaBr
Slab
38  like 37 but trcl=(0 0 0  -1 0 0  0 -1 0  0 0 1) imp:n=1   $LaBr
Slab
39  like 37 but trcl=(0 0 0  0 -1 0  1 0 0  0 0 1)  imp:n=1   $LaBr
Slab
40  like 37 but trcl=(0 0 0  0 1 0  -1 0 0  0 0 1)  imp:n=1   $LaBr
Slab
41  12 -2.70  -53 52 54                              imp:n=1   $Al Shell
42  like 41 but trcl=(0 0 0  -1 0 0  0 -1 0  0 0 1) imp:n=1   $LaBr
Slab
43  like 41 but trcl=(0 0 0  0 -1 0  1 0 0  0 0 1)  imp:n=1   $LaBr
Slab
44  like 41 but trcl=(0 0 0  0 1 0  -1 0 0  0 0 1)  imp:n=1   $LaBr
Slab
45  20 -0.6   -54                                    imp:n=1   $PMT
46  like 45 but trcl=(0 0 0  -1 0 0  0 -1 0  0 0 1) imp:n=1   $LaBr
Slab
47  like 45 but trcl=(0 0 0  0 -1 0  1 0 0  0 0 1)  imp:n=1   $LaBr
Slab
48  like 45 but trcl=(0 0 0  0 1 0  -1 0 0  0 0 1)  imp:n=1   $LaBr
Slab

c     - surface cards -
17 BOX  -16.51 -8.89 -11.43   7.62 0 0   0 17.78 0   0 0 22.86
18 RCC  -12.7  -5.953 -11.43   0 0 22.86   1.42875         $void hole
19 RCC  -12.7  -5.953 -11.43   0 0 22.86   1.27            $Al clad
cylinder
20 RCC  -12.7  -5.953 -8.890   0 0 17.78   1.19380         $He cylinder
21 RCC  -12.7  -1.984 -11.43   0 0 22.86   1.42875         $void hole
22 RCC  -12.7  -1.984 -11.43   0 0 22.86   1.27            $void hole
23 RCC  -12.7  -1.984 -8.890   0 0 17.78   1.19380         $He cylinder
24 RCC  -12.7   1.984 -11.43   0 0 22.86   1.42875         $void hole
25 RCC  -12.7   1.984 -11.43   0 0 22.86   1.27            $Al clad
cylinder
26 RCC  -12.7   1.984 -8.890   0 0 17.78   1.19380         $He cylinder
27 RCC  -12.7   5.953 -11.43   0 0 22.86   1.42875         $void hole
28 RCC  -12.7   5.953 -11.43   0 0 22.86   1.27            $Al clad
cylinder
```

```
29 RCC  -12.7   5.953 -8.890   0 0 17.78   1.19380         $He cylinder
30 SPH   0 0 0 40
31 RCC  -12.7 -5.953  8.890   0 0 2.540   1.19380         $inactive
length
32 RCC  -12.7 -5.953 -11.43   0 0 2.540   1.19380         $inactive
length
33 RCC  -12.7 -1.984  8.890   0 0 2.540   1.19380         $inactive
length
34 RCC  -12.7 -1.984 -11.43   0 0 2.540   1.19380         $inactive
length
35 RCC  -12.7  1.984  8.890   0 0 2.540   1.19380         $inactive
length
36 RCC  -12.7  1.984 -11.43   0 0 2.540   1.19380         $inactive
length
37 RCC  -12.7  5.953  8.890   0 0 2.540   1.19380         $inactive
length
38 RCC  -12.7  5.953 -11.43   0 0 2.540   1.19380         $inactive
length
39 BOX  -16.51 8.900 -11.43   26.035 0 0   0 5.08 0   0 0 22.86
40 BOX  -16.51 -13.97 -13.97   26.035 0 0   0 27.94 0   0 0 2.54
41 RCC   0 0 -3.81     0 0 15.24           3.81
42 RCC   0 0 -10.666   0 0 2.33345133      5.4356             $Pu
cylinder
43 PZ   -8.33254867                                         $Pu
cylinder
44 BOX  -16.51 -8.89 11.43   7.62 0 0   0 17.78 0   0 0 2.54
45 PZ   11.43
46 PZ  -11.43
47 PX   8.89
48 PX  -8.89
49 PY   8.89
50 PY  -8.89
51 BOX -22.51 -17.31 -11.43   46.02 0 0   0  34.32 0   0 0 -5.08  $Poly
slab
52 BOX -8.78  -8.78  -11.32   2.54  0 0   0  14.82 0   0 0  22.75 $LaBr
Slab
53 BOX -8.88  -8.88  -11.42   2.74  0 0   0  15.02 0   0 0  25.39 $Al
Shell
54 BOX -8.78  -8.78   11.43   2.54  0 0   0  14.82 0   0 0   2.44 $PMT

c     - data cards -
mode n
print
sdef   pos=0 0 -9.499274335 axs=0 0 1 rad=d2 ext=d3 erg=d1
si2    0 5.4356
si3   -1.166725665 1.166725665
c     si1    H
c     sp1   -3  0.799 4.903
c       PuO2 (a,n) Spectrum, calculated.  DHB '05
si1  h 0.00E+00 2.00E-01 4.00E-01 6.00E-01 8.00E-01 1.00E+00
       1.20E+00 1.40E+00 1.60E+00 1.80E+00 2.00E+00 2.20E+00
       2.40E+00 2.60E+00 2.80E+00 3.00E+00 3.20E+00 3.40E+00
       3.60E+00 3.80E+00 4.00E+00 4.20E+00 4.40E+00 4.60E+00
       4.80E+00 5.00E+00 5.20E+00 5.40E+00 5.60E+00 5.80E+00
```

```
       6.00E+00 6.20E+00 6.40E+00 6.60E+00 6.80E+00 7.00E+00
       7.20E+00 7.40E+00 7.60E+00 7.80E+00 8.00E+00 8.20E+00
       8.40E+00 8.60E+00 8.80E+00 9.00E+00 9.20E+00 9.40E+00
       9.60E+00 9.80E+00 1.00E+01 1.02E+01 1.04E+01 1.06E+01
       1.08E+01 1.10E+01 1.12E+01
sp1  d 0 1.40E-02 2.02E-02 1.93E-02 1.67E-02 1.89E-02 2.52E-02
         3.42E-02 4.54E-02 5.84E-02 7.62E-02 9.14E-02 1.05E-01
         1.06E-01 9.80E-02 8.36E-02 6.64E-02 5.08E-02 3.39E-02
         1.88E-02 9.46E-03 3.63E-03 1.39E-03 9.54E-04 7.04E-04
         5.53E-04 3.74E-04 2.08E-04 3.57E-05 3.40E-06 3.57E-08
         0.00E+00 0.00E+00 0.00E+00 0.00E+00 0.00E+00 0.00E+00
         0.00E+00 0.00E+00 0.00E+00 0.00E+00 0.00E+00 0.00E+00
         0.00E+00 0.00E+00 0.00E+00 0.00E+00 0.00E+00 0.00E+00
         0.00E+00 0.00E+00 0.00E+00 0.00E+00 0.00E+00 0.00E+00
         0.00E+00 0.00E+00
fq0   e t f
f4:n  10 11 12 13 t
fm4   -1 13 103
sd4    1 1 1 1 1
t4     450 6850 1E12
f14:n ((10 11 12 13) < 24)
fm14   -1 13 103
sd14    1
f24:n ((10 11 12 13) < 25)
fm24   -1 13 103
sd24    1
f34:n ((10 11 12 13) < 26)
fm34   -1 13 103
sd34    1
f44:n ((10 11 12 13) < 27)
fm44   -1 13 103
sd44    1
f8:n  10 11 12 13 t
ft108   cap 2003
fc108 Mulitplicity Count Rate (Infinite Gate)
f108:n  (10 11 12 13)
ft118  cap 2003 gate 450 2400
fc118 Multiplicity Count Rate (24us Gate)
f118:n  (10 11  12 13)
ft128  cap 2003 gate 450 6400
fc128 Multiplicity Count Rate (64us Gate)
f128:n  (10 11 12 13)
c     t4   300 1100 1900 3500 6700 13100
c f8:p    37
c f18:p  (37 38 39 40)
c ft8   GEB 0.007167 0.019027 -0.141
c ft18  GEB 0.007167 0.019027 -0.141
c e0    0.01  4000i  1.5
m11    6000.60c 0.333 1001.60c 0.667         $HDPE density=0.96 g/cm3
mt11   poly.01t
m12   13027.60c 1.000                        $Al   density=2.70 g/cm3
m13    2003.60c 1.000                        $He-3,10 atm,den=2.4463e-4
at/barn-cm
m14    8016.60c 0.210 7014.60c 0.790         $air
```

```
m15   14000.60c 0.334 8016.60c 0.666         $glass
m16   94238.60c -0.00048891
      94239.60c -0.72910337
      94240.60c -0.14524399
      94241.60c -0.00412629
      94242.60c -0.00306266
      95241.60c -0.00846288
       8016.60c -0.11797470
c      1001.60c -                            $Pu mix sample
m17   26000 1                               $Iron box
m18   98252.60c 1.000                       $Cf-252 source density
10e-20
m19    1001.60c -0.018112917
       6012.60c -0.114265632
       8016.60c -0.016921527
      57138.31c -0.000280893
      57139.31c -0.311822943
      35079.31c -0.273018919
      35081.31c -0.265586169                  $LaBr Crystal
m20    8016  .324  7014  .593  14000  .083     $Glass/Air Mix
nps   10000000

tmesh
rmesh1:n flux
cora1 -25 99i 25
corb1 -25 99i 25
corc1 -25 25
rmesh2
cora2 -25 99i 25
corb2 -25 99i 25
corc2 -25 25
rmesh3
cora3 -25 99i 25
corb3 -25 99i 25
corc3 -25 25
endmd
```

Pu-238 Deck

```
MCNP Project (HANDHELD)
c     - cell card -
1   11 -0.96     18  21  24  27       u=1     imp:p=1     $poly box
2   14 -0.001293    -18  19           u=1     imp:p=1     $air space
3   14 -0.001293    -21  22           u=1     imp:p=1     $air space
4   14 -0.001293    -24  25           u=1     imp:p=1     $air space
5   14 -0.001293    -27  28           u=1     imp:p=1     $air space
6   12 -2.70        -19  20  31  32   u=1     imp:p=1     $Al clad
7   12 -2.70        -22  23  33  34   u=1     imp:p=1     $Al clad
8   12 -2.70        -25  26  35  36   u=1     imp:p=1     $Al clad
9   12 -2.70        -28  29  37  38   u=1     imp:p=1     $Al clad
10  13  2.4463e-4   -20              u=1     imp:p=1     $active He
tube
11  13  2.4463e-4   -23              u=1     imp:p=1     $active He
tube
12  13  2.4463e-4   -26              u=1     imp:p=1     $active He
tube
13  13  2.4463e-4   -29              u=1     imp:p=1     $active He
tube
14   0               30                      imp:p=0     $outside
universe
15  14 -0.001293    -30 #24 #25 #26 #33 #34
                        #31 #32 #27 #36 #30
                        #37 #38 #39 #40 #41
                        #42 #43 #44 #45 #46
                        #47 #48      imp:p=1     $sphere
16  13  2.4463e-4   -31               u=1     imp:p=1     $inactive
length
17  13  2.4463e-4   -32              u=1     imp:p=1     $inactive
length
18  13  2.4463e-4   -33              u=1     imp:p=1     $inactive
length
19  13  2.4463e-4   -34              u=1     imp:p=1     $inactive
length
20  13  2.4463e-4   -35              u=1     imp:p=1     $inactive
length
21  13  2.4463e-4   -36              u=1     imp:p=1     $inactive
length
22  13  2.4463e-4   -37              u=1     imp:p=1     $inactive
length
23  13  2.4463e-4   -38              u=1     imp:p=1     $inactive
length
24   0                     -17     fill=1          imp:p=1   $poly box
with tubes
25  like 24 but trcl=(0 0 0  -1 0 0  0 -1 0  0 0 1) imp:p=1   $opposite
poly/tubes
26  like 24 but trcl=(0 0 0  0 -1 0  1 0 0  0 0 1)  imp:p=1
$poly/tube slab
27  like 24 but trcl=(0 0 0  0 1 0  -1 0 0  0 0 1)  imp:p=1
$polt/tubes
```

```
c 29  15 -2.5        -41  42                          imp:p=1   $glass
jar
30  16 -0.900          -42 -43                       imp:p=1   $Pu mix
sample
c 35  18 -10e-20     -45 46 -47 48 -49 50             imp:p=1   $Cf-252
31  17 -2.0            -44                           imp:p=1   $metal
top
32  like 31 but trcl=(0 0 0  -1 0 0  0 -1 0  0 0 1) imp:p=1   $metal
top
33  like 31 but trcl=(0 0 0  0 -1 0  1 0 0  0 0 1)  imp:p=1   $metal
top
34  like 31 but trcl=(0 0 0  0 1 0  -1 0 0  0 0 1)  imp:p=1   $metal
top
36  11 -0.96  -51                                   imp:p=1   $bottom
poly slab
37  19 -3.00  -52 #41                                  imp:p=1   $LaBr
Slab
38  like 37 but trcl=(0 0 0  -1 0 0  0 -1 0  0 0 1) imp:p=1   $LaBr
Slab
39  like 37 but trcl=(0 0 0  0 -1 0  1 0 0  0 0 1)  imp:p=1   $LaBr
Slab
40  like 37 but trcl=(0 0 0  0 1 0  -1 0 0  0 0 1)  imp:p=1   $LaBr
Slab
41  12 -2.70  -53 52 54                              imp:p=1   $Al Shell
42  like 41 but trcl=(0 0 0  -1 0 0  0 -1 0  0 0 1) imp:p=1   $LaBr
Slab
43  like 41 but trcl=(0 0 0  0 -1 0  1 0 0  0 0 1)  imp:p=1   $LaBr
Slab
44  like 41 but trcl=(0 0 0  0 1 0  -1 0 0  0 0 1)  imp:p=1   $LaBr
Slab
45  20 -0.6   -54                                    imp:p=1   $PMT
46  like 45 but trcl=(0 0 0  -1 0 0  0 -1 0  0 0 1) imp:p=1   $LaBr
Slab
47  like 45 but trcl=(0 0 0  0 -1 0  1 0 0  0 0 1)  imp:p=1   $LaBr
Slab
48  like 45 but trcl=(0 0 0  0 1 0  -1 0 0  0 0 1)  imp:p=1   $LaBr
Slab

c     - surface cards -
17 BOX  -16.51 -8.89 -11.43   7.62 0 0   0 17.78 0   0 0 22.86
18 RCC  -12.7  -5.953 -11.43   0 0 22.86   1.42875         $void hole
19 RCC  -12.7  -5.953 -11.43   0 0 22.86   1.27            $Al clad
cylinder
20 RCC  -12.7  -5.953 -8.890   0 0 17.78   1.19380         $He cylinder
21 RCC  -12.7  -1.984 -11.43   0 0 22.86   1.42875         $void hole
22 RCC  -12.7  -1.984 -11.43   0 0 22.86   1.27            $void hole
23 RCC  -12.7  -1.984 -8.890   0 0 17.78   1.19380         $He cylinder
24 RCC  -12.7   1.984 -11.43   0 0 22.86   1.42875         $void hole
25 RCC  -12.7   1.984 -11.43   0 0 22.86   1.27            $Al clad
cylinder
26 RCC  -12.7   1.984 -8.890   0 0 17.78   1.19380         $He cylinder
27 RCC  -12.7   5.953 -11.43   0 0 22.86   1.42875         $void hole
28 RCC  -12.7   5.953 -11.43   0 0 22.86   1.27            $Al clad
cylinder
```

```
29 RCC  -12.7   5.953 -8.890   0 0 17.78   1.19380         $He cylinder
30 SPH   0 0 0 40
31 RCC  -12.7 -5.953  8.890   0 0 2.540   1.19380         $inactive
length
32 RCC  -12.7 -5.953 -11.43   0 0 2.540   1.19380         $inactive
length
33 RCC  -12.7 -1.984  8.890   0 0 2.540   1.19380         $inactive
length
34 RCC  -12.7 -1.984 -11.43   0 0 2.540   1.19380         $inactive
length
35 RCC  -12.7  1.984  8.890   0 0 2.540   1.19380         $inactive
length
36 RCC  -12.7  1.984 -11.43   0 0 2.540   1.19380         $inactive
length
37 RCC  -12.7  5.953  8.890   0 0 2.540   1.19380         $inactive
length
38 RCC  -12.7  5.953 -11.43   0 0 2.540   1.19380         $inactive
length
39 BOX  -16.51 8.900 -11.43   26.035 0 0   0 5.08 0   0 0 22.86
40 BOX  -16.51 -13.97 -13.97   26.035 0 0   0 27.94 0   0 0 2.54
41 RCC   0 0 -3.81     0 0 15.24           3.81
42 RCC   0 0 -10.666   0 0 2.33345133      5.4356             $Pu
cylinder
43 PZ   -8.33254867                                         $Pu
cylinder
44 BOX  -16.51 -8.89 11.43   7.62 0 0   0 17.78 0   0 0 2.54
45 PZ   11.43
46 PZ  -11.43
47 PX   8.89
48 PX  -8.89
49 PY   8.89
50 PY  -8.89
51 BOX -22.51 -17.31 -11.43   46.02 0 0   0  34.32 0   0 0 -5.08  $Poly
slab
52 BOX -8.78  -8.78  -11.32   2.54  0 0   0  14.82 0   0 0  22.75 $LaBr
Slab
53 BOX -8.88  -8.88  -11.42   2.74  0 0   0  15.02 0   0 0  25.39 $Al
Shell
54 BOX -8.78  -8.78   11.43   2.54  0 0   0  14.82 0   0 0   2.44 $PMT

c     - data cards -
mode p
print
sdef    pos=0 0 -9.499274335 ERG=d1 axs=0 0 1 rad=d2 ext=d3
si1  L  0.04348  0.09986  0.15268  0.76641
sp1     2.49E+08 4.59E+07 6.05E+06 1.39E+05
si2     0 5.4356
si3    -1.166725665 1.166725665
c fq0   e t f
c f4:n  10 11 12 13 t
c fm4   -1 13 103
c sd4    1 1 1 1 1
c t4     450 6850 1E12
c f14:n ((10 11 12 13) < 24)
```

```
c fm14   -1 13 103
c sd14    1
c f24:n ((10 11 12 13) < 25)
c fm24   -1 13 103
c sd24    1
c f34:n ((10 11 12 13) < 26)
c fm34   -1 13 103
c sd34    1
c f44:n ((10 11 12 13) < 27)
c fm44   -1 13 103
c sd44    1
c f8:n  10 11 12 13 t
c ft108   cap 2003
c fc108 Mulitplicity Count Rate (Infinite Gate)
c f108:n  (10 11 12 13)
c ft118  cap 2003 gate 450 2400
c fc118 Multiplicity Count Rate (24us Gate)
c f118:n  (10 11  12 13)
c ft128  cap 2003 gate 450 6400
c fc128 Multiplicity Count Rate (64us Gate)
c f128:n  (10 11 12 13)
c     t4   300 1100 1900 3500 6700 13100
c sdef  pos=0 0 -9.499274335 ERG=0.667
f8:p    37
f18:p  (37 38 39 40)
ft8   GEB 0.007167 0.019027 -0.141
ft18  GEB 0.007167 0.019027 -0.141
e0    0.01  4000i  1.5
m11    6000.60c 0.333 1001.60c 0.667         $HDPE density=0.96 g/cm3
mt11   poly.01t
m12   13027.60c 1.000                        $Al   density=2.70 g/cm3
m13    2003.60c 1.000                        $He-3,10 atm,den=2.4463e-4
at/barn-cm
m14    8016.60c 0.210 7014.60c 0.790         $air
m15   14000.60c 0.334 8016.60c 0.666         $glass
m16   94238.60c -0.00048891
      94239.60c -0.72910337
      94240.60c -0.14524399
      94241.60c -0.00412629
      94242.60c -0.00306266
      95241.60c -0.00846288
       8016.60c -0.11797470
c      1001.60c -                            $Pu mix sample
m17   26000 1                                $Iron box
m18   98252.60c 1.000                        $Cf-252 source density
10e-20
m19    1001.60c -0.018112917
       6012.60c -0.114265632
       8016.60c -0.016921527
      57138.31c -0.000280893
      57139.31c -0.311822943
      35079.31c -0.273018919
      35081.31c -0.265586169                   $LaBr Crystal
m20    8016  .324  7014  .593  14000  .083     $Glass/Air Mix
```

```
nps   100000000

tmesh
rmesh1:n flux
cora1 -25 99i 25
corb1 -25 99i 25
corc1 -25 25
rmesh2
cora2 -25 99i 25
corb2 -25 99i 25
corc2 -25 25
rmesh3
cora3 -25 99i 25
corb3 -25 99i 25
corc3 -25 25
endmd
```

Pu-239 Input Deck

```
MCNP Project (HANDHELD)
c     - cell card -
1   11 -0.96     18  21  24  27       u=1     imp:p=1     $poly box
2   14 -0.001293    -18  19           u=1     imp:p=1     $air space
3   14 -0.001293    -21  22           u=1     imp:p=1     $air space
4   14 -0.001293    -24  25           u=1     imp:p=1     $air space
5   14 -0.001293    -27  28           u=1     imp:p=1     $air space
6   12 -2.70        -19  20  31  32   u=1     imp:p=1     $Al clad
7   12 -2.70        -22  23  33  34   u=1     imp:p=1     $Al clad
8   12 -2.70        -25  26  35  36   u=1     imp:p=1     $Al clad
9   12 -2.70        -28  29  37  38   u=1     imp:p=1     $Al clad
10  13  2.4463e-4   -20              u=1     imp:p=1     $active He
tube
11  13  2.4463e-4   -23              u=1     imp:p=1     $active He
tube
12  13  2.4463e-4   -26              u=1     imp:p=1     $active He
tube
13  13  2.4463e-4   -29              u=1     imp:p=1     $active He
tube
14   0               30                      imp:p=0     $outside
universe
15  14 -0.001293    -30 #24 #25 #26 #33 #34
                        #31 #32 #27 #36 #30
                        #37 #38 #39 #40 #41
                        #42 #43 #44 #45 #46
                        #47 #48      imp:p=1     $sphere
16  13  2.4463e-4   -31               u=1     imp:p=1     $inactive
length
17  13  2.4463e-4   -32              u=1     imp:p=1     $inactive
length
18  13  2.4463e-4   -33              u=1     imp:p=1     $inactive
length
19  13  2.4463e-4   -34              u=1     imp:p=1     $inactive
length
20  13  2.4463e-4   -35              u=1     imp:p=1     $inactive
length
21  13  2.4463e-4   -36              u=1     imp:p=1     $inactive
length
22  13  2.4463e-4   -37              u=1     imp:p=1     $inactive
length
23  13  2.4463e-4   -38              u=1     imp:p=1     $inactive
length
24   0                     -17     fill=1          imp:p=1   $poly box
with tubes
25  like 24 but trcl=(0 0 0  -1 0 0  0 -1 0  0 0 1) imp:p=1   $opposite
poly/tubes
26  like 24 but trcl=(0 0 0  0 -1 0  1 0 0  0 0 1)  imp:p=1
$poly/tube slab
27  like 24 but trcl=(0 0 0  0 1 0  -1 0 0  0 0 1)  imp:p=1
$polt/tubes
```

```
c 29  15 -2.5        -41  42                          imp:p=1   $glass
jar
30  16 -0.900          -42 -43                       imp:p=1   $Pu mix
sample
c 35  18 -10e-20     -45 46 -47 48 -49 50             imp:p=1   $Cf-252
31  17 -2.0            -44                           imp:p=1   $metal
top
32  like 31 but trcl=(0 0 0  -1 0 0  0 -1 0  0 0 1) imp:p=1   $metal
top
33  like 31 but trcl=(0 0 0  0 -1 0  1 0 0  0 0 1)  imp:p=1   $metal
top
34  like 31 but trcl=(0 0 0  0 1 0  -1 0 0  0 0 1)  imp:p=1   $metal
top
36  11 -0.96  -51                                   imp:p=1   $bottom
poly slab
37  19 -3.00  -52 #41                                  imp:p=1   $LaBr
Slab
38  like 37 but trcl=(0 0 0  -1 0 0  0 -1 0  0 0 1) imp:p=1   $LaBr
Slab
39  like 37 but trcl=(0 0 0  0 -1 0  1 0 0  0 0 1)  imp:p=1   $LaBr
Slab
40  like 37 but trcl=(0 0 0  0 1 0  -1 0 0  0 0 1)  imp:p=1   $LaBr
Slab
41  12 -2.70  -53 52 54                              imp:p=1   $Al Shell
42  like 41 but trcl=(0 0 0  -1 0 0  0 -1 0  0 0 1) imp:p=1   $LaBr
Slab
43  like 41 but trcl=(0 0 0  0 -1 0  1 0 0  0 0 1)  imp:p=1   $LaBr
Slab
44  like 41 but trcl=(0 0 0  0 1 0  -1 0 0  0 0 1)  imp:p=1   $LaBr
Slab
45  20 -0.6   -54                                    imp:p=1   $PMT
46  like 45 but trcl=(0 0 0  -1 0 0  0 -1 0  0 0 1) imp:p=1   $LaBr
Slab
47  like 45 but trcl=(0 0 0  0 -1 0  1 0 0  0 0 1)  imp:p=1   $LaBr
Slab
48  like 45 but trcl=(0 0 0  0 1 0  -1 0 0  0 0 1)  imp:p=1   $LaBr
Slab

c     - surface cards -
17 BOX  -16.51 -8.89 -11.43   7.62 0 0   0 17.78 0   0 0 22.86
18 RCC  -12.7  -5.953 -11.43   0 0 22.86   1.42875         $void hole
19 RCC  -12.7  -5.953 -11.43   0 0 22.86   1.27            $Al clad
cylinder
20 RCC  -12.7  -5.953 -8.890   0 0 17.78   1.19380         $He cylinder
21 RCC  -12.7  -1.984 -11.43   0 0 22.86   1.42875         $void hole
22 RCC  -12.7  -1.984 -11.43   0 0 22.86   1.27            $void hole
23 RCC  -12.7  -1.984 -8.890   0 0 17.78   1.19380         $He cylinder
24 RCC  -12.7   1.984 -11.43   0 0 22.86   1.42875         $void hole
25 RCC  -12.7   1.984 -11.43   0 0 22.86   1.27            $Al clad
cylinder
26 RCC  -12.7   1.984 -8.890   0 0 17.78   1.19380         $He cylinder
27 RCC  -12.7   5.953 -11.43   0 0 22.86   1.42875         $void hole
28 RCC  -12.7   5.953 -11.43   0 0 22.86   1.27            $Al clad
cylinder
```

```
29 RCC  -12.7   5.953 -8.890   0 0 17.78   1.19380         $He cylinder
30 SPH   0 0 0 40
31 RCC  -12.7 -5.953  8.890   0 0 2.540   1.19380         $inactive
length
32 RCC  -12.7 -5.953 -11.43   0 0 2.540   1.19380         $inactive
length
33 RCC  -12.7 -1.984  8.890   0 0 2.540   1.19380         $inactive
length
34 RCC  -12.7 -1.984 -11.43   0 0 2.540   1.19380         $inactive
length
35 RCC  -12.7  1.984  8.890   0 0 2.540   1.19380         $inactive
length
36 RCC  -12.7  1.984 -11.43   0 0 2.540   1.19380         $inactive
length
37 RCC  -12.7  5.953  8.890   0 0 2.540   1.19380         $inactive
length
38 RCC  -12.7  5.953 -11.43   0 0 2.540   1.19380         $inactive
length
39 BOX  -16.51 8.900 -11.43   26.035 0 0   0 5.08 0   0 0 22.86
40 BOX  -16.51 -13.97 -13.97   26.035 0 0   0 27.94 0   0 0 2.54
41 RCC   0 0 -3.81     0 0 15.24           3.81
42 RCC   0 0 -10.666   0 0 2.33345133      5.4356             $Pu
cylinder
43 PZ   -8.33254867                                          $Pu
cylinder
44 BOX  -16.51 -8.89 11.43   7.62 0 0   0 17.78 0   0 0 2.54
45 PZ   11.43
46 PZ  -11.43
47 PX   8.89
48 PX  -8.89
49 PY   8.89
50 PY  -8.89
51 BOX -22.51 -17.31 -11.43   46.02 0 0   0  34.32 0   0 0 -5.08  $Poly
slab
52 BOX -8.78  -8.78  -11.32   2.54  0 0   0  14.82 0   0 0  22.75 $LaBr
Slab
53 BOX -8.88  -8.88  -11.42   2.74  0 0   0  15.02 0   0 0  25.39 $Al
Shell
54 BOX -8.78  -8.78   11.43   2.54  0 0   0  14.82 0   0 0   2.44 $PMT

c     - data cards -
mode p
print
sdef    pos=0 0 -9.499274335 ERG=d1 axs=0 0 1 rad=d2 ext=d3
si1  L  0.05163  0.09878  0.12929  0.20354
        0.34501  0.37504  0.41371  0.64597
        0.71771  0.094658
sp1     6.19E+05 2.80E+04 1.44E+05 1.28E+04
        1.25E+04 3.60E+04 3.42E+04 3.42E+02
        6.29E+01 9.6813E4
si2     0 5.4356
si3    -1.166725665 1.166725665
c fq0   e t f
c f4:n  10 11 12 13 t
```

```
c fm4   -1 13 103
c sd4    1 1 1 1 1
c t4     450 6850 1E12
c f14:n ((10 11 12 13) < 24)
c fm14   -1 13 103
c sd14    1
c f24:n ((10 11 12 13) < 25)
c fm24   -1 13 103
c sd24    1
c f34:n ((10 11 12 13) < 26)
c fm34   -1 13 103
c sd34    1
c f44:n ((10 11 12 13) < 27)
c fm44   -1 13 103
c sd44    1
c f8:n  10 11 12 13 t
c ft108   cap 2003
c fc108 Mulitplicity Count Rate (Infinite Gate)
c f108:n  (10 11 12 13)
c ft118  cap 2003 gate 450 2400
c fc118 Multiplicity Count Rate (24us Gate)
c f118:n  (10 11  12 13)
c ft128  cap 2003 gate 450 6400
c fc128 Multiplicity Count Rate (64us Gate)
c f128:n  (10 11 12 13)
c     t4   300 1100 1900 3500 6700 13100
c sdef  pos=0 0 -9.499274335 ERG=0.667
f8:p    37
f18:p  (37 38 39 40)
ft8   GEB 0.007167 0.019027 -0.141
ft18  GEB 0.007167 0.019027 -0.141
e0    0.01  4000i  1.5
m11    6000.60c 0.333 1001.60c 0.667         $HDPE density=0.96 g/cm3
mt11   poly.01t
m12   13027.60c 1.000                        $Al   density=2.70 g/cm3
m13    2003.60c 1.000                        $He-3,10 atm,den=2.4463e-4
at/barn-cm
m14    8016.60c 0.210 7014.60c 0.790         $air
m15   14000.60c 0.334 8016.60c 0.666         $glass
m16   94238.60c -0.00048891
      94239.60c -0.72910337
      94240.60c -0.14524399
      94241.60c -0.00412629
      94242.60c -0.00306266
      95241.60c -0.00846288
       8016.60c -0.11797470
c      1001.60c -                            $Pu mix sample
m17   26000 1                                $Iron box
m18   98252.60c 1.000                        $Cf-252 source density
10e-20
m19    1001.60c -0.018112917
       6012.60c -0.114265632
       8016.60c -0.016921527
      57138.31c -0.000280893
```

```
      57139.31c -0.311822943
      35079.31c -0.273018919
      35081.31c -0.265586169                    $LaBr Crystal
m20    8016  .324  7014  .593  14000  .083     $Glass/Air Mix
nps   100000000

tmesh
rmesh1:n flux
cora1 -25 99i 25
corb1 -25 99i 25
corc1 -25 25
rmesh2
cora2 -25 99i 25
corb2 -25 99i 25
corc2 -25 25
rmesh3
cora3 -25 99i 25
corb3 -25 99i 25
corc3 -25 25
endmd
```

Pu-240 Input Deck

```
MCNP Project (HANDHELD)
c     - cell card -
1   11 -0.96     18  21  24  27       u=1     imp:p=1     $poly box
2   14 -0.001293    -18  19           u=1     imp:p=1     $air space
3   14 -0.001293    -21  22           u=1     imp:p=1     $air space
4   14 -0.001293    -24  25           u=1     imp:p=1     $air space
5   14 -0.001293    -27  28           u=1     imp:p=1     $air space
6   12 -2.70        -19  20  31  32   u=1     imp:p=1     $Al clad
7   12 -2.70        -22  23  33  34   u=1     imp:p=1     $Al clad
8   12 -2.70        -25  26  35  36   u=1     imp:p=1     $Al clad
9   12 -2.70        -28  29  37  38   u=1     imp:p=1     $Al clad
10  13  2.4463e-4   -20              u=1     imp:p=1     $active He
tube
11  13  2.4463e-4   -23              u=1     imp:p=1     $active He
tube
12  13  2.4463e-4   -26              u=1     imp:p=1     $active He
tube
13  13  2.4463e-4   -29              u=1     imp:p=1     $active He
tube
14   0               30                      imp:p=0     $outside
universe
15  14 -0.001293    -30 #24 #25 #26 #33 #34
                        #31 #32 #27 #36 #30
                        #37 #38 #39 #40 #41
                        #42 #43 #44 #45 #46
                        #47 #48      imp:p=1     $sphere
16  13  2.4463e-4   -31               u=1     imp:p=1     $inactive
length
17  13  2.4463e-4   -32              u=1     imp:p=1     $inactive
length
18  13  2.4463e-4   -33              u=1     imp:p=1     $inactive
length
19  13  2.4463e-4   -34              u=1     imp:p=1     $inactive
length
20  13  2.4463e-4   -35              u=1     imp:p=1     $inactive
length
21  13  2.4463e-4   -36              u=1     imp:p=1     $inactive
length
22  13  2.4463e-4   -37              u=1     imp:p=1     $inactive
length
23  13  2.4463e-4   -38              u=1     imp:p=1     $inactive
length
24   0                     -17     fill=1          imp:p=1   $poly box
with tubes
25  like 24 but trcl=(0 0 0  -1 0 0  0 -1 0  0 0 1) imp:p=1   $opposite
poly/tubes
26  like 24 but trcl=(0 0 0  0 -1 0  1 0 0  0 0 1)  imp:p=1
$poly/tube slab
27  like 24 but trcl=(0 0 0  0 1 0  -1 0 0  0 0 1)  imp:p=1
$polt/tubes
```

```
c 29  15 -2.5        -41  42                          imp:p=1   $glass
jar
30  16 -0.900          -42 -43                       imp:p=1   $Pu mix
sample
c 35  18 -10e-20     -45 46 -47 48 -49 50             imp:p=1   $Cf-252
31  17 -2.0            -44                           imp:p=1   $metal
top
32  like 31 but trcl=(0 0 0  -1 0 0  0 -1 0  0 0 1) imp:p=1   $metal
top
33  like 31 but trcl=(0 0 0  0 -1 0  1 0 0  0 0 1)  imp:p=1   $metal
top
34  like 31 but trcl=(0 0 0  0 1 0  -1 0 0  0 0 1)  imp:p=1   $metal
top
36  11 -0.96  -51                                   imp:p=1   $bottom
poly slab
37  19 -3.00  -52 #41                                  imp:p=1   $LaBr
Slab
38  like 37 but trcl=(0 0 0  -1 0 0  0 -1 0  0 0 1) imp:p=1   $LaBr
Slab
39  like 37 but trcl=(0 0 0  0 -1 0  1 0 0  0 0 1)  imp:p=1   $LaBr
Slab
40  like 37 but trcl=(0 0 0  0 1 0  -1 0 0  0 0 1)  imp:p=1   $LaBr
Slab
41  12 -2.70  -53 52 54                              imp:p=1   $Al Shell
42  like 41 but trcl=(0 0 0  -1 0 0  0 -1 0  0 0 1) imp:p=1   $LaBr
Slab
43  like 41 but trcl=(0 0 0  0 -1 0  1 0 0  0 0 1)  imp:p=1   $LaBr
Slab
44  like 41 but trcl=(0 0 0  0 1 0  -1 0 0  0 0 1)  imp:p=1   $LaBr
Slab
45  20 -0.6   -54                                    imp:p=1   $PMT
46  like 45 but trcl=(0 0 0  -1 0 0  0 -1 0  0 0 1) imp:p=1   $LaBr
Slab
47  like 45 but trcl=(0 0 0  0 -1 0  1 0 0  0 0 1)  imp:p=1   $LaBr
Slab
48  like 45 but trcl=(0 0 0  0 1 0  -1 0 0  0 0 1)  imp:p=1   $LaBr
Slab

c     - surface cards -
17 BOX  -16.51 -8.89 -11.43   7.62 0 0   0 17.78 0   0 0 22.86
18 RCC  -12.7  -5.953 -11.43   0 0 22.86   1.42875         $void hole
19 RCC  -12.7  -5.953 -11.43   0 0 22.86   1.27            $Al clad
cylinder
20 RCC  -12.7  -5.953 -8.890   0 0 17.78   1.19380         $He cylinder
21 RCC  -12.7  -1.984 -11.43   0 0 22.86   1.42875         $void hole
22 RCC  -12.7  -1.984 -11.43   0 0 22.86   1.27            $void hole
23 RCC  -12.7  -1.984 -8.890   0 0 17.78   1.19380         $He cylinder
24 RCC  -12.7   1.984 -11.43   0 0 22.86   1.42875         $void hole
25 RCC  -12.7   1.984 -11.43   0 0 22.86   1.27            $Al clad
cylinder
26 RCC  -12.7   1.984 -8.890   0 0 17.78   1.19380         $He cylinder
27 RCC  -12.7   5.953 -11.43   0 0 22.86   1.42875         $void hole
28 RCC  -12.7   5.953 -11.43   0 0 22.86   1.27            $Al clad
cylinder
```

```
29 RCC  -12.7   5.953 -8.890   0 0 17.78   1.19380         $He cylinder
30 SPH   0 0 0 40
31 RCC  -12.7 -5.953  8.890   0 0 2.540   1.19380         $inactive
length
32 RCC  -12.7 -5.953 -11.43   0 0 2.540   1.19380         $inactive
length
33 RCC  -12.7 -1.984  8.890   0 0 2.540   1.19380         $inactive
length
34 RCC  -12.7 -1.984 -11.43   0 0 2.540   1.19380         $inactive
length
35 RCC  -12.7  1.984  8.890   0 0 2.540   1.19380         $inactive
length
36 RCC  -12.7  1.984 -11.43   0 0 2.540   1.19380         $inactive
length
37 RCC  -12.7  5.953  8.890   0 0 2.540   1.19380         $inactive
length
38 RCC  -12.7  5.953 -11.43   0 0 2.540   1.19380         $inactive
length
39 BOX  -16.51 8.900 -11.43   26.035 0 0   0 5.08 0   0 0 22.86
40 BOX  -16.51 -13.97 -13.97   26.035 0 0   0 27.94 0   0 0 2.54
41 RCC   0 0 -3.81     0 0 15.24           3.81
42 RCC   0 0 -10.666   0 0 2.33345133      5.4356             $Pu
cylinder
43 PZ   -8.33254867                                         $Pu
cylinder
44 BOX  -16.51 -8.89 11.43   7.62 0 0   0 17.78 0   0 0 2.54
45 PZ   11.43
46 PZ  -11.43
47 PX   8.89
48 PX  -8.89
49 PY   8.89
50 PY  -8.89
51 BOX -22.51 -17.31 -11.43   46.02 0 0   0  34.32 0   0 0 -5.08  $Poly
slab
52 BOX -8.78  -8.78  -11.32   2.54  0 0   0  14.82 0   0 0  22.75 $LaBr
Slab
53 BOX -8.88  -8.88  -11.42   2.74  0 0   0  15.02 0   0 0  25.39 $Al
Shell
54 BOX -8.78  -8.78   11.43   2.54  0 0   0  14.82 0   0 0   2.44 $PMT

c     - data cards -
mode p
print
sdef    pos=0 0 -9.499274335 ERG=d1 axs=0 0 1 rad=d2 ext=d3
si1  L  0.04523  0.10424  0.16028  0.64248
sp1     3.80E+06 5.86E+05 3.38E+04 1.05E+03
si2     0 5.4356
si3    -1.166725665 1.166725665
c fq0   e t f
c f4:n  10 11 12 13 t
c fm4   -1 13 103
c sd4    1 1 1 1 1
c t4     450 6850 1E12
c f14:n ((10 11 12 13) < 24)
```

```
c fm14   -1 13 103
c sd14    1
c f24:n ((10 11 12 13) < 25)
c fm24   -1 13 103
c sd24    1
c f34:n ((10 11 12 13) < 26)
c fm34   -1 13 103
c sd34    1
c f44:n ((10 11 12 13) < 27)
c fm44   -1 13 103
c sd44    1
c f8:n  10 11 12 13 t
c ft108   cap 2003
c fc108 Mulitplicity Count Rate (Infinite Gate)
c f108:n  (10 11 12 13)
c ft118  cap 2003 gate 450 2400
c fc118 Multiplicity Count Rate (24us Gate)
c f118:n  (10 11  12 13)
c ft128  cap 2003 gate 450 6400
c fc128 Multiplicity Count Rate (64us Gate)
c f128:n  (10 11 12 13)
c     t4   300 1100 1900 3500 6700 13100
c sdef  pos=0 0 -9.499274335 ERG=0.667
f8:p    37
f18:p  (37 38 39 40)
ft8   GEB 0.007167 0.019027 -0.141
ft18  GEB 0.007167 0.019027 -0.141
e0    0.01  4000i  1.5
m11    6000.60c 0.333 1001.60c 0.667         $HDPE density=0.96 g/cm3
mt11   poly.01t
m12   13027.60c 1.000                        $Al   density=2.70 g/cm3
m13    2003.60c 1.000                        $He-3,10 atm,den=2.4463e-4
at/barn-cm
m14    8016.60c 0.210 7014.60c 0.790         $air
m15   14000.60c 0.334 8016.60c 0.666         $glass
m16   94238.60c -0.00048891
      94239.60c -0.72910337
      94240.60c -0.14524399
      94241.60c -0.00412629
      94242.60c -0.00306266
      95241.60c -0.00846288
       8016.60c -0.11797470
c      1001.60c -                            $Pu mix sample
m17   26000 1                                $Iron box
m18   98252.60c 1.000                        $Cf-252 source density
10e-20
m19    1001.60c -0.018112917
       6012.60c -0.114265632
       8016.60c -0.016921527
      57138.31c -0.000280893
      57139.31c -0.311822943
      35079.31c -0.273018919
      35081.31c -0.265586169                   $LaBr Crystal
m20    8016  .324  7014  .593  14000  .083     $Glass/Air Mix
```

```
nps   100000000

tmesh
rmesh1:n flux
cora1 -25 99i 25
corb1 -25 99i 25
corc1 -25 25
rmesh2
cora2 -25 99i 25
corb2 -25 99i 25
corc2 -25 25
rmesh3
cora3 -25 99i 25
corb3 -25 99i 25
corc3 -25 25
endmd
```

Pu-241 Input Deck

```
MCNP Project (HANDHELD)
c     - cell card -
1   11 -0.96     18  21  24  27       u=1     imp:p=1     $poly box
2   14 -0.001293    -18  19           u=1     imp:p=1     $air space
3   14 -0.001293    -21  22           u=1     imp:p=1     $air space
4   14 -0.001293    -24  25           u=1     imp:p=1     $air space
5   14 -0.001293    -27  28           u=1     imp:p=1     $air space
6   12 -2.70        -19  20  31  32   u=1     imp:p=1     $Al clad
7   12 -2.70        -22  23  33  34   u=1     imp:p=1     $Al clad
8   12 -2.70        -25  26  35  36   u=1     imp:p=1     $Al clad
9   12 -2.70        -28  29  37  38   u=1     imp:p=1     $Al clad
10  13  2.4463e-4   -20              u=1     imp:p=1     $active He
tube
11  13  2.4463e-4   -23              u=1     imp:p=1     $active He
tube
12  13  2.4463e-4   -26              u=1     imp:p=1     $active He
tube
13  13  2.4463e-4   -29              u=1     imp:p=1     $active He
tube
14   0               30                      imp:p=0     $outside
universe
15  14 -0.001293    -30 #24 #25 #26 #33 #34
                        #31 #32 #27 #36 #30
                        #37 #38 #39 #40 #41
                        #42 #43 #44 #45 #46
                        #47 #48      imp:p=1     $sphere
16  13  2.4463e-4   -31               u=1     imp:p=1     $inactive
length
17  13  2.4463e-4   -32              u=1     imp:p=1     $inactive
length
18  13  2.4463e-4   -33              u=1     imp:p=1     $inactive
length
19  13  2.4463e-4   -34              u=1     imp:p=1     $inactive
length
20  13  2.4463e-4   -35              u=1     imp:p=1     $inactive
length
21  13  2.4463e-4   -36              u=1     imp:p=1     $inactive
length
22  13  2.4463e-4   -37              u=1     imp:p=1     $inactive
length
23  13  2.4463e-4   -38              u=1     imp:p=1     $inactive
length
24   0                     -17     fill=1          imp:p=1   $poly box
with tubes
25  like 24 but trcl=(0 0 0  -1 0 0  0 -1 0  0 0 1) imp:p=1   $opposite
poly/tubes
26  like 24 but trcl=(0 0 0  0 -1 0  1 0 0  0 0 1)  imp:p=1
$poly/tube slab
27  like 24 but trcl=(0 0 0  0 1 0  -1 0 0  0 0 1)  imp:p=1
$polt/tubes
```

```
c 29  15 -2.5        -41  42                          imp:p=1   $glass
jar
30  16 -0.900          -42 -43                       imp:p=1   $Pu mix
sample
c 35  18 -10e-20     -45 46 -47 48 -49 50             imp:p=1   $Cf-252
31  17 -2.0            -44                           imp:p=1   $metal
top
32  like 31 but trcl=(0 0 0  -1 0 0  0 -1 0  0 0 1) imp:p=1   $metal
top
33  like 31 but trcl=(0 0 0  0 -1 0  1 0 0  0 0 1)  imp:p=1   $metal
top
34  like 31 but trcl=(0 0 0  0 1 0  -1 0 0  0 0 1)  imp:p=1   $metal
top
36  11 -0.96  -51                                   imp:p=1   $bottom
poly slab
37  19 -3.00  -52 #41                                  imp:p=1   $LaBr
Slab
38  like 37 but trcl=(0 0 0  -1 0 0  0 -1 0  0 0 1) imp:p=1   $LaBr
Slab
39  like 37 but trcl=(0 0 0  0 -1 0  1 0 0  0 0 1)  imp:p=1   $LaBr
Slab
40  like 37 but trcl=(0 0 0  0 1 0  -1 0 0  0 0 1)  imp:p=1   $LaBr
Slab
41  12 -2.70  -53 52 54                              imp:p=1   $Al Shell
42  like 41 but trcl=(0 0 0  -1 0 0  0 -1 0  0 0 1) imp:p=1   $LaBr
Slab
43  like 41 but trcl=(0 0 0  0 -1 0  1 0 0  0 0 1)  imp:p=1   $LaBr
Slab
44  like 41 but trcl=(0 0 0  0 1 0  -1 0 0  0 0 1)  imp:p=1   $LaBr
Slab
45  20 -0.6   -54                                    imp:p=1   $PMT
46  like 45 but trcl=(0 0 0  -1 0 0  0 -1 0  0 0 1) imp:p=1   $LaBr
Slab
47  like 45 but trcl=(0 0 0  0 -1 0  1 0 0  0 0 1)  imp:p=1   $LaBr
Slab
48  like 45 but trcl=(0 0 0  0 1 0  -1 0 0  0 0 1)  imp:p=1   $LaBr
Slab

c     - surface cards -
17 BOX  -16.51 -8.89 -11.43   7.62 0 0   0 17.78 0   0 0 22.86
18 RCC  -12.7  -5.953 -11.43   0 0 22.86   1.42875         $void hole
19 RCC  -12.7  -5.953 -11.43   0 0 22.86   1.27            $Al clad
cylinder
20 RCC  -12.7  -5.953 -8.890   0 0 17.78   1.19380         $He cylinder
21 RCC  -12.7  -1.984 -11.43   0 0 22.86   1.42875         $void hole
22 RCC  -12.7  -1.984 -11.43   0 0 22.86   1.27            $void hole
23 RCC  -12.7  -1.984 -8.890   0 0 17.78   1.19380         $He cylinder
24 RCC  -12.7   1.984 -11.43   0 0 22.86   1.42875         $void hole
25 RCC  -12.7   1.984 -11.43   0 0 22.86   1.27            $Al clad
cylinder
26 RCC  -12.7   1.984 -8.890   0 0 17.78   1.19380         $He cylinder
27 RCC  -12.7   5.953 -11.43   0 0 22.86   1.42875         $void hole
28 RCC  -12.7   5.953 -11.43   0 0 22.86   1.27            $Al clad
cylinder
```

```
29 RCC  -12.7   5.953 -8.890   0 0 17.78   1.19380         $He cylinder
30 SPH   0 0 0 40
31 RCC  -12.7 -5.953  8.890   0 0 2.540   1.19380         $inactive
length
32 RCC  -12.7 -5.953 -11.43   0 0 2.540   1.19380         $inactive
length
33 RCC  -12.7 -1.984  8.890   0 0 2.540   1.19380         $inactive
length
34 RCC  -12.7 -1.984 -11.43   0 0 2.540   1.19380         $inactive
length
35 RCC  -12.7  1.984  8.890   0 0 2.540   1.19380         $inactive
length
36 RCC  -12.7  1.984 -11.43   0 0 2.540   1.19380         $inactive
length
37 RCC  -12.7  5.953  8.890   0 0 2.540   1.19380         $inactive
length
38 RCC  -12.7  5.953 -11.43   0 0 2.540   1.19380         $inactive
length
39 BOX  -16.51 8.900 -11.43   26.035 0 0   0 5.08 0   0 0 22.86
40 BOX  -16.51 -13.97 -13.97   26.035 0 0   0 27.94 0   0 0 2.54
41 RCC   0 0 -3.81     0 0 15.24           3.81
42 RCC   0 0 -10.666   0 0 2.33345133      5.4356             $Pu
cylinder
43 PZ   -8.33254867                                         $Pu
cylinder
44 BOX  -16.51 -8.89 11.43   7.62 0 0   0 17.78 0   0 0 2.54
45 PZ   11.43
46 PZ  -11.43
47 PX   8.89
48 PX  -8.89
49 PY   8.89
50 PY  -8.89
51 BOX -22.51 -17.31 -11.43   46.02 0 0   0  34.32 0   0 0 -5.08  $Poly
slab
52 BOX -8.78  -8.78  -11.32   2.54  0 0   0  14.82 0   0 0  22.75 $LaBr
Slab
53 BOX -8.88  -8.88  -11.42   2.74  0 0   0  15.02 0   0 0  25.39 $Al
Shell
54 BOX -8.78  -8.78   11.43   2.54  0 0   0  14.82 0   0 0   2.44 $PMT

c     - data cards -
mode p
print
sdef    pos=0 0 -9.499274335 ERG=d1 axs=0 0 1 rad=d2 ext=d3
si1  L  0.10368  0.14857  0.16458  0.20800
        0.33235  0.37093  0.09466
sp1     3.86E+06 7.15E+06 1.73E+05 2.04E+7
        1.14E+06 1.04E+05 1.159E+07
si2     0 5.4356
si3    -1.166725665 1.166725665
c fq0   e t f
c f4:n  10 11 12 13 t
c fm4   -1 13 103
c sd4    1 1 1 1 1
```

```
c t4     450 6850 1E12
c f14:n ((10 11 12 13) < 24)
c fm14   -1 13 103
c sd14    1
c f24:n ((10 11 12 13) < 25)
c fm24   -1 13 103
c sd24    1
c f34:n ((10 11 12 13) < 26)
c fm34   -1 13 103
c sd34    1
c f44:n ((10 11 12 13) < 27)
c fm44   -1 13 103
c sd44    1
c f8:n  10 11 12 13 t
c ft108   cap 2003
c fc108 Mulitplicity Count Rate (Infinite Gate)
c f108:n  (10 11 12 13)
c ft118  cap 2003 gate 450 2400
c fc118 Multiplicity Count Rate (24us Gate)
c f118:n  (10 11  12 13)
c ft128  cap 2003 gate 450 6400
c fc128 Multiplicity Count Rate (64us Gate)
c f128:n  (10 11 12 13)
c     t4   300 1100 1900 3500 6700 13100
c sdef  pos=0 0 -9.499274335 ERG=0.667
f8:p    37
f18:p  (37 38 39 40)
ft8   GEB 0.007167 0.019027 -0.141
ft18  GEB 0.007167 0.019027 -0.141
e0    0.01  4000i  1.5
m11    6000.60c 0.333 1001.60c 0.667         $HDPE density=0.96 g/cm3
mt11   poly.01t
m12   13027.60c 1.000                        $Al   density=2.70 g/cm3
m13    2003.60c 1.000                        $He-3,10 atm,den=2.4463e-4
at/barn-cm
m14    8016.60c 0.210 7014.60c 0.790         $air
m15   14000.60c 0.334 8016.60c 0.666         $glass
m16   94238.60c -0.00048891
      94239.60c -0.72910337
      94240.60c -0.14524399
      94241.60c -0.00412629
      94242.60c -0.00306266
      95241.60c -0.00846288
       8016.60c -0.11797470
c      1001.60c -                            $Pu mix sample
m17   26000 1                                $Iron box
m18   98252.60c 1.000                        $Cf-252 source density
10e-20
m19    1001.60c -0.018112917
       6012.60c -0.114265632
       8016.60c -0.016921527
      57138.31c -0.000280893
      57139.31c -0.311822943
      35079.31c -0.273018919
```

```
      35081.31c -0.265586169                    $LaBr Crystal
m20    8016  .324  7014  .593  14000  .083     $Glass/Air Mix
nps   100000000

tmesh
rmesh1:n flux
cora1 -25 99i 25
corb1 -25 99i 25
corc1 -25 25
rmesh2
cora2 -25 99i 25
corb2 -25 99i 25
corc2 -25 25
rmesh3
cora3 -25 99i 25
corb3 -25 99i 25
corc3 -25 25
endmd
```

Am-251 59 keV Input Deck

```
MCNP Project (HANDHELD)
c     - cell card -
1   11 -0.96     18  21  24  27       u=1     imp:p=1     $poly box
2   14 -0.001293    -18  19           u=1     imp:p=1     $air space
3   14 -0.001293    -21  22           u=1     imp:p=1     $air space
4   14 -0.001293    -24  25           u=1     imp:p=1     $air space
5   14 -0.001293    -27  28           u=1     imp:p=1     $air space
6   12 -2.70        -19  20  31  32   u=1     imp:p=1     $Al clad
7   12 -2.70        -22  23  33  34   u=1     imp:p=1     $Al clad
8   12 -2.70        -25  26  35  36   u=1     imp:p=1     $Al clad
9   12 -2.70        -28  29  37  38   u=1     imp:p=1     $Al clad
10  13  2.4463e-4   -20              u=1     imp:p=1     $active He
tube
11  13  2.4463e-4   -23              u=1     imp:p=1     $active He
tube
12  13  2.4463e-4   -26              u=1     imp:p=1     $active He
tube
13  13  2.4463e-4   -29              u=1     imp:p=1     $active He
tube
14   0               30                      imp:p=0     $outside
universe
15  14 -0.001293    -30 #24 #25 #26 #33 #34
                        #31 #32 #27 #36 #30
                        #37 #38 #39 #40 #41
                        #42 #43 #44 #45 #46
                        #47 #48      imp:p=1     $sphere
16  13  2.4463e-4   -31               u=1     imp:p=1     $inactive
length
17  13  2.4463e-4   -32              u=1     imp:p=1     $inactive
length
18  13  2.4463e-4   -33              u=1     imp:p=1     $inactive
length
19  13  2.4463e-4   -34              u=1     imp:p=1     $inactive
length
20  13  2.4463e-4   -35              u=1     imp:p=1     $inactive
length
21  13  2.4463e-4   -36              u=1     imp:p=1     $inactive
length
22  13  2.4463e-4   -37              u=1     imp:p=1     $inactive
length
23  13  2.4463e-4   -38              u=1     imp:p=1     $inactive
length
24   0                     -17     fill=1          imp:p=1   $poly box
with tubes
25  like 24 but trcl=(0 0 0  -1 0 0  0 -1 0  0 0 1) imp:p=1   $opposite
poly/tubes
26  like 24 but trcl=(0 0 0  0 -1 0  1 0 0  0 0 1)  imp:p=1
$poly/tube slab
27  like 24 but trcl=(0 0 0  0 1 0  -1 0 0  0 0 1)  imp:p=1
$polt/tubes
```

```
c 29  15 -2.5        -41  42                          imp:p=1   $glass
jar
30  16 -0.900          -42                       imp:p=1   $Pu mix
sample
c 35  18 -10e-20     -45 46 -47 48 -49 50            imp:p=1   $Cf-252
31  17 -2.0            -44                          imp:p=1   $metal
top
32  like 31 but trcl=(0 0 0  -1 0 0  0 -1 0  0 0 1) imp:p=1   $metal
top
33  like 31 but trcl=(0 0 0  0 -1 0  1 0 0  0 0 1)  imp:p=1   $metal
top
34  like 31 but trcl=(0 0 0  0 1 0  -1 0 0  0 0 1)  imp:p=1   $metal
top
36  11 -0.96  -51                                   imp:p=1   $bottom
poly slab
37  19 -2.59  -52 #41                                  imp:p=1   $LaBr
Slab
38  like 37 but trcl=(0 0 0  -1 0 0  0 -1 0  0 0 1) imp:p=1   $LaBr
Slab
39  like 37 but trcl=(0 0 0  0 -1 0  1 0 0  0 0 1)  imp:p=1   $LaBr
Slab
40  like 37 but trcl=(0 0 0  0 1 0  -1 0 0  0 0 1)  imp:p=1   $LaBr
Slab
41  12 -2.70  -53 52 54                              imp:p=1   $Al Shell
42  like 41 but trcl=(0 0 0  -1 0 0  0 -1 0  0 0 1) imp:p=1   $LaBr
Slab
43  like 41 but trcl=(0 0 0  0 -1 0  1 0 0  0 0 1)  imp:p=1   $LaBr
Slab
44  like 41 but trcl=(0 0 0  0 1 0  -1 0 0  0 0 1)  imp:p=1   $LaBr
Slab
45  20 -0.6   -54                                   imp:p=1   $PMT
46  like 45 but trcl=(0 0 0  -1 0 0  0 -1 0  0 0 1) imp:p=1   $LaBr
Slab
47  like 45 but trcl=(0 0 0  0 -1 0  1 0 0  0 0 1)  imp:p=1   $LaBr
Slab
48  like 45 but trcl=(0 0 0  0 1 0  -1 0 0  0 0 1)  imp:p=1   $LaBr
Slab

c     - surface cards -
17 BOX  -16.51 -8.89 -11.43   7.62 0 0   0 17.78 0   0 0 22.86
18 RCC  -12.7  -5.953 -11.43   0 0 22.86   1.42875         $void hole
19 RCC  -12.7  -5.953 -11.43   0 0 22.86   1.27            $Al clad
cylinder
20 RCC  -12.7  -5.953 -8.890   0 0 17.78   1.19380         $He cylinder
21 RCC  -12.7  -1.984 -11.43   0 0 22.86   1.42875         $void hole
22 RCC  -12.7  -1.984 -11.43   0 0 22.86   1.27            $void hole
23 RCC  -12.7  -1.984 -8.890   0 0 17.78   1.19380         $He cylinder
24 RCC  -12.7   1.984 -11.43   0 0 22.86   1.42875         $void hole
25 RCC  -12.7   1.984 -11.43   0 0 22.86   1.27            $Al clad
cylinder
26 RCC  -12.7   1.984 -8.890   0 0 17.78   1.19380         $He cylinder
27 RCC  -12.7   5.953 -11.43   0 0 22.86   1.42875         $void hole
28 RCC  -12.7   5.953 -11.43   0 0 22.86   1.27            $Al clad
cylinder
```

```
29 RCC  -12.7   5.953 -8.890   0 0 17.78   1.19380         $He cylinder
30 SPH   0 0 0 40
31 RCC  -12.7 -5.953  8.890   0 0 2.540   1.19380         $inactive
length
32 RCC  -12.7 -5.953 -11.43   0 0 2.540   1.19380         $inactive
length
33 RCC  -12.7 -1.984  8.890   0 0 2.540   1.19380         $inactive
length
34 RCC  -12.7 -1.984 -11.43   0 0 2.540   1.19380         $inactive
length
35 RCC  -12.7  1.984  8.890   0 0 2.540   1.19380         $inactive
length
36 RCC  -12.7  1.984 -11.43   0 0 2.540   1.19380         $inactive
length
37 RCC  -12.7  5.953  8.890   0 0 2.540   1.19380         $inactive
length
38 RCC  -12.7  5.953 -11.43   0 0 2.540   1.19380         $inactive
length
39 BOX  -16.51 8.900 -11.43   26.035 0 0   0 5.08 0   0 0 22.86
40 BOX  -16.51 -13.97 -13.97   26.035 0 0   0 27.94 0   0 0 2.54
41 RCC   0 0 -3.81     0 0 15.24           3.81
42 RCC   0 0 -10.666   0 0 2.33345133      5.4356             $Pu
cylinder
c 43 PZ   -8.33254867                                          $Pu
cylinder
44 BOX  -16.51 -8.89 11.43   7.62 0 0   0 17.78 0   0 0 2.54
45 PZ   11.43
46 PZ  -11.43
47 PX   8.89
48 PX  -8.89
49 PY   8.89
50 PY  -8.89
51 BOX -22.51 -17.31 -11.43   46.02 0 0   0  34.32 0   0 0 -5.08  $Poly
slab
52 BOX -8.78  -8.78  -11.32   2.54  0 0   0  14.82 0   0 0  22.75 $LaBr
Slab
53 BOX -8.88  -8.88  -11.42   2.74  0 0   0  15.02 0   0 0  25.39 $Al
Shell
54 BOX -8.78  -8.78   11.43   2.54  0 0   0  14.82 0   0 0   2.44 $PMT

c     - data cards -
mode p
print
sdef    pos=0 0 -9.499274335 ERG=.05954 axs=0 0 1 rad=d2 ext=d3
si2     0 5.4356
si3    -1.166725665 1.166725665
c fq0   e t f
c f4:n  10 11 12 13 t
c fm4   -1 13 103
c sd4    1 1 1 1 1
c t4     450 6850 1E12
c f14:n ((10 11 12 13) < 24)
c fm14   -1 13 103
c sd14    1
```

```
c f24:n ((10 11 12 13) < 25)
c fm24   -1 13 103
c sd24    1
c f34:n ((10 11 12 13) < 26)
c fm34   -1 13 103
c sd34    1
c f44:n ((10 11 12 13) < 27)
c fm44   -1 13 103
c sd44    1
c f8:n  10 11 12 13 t
c ft108   cap 2003
c fc108 Mulitplicity Count Rate (Infinite Gate)
c f108:n  (10 11 12 13)
c ft118  cap 2003 gate 450 2400
c fc118 Multiplicity Count Rate (24us Gate)
c f118:n  (10 11  12 13)
c ft128  cap 2003 gate 450 6400
c fc128 Multiplicity Count Rate (64us Gate)
c f128:n  (10 11 12 13)
c     t4   300 1100 1900 3500 6700 13100
c sdef  pos=0 0 -9.499274335 ERG=0.667
f8:p    37
f18:p  (37 38 39 40)
ft8   GEB 0.007167 0.019027 -0.141
ft18  GEB 0.007167 0.019027 -0.141
e0    0.01  4000i  1.5
m11    6000.60c 0.333 1001.60c 0.667         $HDPE density=0.96 g/cm3
mt11   poly.01t
m12   13027.60c 1.000                        $Al   density=2.70 g/cm3
m13    2003.60c 1.000                        $He-3,10 atm,den=2.4463e-4
at/barn-cm
m14    8016.60c 0.210 7014.60c 0.790         $air
m15   14000.60c 0.334 8016.60c 0.666         $glass
m16   94238.60c -0.00048891
      94239.60c -0.72910337
      94240.60c -0.14524399
      94241.60c -0.00412629
      94242.60c -0.00306266
      95241.60c -0.00846288
       8016.60c -0.11797470
c      1001.60c -                            $Pu mix sample
m17   26000 1                                $Iron box
m18   98252.60c 1.000                        $Cf-252 source density
10e-20
m19    1001.60c -0.018112917
       6012.60c -0.114265632
       8016.60c -0.016921527
      57138.31c -0.000280893
      57139.31c -0.311822943
      35079.31c -0.273018919
      35081.31c -0.265586169                   $LaBr Crystal
m20    8016  .324  7014  .593  14000  .083     $Glass/Air Mix
nps   1000000000
```

```
tmesh
rmesh1:n flux
cora1 -25 99i 25
corb1 -25 99i 25
corc1 -25 25
rmesh2
cora2 -25 99i 25
corb2 -25 99i 25
corc2 -25 25
rmesh3
cora3 -25 99i 25
corb3 -25 99i 25
corc3 -25 25
endmd
```

Am-241 >60 keV Input Deck

```
MCNP Project (HANDHELD)
c     - cell card -
1   11 -0.96     18  21  24  27       u=1     imp:p=1     $poly box
2   14 -0.001293    -18  19           u=1     imp:p=1     $air space
3   14 -0.001293    -21  22           u=1     imp:p=1     $air space
4   14 -0.001293    -24  25           u=1     imp:p=1     $air space
5   14 -0.001293    -27  28           u=1     imp:p=1     $air space
6   12 -2.70        -19  20  31  32   u=1     imp:p=1     $Al clad
7   12 -2.70        -22  23  33  34   u=1     imp:p=1     $Al clad
8   12 -2.70        -25  26  35  36   u=1     imp:p=1     $Al clad
9   12 -2.70        -28  29  37  38   u=1     imp:p=1     $Al clad
10  13  2.4463e-4   -20              u=1     imp:p=1     $active He
tube
11  13  2.4463e-4   -23              u=1     imp:p=1     $active He
tube
12  13  2.4463e-4   -26              u=1     imp:p=1     $active He
tube
13  13  2.4463e-4   -29              u=1     imp:p=1     $active He
tube
14   0               30                      imp:p=0     $outside
universe
15  14 -0.001293    -30 #24 #25 #26 #33 #34
                        #31 #32 #27 #36 #30
                        #37 #38 #39 #40 #41
                        #42 #43 #44 #45 #46
                        #47 #48      imp:p=1     $sphere
16  13  2.4463e-4   -31               u=1     imp:p=1     $inactive
length
17  13  2.4463e-4   -32               u=1     imp:p=1     $inactive
length
18  13  2.4463e-4   -33               u=1     imp:p=1     $inactive
length
19  13  2.4463e-4   -34               u=1     imp:p=1     $inactive
length
20  13  2.4463e-4   -35               u=1     imp:p=1     $inactive
length
21  13  2.4463e-4   -36               u=1     imp:p=1     $inactive
length
22  13  2.4463e-4   -37               u=1     imp:p=1     $inactive
length
23  13  2.4463e-4   -38               u=1     imp:p=1     $inactive
length
24   0                     -17     fill=1          imp:p=1   $poly box
with tubes
25  like 24 but trcl=(0 0 0  -1 0 0  0 -1 0  0 0 1) imp:p=1   $opposite
poly/tubes
26  like 24 but trcl=(0 0 0  0 -1 0  1 0 0  0 0 1)  imp:p=1
$poly/tube slab
```

```
27  like 24 but trcl=(0 0 0  0 1 0  -1 0 0  0 0 1)  imp:p=1
$polt/tubes
c 29  15 -2.5        -41  42                          imp:p=1   $glass
jar
30  16 -0.900          -42                      imp:p=1   $Pu mix
sample
c 35  18 -10e-20     -45 46 -47 48 -49 50             imp:p=1   $Cf-252
31  17 -2.0            -44                          imp:p=1   $metal
top
32  like 31 but trcl=(0 0 0  -1 0 0  0 -1 0  0 0 1) imp:p=1   $metal
top
33  like 31 but trcl=(0 0 0  0 -1 0  1 0 0  0 0 1)  imp:p=1   $metal
top
34  like 31 but trcl=(0 0 0  0 1 0  -1 0 0  0 0 1)  imp:p=1   $metal
top
36  11 -0.96  -51                                   imp:p=1   $bottom
poly slab
37  19 -2.59  -52 #41                                  imp:p=1   $LaBr
Slab
38  like 37 but trcl=(0 0 0  -1 0 0  0 -1 0  0 0 1) imp:p=1   $LaBr
Slab
39  like 37 but trcl=(0 0 0  0 -1 0  1 0 0  0 0 1)  imp:p=1   $LaBr
Slab
40  like 37 but trcl=(0 0 0  0 1 0  -1 0 0  0 0 1)  imp:p=1   $LaBr
Slab
41  12 -2.70  -53 52 54                              imp:p=1   $Al Shell
42  like 41 but trcl=(0 0 0  -1 0 0  0 -1 0  0 0 1) imp:p=1   $LaBr
Slab
43  like 41 but trcl=(0 0 0  0 -1 0  1 0 0  0 0 1)  imp:p=1   $LaBr
Slab
44  like 41 but trcl=(0 0 0  0 1 0  -1 0 0  0 0 1)  imp:p=1   $LaBr
Slab
45  20 -0.6   -54                                   imp:p=1   $PMT
46  like 45 but trcl=(0 0 0  -1 0 0  0 -1 0  0 0 1) imp:p=1   $LaBr
Slab
47  like 45 but trcl=(0 0 0  0 -1 0  1 0 0  0 0 1)  imp:p=1   $LaBr
Slab
48  like 45 but trcl=(0 0 0  0 1 0  -1 0 0  0 0 1)  imp:p=1   $LaBr
Slab

c     - surface cards -
17 BOX  -16.51 -8.89 -11.43   7.62 0 0   0 17.78 0   0 0 22.86
18 RCC  -12.7  -5.953 -11.43   0 0 22.86   1.42875         $void hole
19 RCC  -12.7  -5.953 -11.43   0 0 22.86   1.27            $Al clad
cylinder
20 RCC  -12.7  -5.953 -8.890   0 0 17.78   1.19380         $He cylinder
21 RCC  -12.7  -1.984 -11.43   0 0 22.86   1.42875         $void hole
22 RCC  -12.7  -1.984 -11.43   0 0 22.86   1.27            $void hole
23 RCC  -12.7  -1.984 -8.890   0 0 17.78   1.19380         $He cylinder
24 RCC  -12.7   1.984 -11.43   0 0 22.86   1.42875         $void hole
25 RCC  -12.7   1.984 -11.43   0 0 22.86   1.27            $Al clad
cylinder
26 RCC  -12.7   1.984 -8.890   0 0 17.78   1.19380         $He cylinder
27 RCC  -12.7   5.953 -11.43   0 0 22.86   1.42875         $void hole
```

```
28 RCC  -12.7   5.953 -11.43   0 0 22.86   1.27            $Al clad
cylinder
29 RCC  -12.7   5.953 -8.890   0 0 17.78   1.19380         $He cylinder
30 SPH   0 0 0 40
31 RCC  -12.7 -5.953  8.890   0 0 2.540   1.19380         $inactive
length
32 RCC  -12.7 -5.953 -11.43   0 0 2.540   1.19380         $inactive
length
33 RCC  -12.7 -1.984  8.890   0 0 2.540   1.19380         $inactive
length
34 RCC  -12.7 -1.984 -11.43   0 0 2.540   1.19380         $inactive
length
35 RCC  -12.7  1.984  8.890   0 0 2.540   1.19380         $inactive
length
36 RCC  -12.7  1.984 -11.43   0 0 2.540   1.19380         $inactive
length
37 RCC  -12.7  5.953  8.890   0 0 2.540   1.19380         $inactive
length
38 RCC  -12.7  5.953 -11.43   0 0 2.540   1.19380         $inactive
length
39 BOX  -16.51 8.900 -11.43   26.035 0 0   0 5.08 0   0 0 22.86
40 BOX  -16.51 -13.97 -13.97   26.035 0 0   0 27.94 0   0 0 2.54
41 RCC   0 0 -3.81     0 0 15.24           3.81
42 RCC   0 0 -10.666   0 0 2.33345133      5.4356             $Pu
cylinder
c 43 PZ   -8.33254867                                          $Pu
cylinder
44 BOX  -16.51 -8.89 11.43   7.62 0 0   0 17.78 0   0 0 2.54
45 PZ   11.43
46 PZ  -11.43
47 PX   8.89
48 PX  -8.89
49 PY   8.89
50 PY  -8.89
51 BOX -22.51 -17.31 -11.43   46.02 0 0   0  34.32 0   0 0 -5.08  $Poly
slab
52 BOX -8.78  -8.78  -11.32   2.54  0 0   0  14.82 0   0 0  22.75 $LaBr
Slab
53 BOX -8.88  -8.88  -11.42   2.74  0 0   0  15.02 0   0 0  25.39 $Al
Shell
54 BOX -8.78  -8.78   11.43   2.54  0 0   0  14.82 0   0 0   2.44 $PMT

c     - data cards -
mode p
print
sdef    pos=0 0 -9.499274335 ERG=d1 axs=0 0 1 rad=d2 ext=d3
si1  L  0.09895  0.10297  0.12529
        0.33540  0.66242  0.72199  0.20800
sp1     2.57E+07 2.47E+07 5.16E+06
        6.28E+05 4.61E+05 2.48E+05 1.00E+06
si2     0 5.4356
si3    -1.166725665 1.166725665
c fq0   e t f
c f4:n  10 11 12 13 t
```

```
c fm4   -1 13 103
c sd4    1 1 1 1 1
c t4     450 6850 1E12
c f14:n ((10 11 12 13) < 24)
c fm14   -1 13 103
c sd14    1
c f24:n ((10 11 12 13) < 25)
c fm24   -1 13 103
c sd24    1
c f34:n ((10 11 12 13) < 26)
c fm34   -1 13 103
c sd34    1
c f44:n ((10 11 12 13) < 27)
c fm44   -1 13 103
c sd44    1
c f8:n  10 11 12 13 t
c ft108   cap 2003
c fc108 Mulitplicity Count Rate (Infinite Gate)
c f108:n  (10 11 12 13)
c ft118  cap 2003 gate 450 2400
c fc118 Multiplicity Count Rate (24us Gate)
c f118:n  (10 11  12 13)
c ft128  cap 2003 gate 450 6400
c fc128 Multiplicity Count Rate (64us Gate)
c f128:n  (10 11 12 13)
c     t4   300 1100 1900 3500 6700 13100
c sdef  pos=0 0 -9.499274335 ERG=0.667
f8:p    37
f18:p  (37 38 39 40)
ft8   GEB 0.007167 0.019027 -0.141
ft18  GEB 0.007167 0.019027 -0.141
e0    0.01  4000i  1.5
m11    6000.60c 0.333 1001.60c 0.667         $HDPE density=0.96 g/cm3
mt11   poly.01t
m12   13027.60c 1.000                        $Al   density=2.70 g/cm3
m13    2003.60c 1.000                        $He-3,10 atm,den=2.4463e-4
at/barn-cm
m14    8016.60c 0.210 7014.60c 0.790         $air
m15   14000.60c 0.334 8016.60c 0.666         $glass
m16   94238.60c -0.00048891
      94239.60c -0.72910337
      94240.60c -0.14524399
      94241.60c -0.00412629
      94242.60c -0.00306266
      95241.60c -0.00846288
       8016.60c -0.11797470
c      1001.60c -                            $Pu mix sample
m17   26000 1                                $Iron box
m18   98252.60c 1.000                        $Cf-252 source density
10e-20
m19    1001.60c -0.018112917
       6012.60c -0.114265632
       8016.60c -0.016921527
      57138.31c -0.000280893
```

```
      57139.31c -0.311822943
      35079.31c -0.273018919
      35081.31c -0.265586169                    $LaBr Crystal
m20    8016  .324  7014  .593  14000  .083     $Glass/Air Mix
nps   1000000000

tmesh
rmesh1:n flux
cora1 -25 99i 25
corb1 -25 99i 25
corc1 -25 25
rmesh2
cora2 -25 99i 25
corb2 -25 99i 25
corc2 -25 25
rmesh3
cora3 -25 99i 25
corb3 -25 99i 25
corc3 -25 25
endmd
```

VITA

Daniel Canady Strohmeyer received his Bachelor of Science degree in Radiological Health Engineering from Texas A&M University in 2007. He entered the Health Physics graduate program at Texas A&M University in June 2007, and received his Master of Science degree in May 2010. His research interests include nuclear non-proliferation, nuclear safeguards, and nuclear counterterrorism.

Mr. Strohmeyer may be reached at 129 Zachry Engineering Building 3133 TAMU College Station, TX 77843-3133 or by email at danielstrohmeyer@neo.tamu.edu.